



**HAL**  
open science

# Mécanismes d'optimisation de l'utilisation des technologies dans le Home Network

Hanane El Abdellaouy

► **To cite this version:**

Hanane El Abdellaouy. Mécanismes d'optimisation de l'utilisation des technologies dans le Home Network. Computer Science [cs]. Télécom Bretagne; Université de Rennes 1, 2015. English. NNT: . tel-01212832

**HAL Id: tel-01212832**

**<https://hal.science/tel-01212832>**

Submitted on 7 Oct 2015

**HAL** is a multi-disciplinary open access archive for the deposit and dissemination of scientific research documents, whether they are published or not. The documents may come from teaching and research institutions in France or abroad, or from public or private research centers.

L'archive ouverte pluridisciplinaire **HAL**, est destinée au dépôt et à la diffusion de documents scientifiques de niveau recherche, publiés ou non, émanant des établissements d'enseignement et de recherche français ou étrangers, des laboratoires publics ou privés.



**THÈSE / Télécom Bretagne**  
sous le sceau de l'Université européenne de Bretagne  
pour obtenir le grade de Docteur de Télécom Bretagne  
En accréditation conjointe avec l'Ecole doctorale Matisse  
Mention : Informatique

présentée par

**Hanane El Abdellaouy**

préparée dans le département Réseaux, sécurité et multimédia  
Laboratoire Irisa

# Mécanismes d'optimisation de l'utilisation des technologies dans le Home Network

Thèse soutenue le 16 janvier 2015  
Devant le jury composé de :

**Frédéric Guidic**  
Professeur, Université Bretagne-Sud / président

**Congduc Pham**  
Professeur, Université de Pau / rapporteur

**Julien Montavont**  
Maître de conférences, Université de Strasbourg / rapporteur

**Bernard Pottier**  
Professeur, Université de Bretagne Occidentale / rapporteur

**Alexander Pelov**  
Maître de Conférences, Télécom Bretagne / examinateur

**Laurent Toutain**  
Maître de Conférences, Télécom Bretagne / directeur de thèse

**Amor Nafkha**  
Maître de Conférences, Supelec – Rennes / invité

**David Bernard**  
Ingénieur Recherche, FT/Orange Labs – Cesson Sévigné / invité

**Frédéric Weiss**  
Maître de Conférences, Université Rennes 1 / invité

# Thèse de Doctorat

**Sous le sceau de l'Université européenne de Bretagne**

## TELECOM BRETAGNE

En accréditation conjointe avec l'Ecole Doctorale MATISSE

pour obtenir le grade de

### DOCTEUR de Télécom Bretagne

Mention : *Informatique*

par

**Hanane EL ABDELLAOUY**

---

## Mécanismes d'optimisation de l'utilisation des technologies dans le Home Network

*Optimization of routing mechanisms for green home network*

---

### Composition du Jury :

- Rapporteurs :** M. Bernard Pottier, Professeur, Université de Bretagne Occidentale  
M. Congduc Pham, Professeur, Université de Pau  
M. Julien Montavont, Maître de Conférences, Université de Strasbourg
- Examineurs :** M. Frédéric Guidec, Professeur, Université de Bretagne-Sud  
M. Alexander Pelov, Maître de Conférences, Télécom Bretagne (Encadrant)  
M. Laurent Toutain, Professeur, Télécom Bretagne (Directeur de thèse)
- Invités :** M. David Bernard, Ingénieur Recherche, Orange Labs (Encadrant)  
M. Amor Nafkha, Maître de Conférences, Supelec  
M. Frédéric Weiss, Maître de Conférences, Université Rennes 1



# Acknowledgements

This thesis took place in Orange Labs of Rennes within the WIDEs team in the context of a CIFRE contract. I would like then to thank the WIDEs team manager M.Yann Rochefort for giving me this opportunity.

I am most grateful to the people with whom I have most closely worked. First of all, my advisor Dr Alexander Pelov, who followed this work from the early beginning to the manuscript writing. I am grateful for his availability and encouragement. I am also grateful to my thesis director Dr. Laurent Toutain for his opinions, advices and for guiding my work through these three years. I would like to express my gratitude to David Bernard for his support, availability and involvement. Later, I had the pleasure

I would like to thank the members of my Ph.D.-committee for reading my dissertation. I feel greatly honored that they have accepted to evaluate my work.

I am most grateful to my husband, Anass, for his constant care and support throughout the long hours of work and for his listening when I was frustrated. I am especially grateful to my parents, Et-Taleb and Dahmana, my sister, Awatif, and my brothers, Mohammed and Adnane for having supported me during my studies.

I would like to thank Meryem Ouzzif for her support and for her care during my three thesis year at Orange. Finally, during my years with Orange and Telecom Bretagne, I have had many great people as colleagues. I would like to thank them, and especially Siwar, Nahla, Malla, Amin and Amine.



# Abstract

The recent improvements in communication technologies and products in terms of services' diversification have a direct effect on home environment. Nowadays, homes host increasingly sophisticated devices providing a wide range of services such as HDTV, VoIP, multimedia storage, gaming, music and so on. This extension does not come for free. Indeed, Information and Communication Technology-enabled (ICT) devices consume about the quarter of the total power consumption within a typical home network, which puts forward the issue of energy efficiency in the home network. In addition, electromagnetic radiation emissions are increasing within homes and may create fear likely to slow down future innovations for certain community of people. Nevertheless the increasing connectivity may help to solve these problems by disabling redundant devices or select more appropriate paths in the network. The problem can be viewed as a multi-criteria routing protocol generalization with the introduction of new metrics. A home network routing solution has therefore to support additional constraints in conjunction with QoS criteria.

It has been a challenging goal to make path selection based on ecological criteria that are closely linked to the external environment (e.g. EM radiation); instead of the conventional routing metrics inherently dependent on network state (e.g. delay). In this thesis, we develop a new concept of radiation-aware routing algorithm for heterogeneous home networks in order to reduce radiated emissions level within a given area.

The first contribution is the proposal of two models of electromagnetic radiated emissions stemming from Wi-Fi and PLC links based on a set of assumptions and mathematical approximation methods. We have then formulated a link-adaptive radiation-aware routing metric.

The second contribution is the proposal of the Radiant Exposure (RE), which is a new routing metric for finding minimum radiated emissions paths in multi-hop heterogeneous network. The RE of a path is the expected radiated energy in units

of  $\frac{W}{m^2}$ , within the radiation-sensitive area, while transmitting a packet along that path.

The RE metric incorporates the effects of the distance between the radiating sources and the radiation-sensitive area as well as the asymmetry of this radiated energy regarding the two directions of each link. We describe the design and implementation of RE as routing metric that can't any shortest path algorithm. For practical networks, using RE metric also maximizes the network throughput. We show by simulations that using RE metric reduces significantly radiated energy compared to the widely used minimum-hop count metric.

The third contribution consists of proposing a mutli-criteria routing algorithm built upon the well-known normalized weighting function. Such method transforms a multi-objective problem into a mono-objective problem by multiplying each objective function by a weighting factor and summing up all the weighted criteria. We involve the user in the process of selecting weights in line with their preferences. The three criteria considered here are radiant exposure (RE), expected energy consumption and bandwidth.

# Contents

<b>Acknowledgements</b>	<b>i</b>
<b>Abstract</b>	<b>iii</b>
<b>Introduction</b>	<b>iii</b>
<b>Contents</b>	<b>v</b>
<b>List of Figures</b>	<b>ix</b>
<b>List of Tables</b>	<b>xi</b>
<b>Introduction</b>	<b>1</b>
<b>I Backgrounds and Technological Context</b>	<b>5</b>
<b>1 Overview of Green Solutions for Home Networks</b>	<b>7</b>
1.1 Home Networks in Literature . . . . .	7
1.1.1 Devices . . . . .	7
1.1.2 Services & Applications . . . . .	10
1.1.3 User Requirements . . . . .	10
1.1.4 Networking . . . . .	10
1.1.4.1 Convergent Home Network Concept . . . . .	11
1.1.4.2 Home Network as IPv6 Network . . . . .	12
1.2 Routing in Home Network . . . . .	13
1.2.1 Network Type . . . . .	13
1.2.2 Design Goal . . . . .	14
1.2.3 Decision Algorithm . . . . .	14

1.2.4	Route Construction . . . . .	14
1.3	User Requirement for Green Home Network . . . . .	15
1.3.1	Overview . . . . .	15
1.3.2	Energy Efficiency . . . . .	16
1.3.3	Electromagnetic Radiation Awareness . . . . .	19
1.4	Conclusion . . . . .	21
 <b>II Analytical Models of ElectroMagnetic Fields for Home Networks</b>		<b>23</b>
<b>2</b>	<b>Modeling ElectroMagnetic Fields (EMFs) from Wi-Fi</b>	<b>25</b>
2.1	Introduction . . . . .	25
2.2	Choice of Measurement Units . . . . .	26
2.2.1	Electric & Magnetic Fields . . . . .	26
2.2.2	Specific Absorption Rate (SAR) . . . . .	26
2.2.3	Power Density . . . . .	27
2.3	Introduction to Different Modeling Methods . . . . .	27
2.4	Modeling Assumptions . . . . .	29
2.4.1	Emission/Transmission System . . . . .	29
2.4.2	Propagation Environment . . . . .	30
2.4.2.1	Source Point Method . . . . .	30
2.4.2.2	Propagation Channel Model . . . . .	31
2.4.2.3	Path Loss Model . . . . .	31
2.4.3	Expected Packet Time (EPT) Model . . . . .	32
2.4.4	Radiation-Sensitive Area . . . . .	32
2.5	Modeling EMFs from a Wi-Fi Link . . . . .	33
2.5.1	Radiant Exposure (RE) Definition . . . . .	33
2.5.2	Formulation of the RE Metric for Wi-Fi Links . . . . .	33
2.5.3	RE Intuition . . . . .	35
2.6	RE Routing Properties . . . . .	35
2.6.1	Additivity . . . . .	36
2.6.2	Asymmetry . . . . .	39
2.6.3	Isotonicity & Monotonicity . . . . .	41
2.7	RE Qualitative Evaluation . . . . .	41
2.7.1	Interpretations . . . . .	41
2.7.2	Impact of Distance from Radiating Source . . . . .	42
2.7.3	Impact of Link Capacity . . . . .	43
2.8	Model Inaccuracies . . . . .	45
2.9	Summary . . . . .	47

<b>3</b>	<b>Modeling EMFs from Power Line Communication (PLC)</b>	<b>49</b>
3.1	Introduction . . . . .	49
3.2	Fundamentals of PLC Technology . . . . .	50
3.2.1	Operating Principle . . . . .	50
3.2.1.1	Physical Medium . . . . .	50
3.2.1.2	Channel Characterization . . . . .	50
3.2.2	EMFs Related Features . . . . .	51
3.2.2.1	EMFs Issues Related to PLC . . . . .	51
3.2.2.2	Standardization Context . . . . .	51
3.3	Modeling EMFs from a Power Line Communication (PLC) Link . .	52
3.3.1	EMFs Modeling Issues . . . . .	52
3.3.2	Introduction to Different Modeling Methods . . . . .	52
3.3.3	EMFs' Model for a PLC link . . . . .	54
3.3.3.1	Simplified Approach . . . . .	54
3.3.3.2	Introduction to In-Home Wiring Topologies . . . . .	56
3.3.3.3	Electric Current Distribution . . . . .	57
3.3.3.4	Radiated Emissions from a Power Line Using Antenna Theory . . . . .	58
3.3.3.5	Formulation of the RE metric for a PLC Link . . . . .	62
3.3.4	Radiated Energy Cartography . . . . .	64
3.3.5	Model Inaccuracies . . . . .	67
3.4	Conclusions . . . . .	68
<b>III</b>	<b>Green Home Network Routing Solutions</b>	<b>69</b>
<b>4</b>	<b>ElectroMagnetic Radiation-Aware Routing Algorithms</b>	<b>71</b>
4.1	Introduction . . . . .	71
4.2	Preliminaries . . . . .	71
4.2.1	Overview . . . . .	71
4.2.2	Chapter Scope . . . . .	73
4.3	ElectroMagnetic Radiation-Aware Routing Algorithm (EMRARA) for Wireless Multi-Hop Networks . . . . .	73
4.3.1	Network Assumptions . . . . .	73
4.3.2	Network Model . . . . .	73
4.3.3	Algorithm Description . . . . .	74
4.3.4	Computing EPT . . . . .	75
4.4	ElectroMagnetic Radiation-Aware Routing Algorithm for Heterogeneous multi-hop networks (EMRARA-H) . . . . .	79
4.4.1	Network Assumptions . . . . .	79

4.4.2	Network Model . . . . .	79
4.4.3	Link-Adaptive RE Path Cost . . . . .	80
4.4.4	Computing EPT . . . . .	81
4.5	Implementation . . . . .	82
4.6	Results and Evaluations . . . . .	83
4.6.1	Performance Metrics . . . . .	83
4.6.2	Experimental Methodology . . . . .	84
4.6.3	Numerical Results . . . . .	85
4.7	Conclusions . . . . .	96
<b>5</b>	<b>Multi-Criteria ElectroMagnetic Radiation-Aware</b>	
	<b>Routing Algorithms</b>	<b>97</b>
5.1	Introduction . . . . .	97
5.2	Preliminaries . . . . .	98
5.2.1	Overview & Chapter Scope . . . . .	98
5.2.2	From Multi-Criteria to Mono-Criterion Optimization . . . . .	98
5.3	Composite Multi-Criteria Routing Algorithm . . . . .	99
5.3.1	Weighting Function . . . . .	99
5.3.2	Normalization . . . . .	100
5.3.3	Objective Functions . . . . .	100
5.4	Implementation . . . . .	103
5.5	Evaluations & Results . . . . .	104
5.5.1	Experimental Methodology . . . . .	104
5.5.2	Evaluation Metrics . . . . .	104
5.5.3	Numerical Results . . . . .	105
5.6	Limitations . . . . .	110
5.7	Conclusions . . . . .	110
<b>6</b>	<b>Conclusions &amp; Perspectives</b>	<b>113</b>
6.1	Conclusions . . . . .	113
6.2	Perspectives & Future Work . . . . .	115
	<b>Acronyms</b>	<b>117</b>
	<b>A Résumé en Français</b>	<b>121</b>
	<b>List of Publications</b>	<b>127</b>
	<b>Bibliography</b>	<b>129</b>

# List of Figures

1.1	Extended Home Network environment . . . . .	8
1.2	Classification of Extended Home Network components . . . . .	9
1.3	IEEE 1905.1 Abstraction layer in the protocol stack . . . . .	11
1.4	General taxonomy of routing protocols. . . . .	13
1.5	Distribution of the electricity consumption per use for a typical French household [1] . . . . .	15
1.6	Risk perception of EMFs [2] . . . . .	16
1.7	Wireless network partitioning because of a drained device (device A in this example) . . . . .	17
2.1	Isotropic antenna radiation assuming source model point . . . . .	30
2.2	Illustration of the geometric parameters in Equations (2.13)–(2.20). . . . .	36
2.3	Different costs for both directions of the link between $u$ and $v$ . . . . .	40
2.4	Radiant Exposure versus distance from radiating source for different modulation schemes of IEEE 802.11n . . . . .	43
2.5	Radiant Exposure versus an IEEE 802.11n link capacity expressed by distance between transmitter and receiver for different distance from the radiation-sensitive area. . . . .	44
3.1	Block diagram of modeling procedure . . . . .	55
3.2	An example of in-home PLC network . . . . .	56
3.3	Three most conventional in-home wiring topologies . . . . .	57
3.4	Illustration of antenna theory applied for linear PLC line . . . . .	58
3.5	Metric calculation example for a typical wiring topology: Bus topology (Figure 3.3c) with conductors along the perimeter . . . . .	64
3.6	Bus configuration example with corresponding dimensions . . . . .	65
3.7	Power density cartography for bus topology example in Figure 3.6 . . . . .	66

4.1	Semantic schematic of general interactions between different components of a link-state routing protocol for one node. . . . .	72
4.2	Illustration of EMRARA . . . . .	75
4.3	Transmission ranges to MCSs mapping . . . . .	79
4.4	Network topologies examples showing all shortest paths from/to UEs with respect to four radiation-sensitive area positions that EMRARA avoids. . . . .	87
4.5	Normalized CRE within the radiant-sensitive area depicted in Figure 4.4a for $\mathbf{N}=100$ and $\mathbf{PP}=0\%$ . . . . .	88
4.6	Normalized CEC when all UEs are receiving . . . . .	89
4.7	Cumulative relay nodes when all UEs are receiving . . . . .	90
4.8	Normalized cumulative radiant exposure within the radiant-sensitive area depicted in Figure 4.4a for $\mathbf{UEP}=70\%$ . Figures represent 20, 60, 100 nodes, respectively. . . . .	92
4.9	Normalized cumulative radiated power within the radiant-sensitive area depicted in Figure 4.4a for $\mathbf{UEP}=70\%$ . Figures represent 20, 60, 100 nodes, respectively. . . . .	93
4.10	Normalized cumulative energy consumption variations with changes in network size. Figures represents 20, 60, 100 nodes, respectively . . . . .	94
4.11	Cumulative Wi-Fi and PLC (dotted bars) links number variations with changes in network size. Figures represent 20, 60 and 100 nodes respectively. . . . .	95
5.1	Simulation results for the shortest path between the HG and a UE with respect to algorithms of the cluster $\mathcal{G}_1$ . . . . .	107
5.2	Simulation results for the shortest path between the HG and a UE with respect to algorithms of the cluster $\mathcal{G}_2$ . . . . .	108
5.3	Simulation results for the shortest path between the HG and a UE with respect to algorithms of the cluster $\mathcal{G}_3$ . . . . .	109

# List of Tables

1.1	Recapitulative table of surveyed works . . . . .	22
2.1	Overview of electromagnetic radiation simulating methods [3, 4] . . . . .	28
2.2	Quantities and corresponding SI units of the parameters in Equation (2.10) . . . . .	34
2.3	Data rates for 802.11n modulation schemes [5] . . . . .	43
3.1	Limits of radiated emissions at a distance of 10m . . . . .	52
3.2	Electric and magnetic quantities and corresponding SI units. . . . .	62
3.3	Error examples of three integral approximating methods . . . . .	68
4.1	Receiver sensitivity corresponding to IEEE 802.11n modulation schemes [5]. . . . .	78
4.2	Transmission ranges and data rates corresponding to 802.11n MCSs indices. . . . .	78



# Introduction

During the last decade, home networks have constituted a new market for network operators and service providers. This is mainly due to the increasingly augmenting ratio of broadband penetration of households all over the world (e.g. 76% and 83% in households have broadband access in France and United Kingdom respectively [6]). This significant interest in home networking originates from the availability of low cost communication technologies and the increasing number of connected devices. Indeed, according to Cisco [7], fixed Internet residential devices and connections worldwide will grow from 3.8 billion in 2013 to 7.9 billion by 2018.

Although this considerable proliferation of available connected devices and transmission technologies; to date, there is no well-defined home network architecture. This is, *inter alia*, the goal of ongoing research work of an Internet Engineering Task Force (IETF) working group [8].

In many scenarios, the design of home-oriented solutions is guided by several users' requirements: higher throughput, self-management, auto-configuration, ease of use, full automation, energy efficiency, etc. In addition, recent studies [9] state that by 2015, 90% of wireless worldwide traffic will originate indoors, including households. It is therefore a significant challenge to consider the electromagnetic radiation awareness as an additional requirement while designing new home network solutions.

Nevertheless the increasing connectivity may help to solve these problems by disabling redundant devices or selecting more appropriate paths in the network. The problem can be viewed as a multi-criteria routing protocol generalization with the introduction of new metrics. A home network routing solution has therefore to support additional constraints in conjunction with Quality of Service (QoS) criteria.

*In short, this PhD thesis concerns modeling, designing, analyzing and evaluating novel electromagnetic radiation-aware routing metrics and algorithms for both wireless and heterogeneous home network scenarios.*

The remainder of the present dissertation is divided into three parts. Part I introduces the general background and the technological context of our studies. This part consists of a single chapter, namely Chapter 1. Part II pioneers the concept of an electromagnetic-radiation aware routing metric and it consists of two chapters, namely Chapter 2 and Chapter 3. As to Part III, it details our proposals of ElectroMagnetic Radiation Aware Routing Algorithm (EMRARA), ElectroMagnetic Radiation Aware Routing Algorithm for Heterogeneous home network (H-EMRARA) and different multi-criteria routing schemes. This part consists of two chapters, more precisely Chapter 4 and Chapter 5.

## Part I

We begin Chapter 1 by giving a general overview of the broad field of smart homes. We introduce then the most relevant solutions aiming to optimize networking mechanisms within home environment. We finally lay more importance on existing routing solutions that take into account users' green requirements, more precisely energy efficiency and radio-frequency emissions. Throughout these reviews, we emphasize the lack, in the literature, of a routing solution that meets these ecological objectives for a home environment, this has motivated our work.

## Part II

With the aim of satisfying users' green requirements, we present in Chapter 2 the concept of a new and generic radiation-aware metric that can fit any shortest path algorithm. Then, we analytically prove its properties for consistent, loop free and optimal routing based on the well-known algebra [10, 11]. This metric is henceforth called Radiant Exposure (RE). When expressed for a direct link, RE quantifies the expected radiated energy in units of  $\frac{W}{m^2}.s$  while transmitting a packet through that link.

In order to formulate the presented radiation-aware metric for Wi-Fi and PLC links, both (i.e. Wi-Fi and PLC) are the most common technologies in today's households, we detail in Chapter 2 our first model of EMFs emanating from Wi-Fi devices and in Chapter 3 our second model of EMFs from power lines when carrying data signals at high frequencies. But before, we thoroughly discuss in both chapters

the challenging issues of modeling such physical phenomenon for routing purposes. This leads us to assume a set of assumptions and appropriate mathematical methods.

The main contributions of this part is the proposal of two theoretical models providing a single value for each Wi-Fi and PLC link that characterize its contribution to radiated energy during data transmission. This part is partially published in [P1, P2].

## Part III

After presenting, in the previous part, the RE formulation, we detail in Chapter 4 its calculation and implementation procedures in two scenarios: fully wireless and heterogeneous multi-hop home networks. This leads us to extend the initial definition of the RE metric to a link-adaptive path cost formulation. So that the use case where Wi-Fi and PLC links coexist, is covered.

We describe our routing solutions, EMRARA and H-EMRARA, for finding minimum radiated energy paths in wireless and heterogeneous multi-hop networks, respectively. Then, we develop a Python-based simulator wherein we implement required models, metric calculation modules and our algorithms. We carry out extensive simulations to evaluate our algorithms' performances compared to other well-established routing algorithms.

Our last contribution consists in proposing a mutli-criteria routing algorithm built upon the well-known normalized weighting function. Such method transforms a multi-objective problem into a mono-objective problem by multiplying each objective function by a weighting factor and summing up all the weighted criteria. We involve the user in the process of selecting weights in line with his/her preferences. The three criteria considered are RE, expected energy consumption and bandwidth. The results of this part are partially published in [P1, P2].

Finally, the concluding chapter synthesizes the contributions of the present thesis and proposes directions for future research.



Part I

Backgrounds and Technological  
Context



# Overview of Green Solutions for Home Networks

## 1.1 Home Networks in Literature

The recent improvements in technologies have changed the traditional view of the home environment from a simple interconnection of few devices to a complex *full connected home network*<sup>1</sup> including a multitude of different heterogeneous technologies and different types of connected devices offering a wide palette of services and applications (Figure 1.1). It has been almost 20 years since the authors in [13, 14, 15] have imagined the home of the future with an eye towards user needs. More recent surveys have given a bird's eye view of challenges and technological requirements of the broad field of smart homes [16, 17, 18, 19]. The main thrust of the existing works in the field is done to ease daily life by increasing user comfort [15, 20, 21, 22].

From this landscape of home-oriented solutions, we have gleaned a general classification of the building blocks of an *Extended Home Network*<sup>2</sup>, with the aim of precisely defining the fields of our contributions. This classification is depicted in Figure 1.2. We detail in the following these blocks.

### 1.1.1 Devices

The extended home networks are expanding beyond phones and computers to cover all imaginable type of sophisticated devices from TVs and audio equipments, to smart connected appliances and sensors. Saito [19] has proposed a usage-based

---

<sup>1</sup>Called also *Intelligent Home* or *Smart Home*, for example in [12]

<sup>2</sup>It should not be confused with the *Home Network* term that will be used frequently in the next chapters

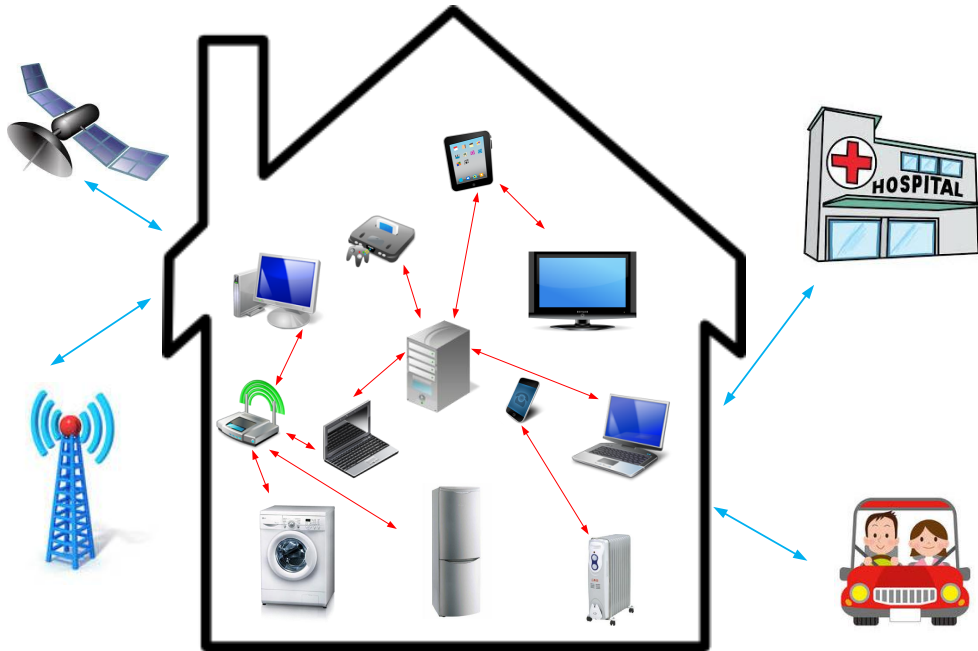


Figure 1.1: Extended Home Network environment

classification of home devices. Here we propose a categorization of home devices based on communication technologies:

**Smart appliances:** Nowadays' dwellings host many kinds of smart and connected appliances (e.g. fridge, washing machine, air conditioning etc.). The ultimate goal of the majority of existing projects and even research works such as [15, 23, 24], is to have a full control of these appliances based on the knowledge of daily user activities. With the diminishing cost of communication chipset, it is safe to consider that all appliances introduced to the market by 2020 will be smart appliances.

**TV and radio devices:** Usually, the Set Top Box (STB) is the device that interconnects one or more TVs to the Home Gateway (HG). The arrival of 3D and 4-K high definition TVs will add more constraints and increased requirements on QoS and more specifically on the bandwidth.

**Sensing/metering devices:** Examples include actuators (e.g. relay, light dimmer, heating valve, etc.) and sensors (e.g. wall switch, water leak, blood pressure, etc.) with the aim of managing and controlling home appliances, collecting measures of some physical parameters and detecting events [25, 16].



**Networking devices:** This category includes bridging and routing devices (e.g. routers, hubs, bridges, etc.) and familiar computing devices such as the desktop personal computers, laptops, tablets, and smartphones. And finally a HG that connects these devices to the Internet through a broadband public provider. Networking devices are usually interconnected via several heterogeneous technologies (Subsection 1.1.4). In the scope of our work, we will consider only this category of devices.

### 1.1.2 Services & Applications

We split home services and applications into two main groups. The first one (broadband communication) includes services yielded by one or more service providers, such as TV broadcasting, Voice over IP (VoIP), etc. The second group of services (control and assistance) consists of applications related to user comfort (e.g. home automation, healthcare, safety, etc.) as well as energy management.

### 1.1.3 User Requirements

With regard to consumer needs, services and applications are more and more greedy for throughput, bandwidth and rely on specific QoS parameters. Hence, within homes, in addition to classical uses of Internet (surfing, downloading, e-mails), we find also real-time applications, such as VoIP, Standard Definition (SD) and High Definition (HD) video stream. Users usually want to enjoy the provided services without any quality degradation. Easiness, self-management and transparency of operations in a home network are of the utmost importance. The basic feature of a consumer product or module is that it must be operable without complicated setups or instruction books. Thus, new modules must be included automatically in the network. Recently, additional ecological considerations have arisen as overriding criteria in the home environment [19, P3]. These green requirements are thoroughly discussed in Section 1.3.

Generally, home oriented solutions are designed to meet the mentioned requirements and make the home network more user friendly by translating users' wishes to technically feasible mechanisms [26, 15, 27, P4]. Finally, the importance of a requirement compared to another one depends entirely on the user profile.

### 1.1.4 Networking

Networking constitutes an important branch of the extended home network field. It involves, as depicted in Figure 1.2, transmission technologies that interconnect home network devices, how these devices could discover each other's presence, addressing

and naming mechanisms, and finally the internal routing protocols. Networking questions in home network have been addressed in the literature from different perspectives. We present in the following two different views.

#### 1.1.4.1 Convergent Home Network Concept

Many academic research and standardization works have attempted to converge wired and wireless communication technologies, within home network, into one unique infrastructure [28]. The concept of *2.5 convergence layer* called also Inter-MAC layer has been first introduced in the framework of the FP7 European project OMEGA [29, 30]. The Inter-MAC sublayer concept has been later adopted by the Institute of Electrical and Electronics Engineers (IEEE) working group 1905 with the aim of taking advantage of the proliferation of technologies in today's home environment to improve the overall connectivity and the end-to-end QoS.

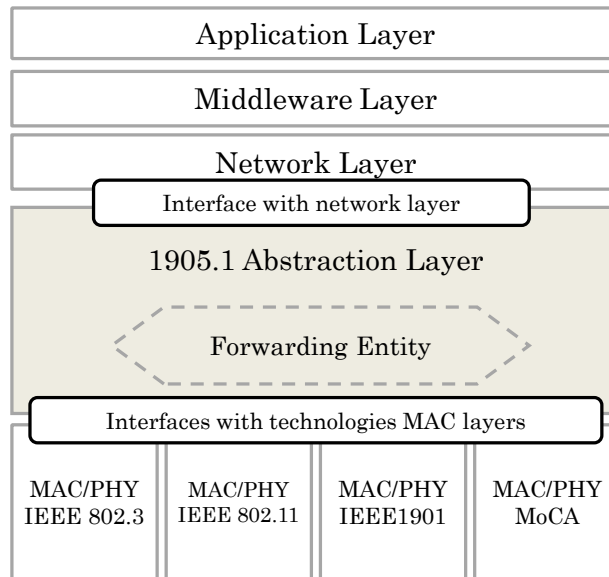


**Figure 1.3:** IEEE 1905.1 Abstraction layer in the protocol stack

As shown in Figure 1.3, the abstraction layer is located on the top of the Medium Access Control (MAC) layers of the different home network technologies: IEEE 1901 over power lines [31], Wi-Fi/IEEE 802.11 [32, 33, 34], Ethernet [35] over twisted pair cable, and Multimedia over Coax Alliance (MoCA) 1.1 over coax [36]. The standard defines a common interface to all these technologies. Thus, upper layers will see a single interface of a home device although this device could support more than one technology. A seamless switching between technologies' interfaces is therefore

guaranteed.

In the scope of the IEEE 1905 standard [37], the accent is put on interfacing mechanisms and messages. On one hand, between MAC layers of home technologies and the abstraction layer, and on the other hand between the abstraction layer and the upper layers (see Figure 1.3). However, to date, the forwarding entity (i.e. how forwarding tables are constructed) is not yet defined, and obviously neither are the path selection mechanisms.

An implementation example of the Inter-MAC sublayer has been proposed and demonstrated through many works [38, 39, 40, 41], each dealing with a specific issue. Authors in [38] introduced the concept of Inter-MAC adaptors which are the interfaces between technologies' MAC layers and the Inter-MAC layer. The key feature of these adaptors is to translate technology-related information into Inter-MAC common semantics as proposed in [39], and this to ensure a total separation between technology-agnostic and technology-dependent parts of the Inter-MAC layer. The concept feasibility has been proven by a reference implementation in [41]. Among Inter-MAC functionalities, the authors in [40] propose a path selection solution based on two QoS metrics. Routing features for home network will be further discussed in Section 1.2.

#### 1.1.4.2 Home Network as IPv6 Network

The IETF working group *homnet* started from the observation that IPv6 is replacing IPv4. So that service providers are more and more deploying IPv6 and HGs are increasingly supporting IPv6 as well. The main goal is then to address issues related to IPv6 introduction, to apply and potentially adapt IETF protocols for home uses while addressing the following requirements [8]:

- Prefix configuration for routers
- Managing routing
- Name resolution
- Service discovery
- Network security

The group intends to achieve these objectives by developing a home network architecture involving multiple routers and subnets. Our contributions of deriving green routing metrics are supposed to be complementary with the ongoing research work on home network within IETF and/or IEEE working groups since these metrics are designed in such a way that they can fit any shortest path algorithm.

## 1.2 Routing in Home Network

Home networks are evolving to include multiple connected devices which require efficient routing mechanisms. In the literature, there are several classifications of routing protocols usually built upon a single criterion; either according to the decision algorithm (*how to calculate the best path related to network information?*) or route construction, called also route discovery (*when to update routes related to traffic availability?*). We propose a general taxonomy which is a super-set of the existing work and includes two other criteria that we deem important for more refined research of a routing solution within home network, namely, network type (*what system was the protocol originally designed for?*) and design goal (*what is the primary objective of the protocol?*). Under each criterion we distinct further categories. These criteria are depicted in Figure 1.4. The aim is to have a global overview of routing protocols. This taxonomy allows us to classify a given protocol and more particularly the target home network protocol as a quadruple of categories, e.g. AODV (network type = ad hoc, design goal = high mobility, decision algorithm = distance vector, route construction = reactive).

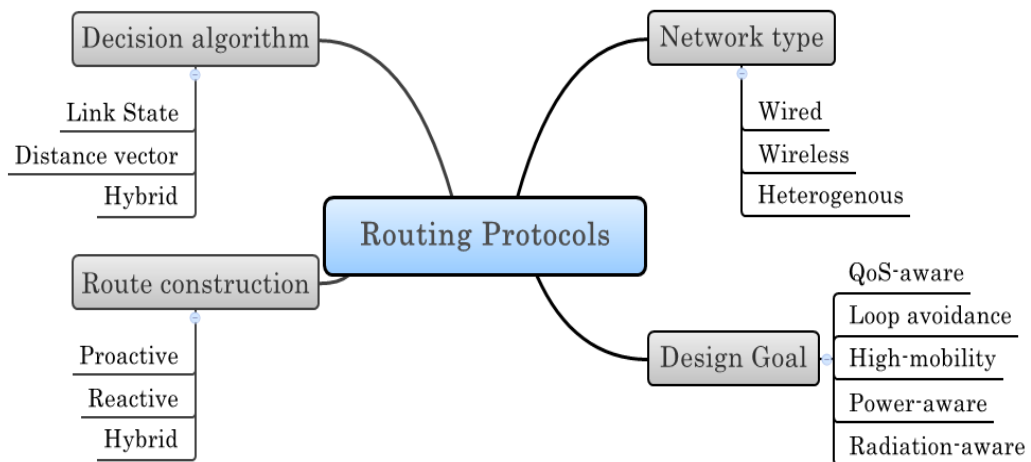


Figure 1.4: General taxonomy of routing protocols.

### 1.2.1 Network Type

Links' nature affects directly both network topology and bandwidth variability. Nodes within a fully wireless network may move frequently and can share the same channel. Hence, a routing protocol for such environment has to tailor to link changes. In contrast, a routing protocol designed for wired networks, does not have the link changes' issue since topology remains unchanged. Power lines are fixed but with a

highly variable shared medium. An extra feature of home networks is that they host all of the mentioned links which will essentially affect the design of routing metrics.

### 1.2.2 Design Goal

A routing protocol is often designed either to overcome shortcomings of an existing one, or to meet specific requirements. Protocols for Mobile Ad hoc NETWORKS (MANETs), for instance, are designed to meet a urgent necessity of high mobility within wireless network. Designing a routing solution for a green home network requires two main criteria, more precisely energy efficiency and reduction of radio-frequency emissions. These two requirements will be discussed in details in Section 1.3.

### 1.2.3 Decision Algorithm

This block answers the question: *how the protocol constructs the routing table at node level?* In other words, the manner that a node computes next hops using network information. Routing protocols are classified based on the content of routing tables into three categories: distance vector, link-state and hybrid protocols. Distance vector protocols use Bellman-Ford algorithm to calculate best paths relying on direct connected neighbors' information. Unlike distance vector, in link-state protocols, each node is aware of the entire network topology. Thus, it uses Dijkstra's algorithm to calculate the shortest path to each destination in the network. Hybrid protocols take advantage from both approaches. Instead of flooding routing updates periodically, they use distance vector to determine best paths and report routing information only when there is a change in the topology. Our algorithms are based on an extension of Dijkstra's algorithm.

### 1.2.4 Route Construction

This block answers the question: *when to update routing information?* Thus, routing protocols can be divided into three categories, proactive (table driven), reactive (on-demand) or hybrid. Proactive protocols maintain fresh routes on each node to all other nodes in the network by updating routing tables periodically. Regarding reactive protocols, routes are constructed solely on demand from a source which has data to send. Hybrid protocols increase scalability while decreasing discovery over-heads. In fact, for nearest nodes, routes are proactively maintained, but for farther ones, routes are constructed on demand. We will not address in the scope of this thesis mechanisms related to route construction.

## 1.3 User Requirement for Green Home Network

### 1.3.1 Overview

The economical and ecological stakes of saving energy are considerable for non-residential environment, e.g. mobile networks, data-centers [42]. Many industry and research works focus then on *greening*<sup>3</sup> cellular networks [44, 45] and Internet wired network [43].

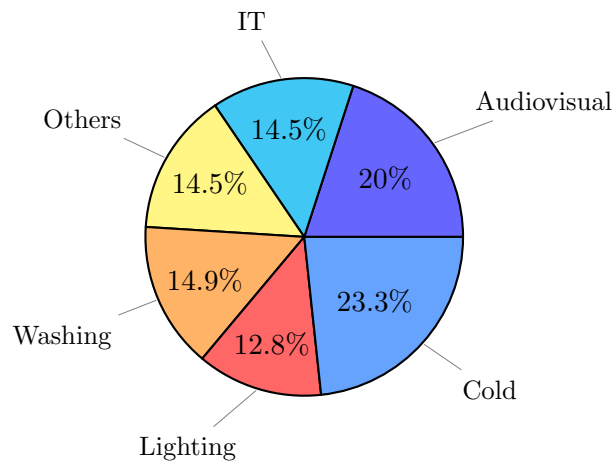


**Figure 1.5:** Distribution of the electricity consumption per use for a typical French household [1]

Nevertheless, with the increasing interest in home networks, it become critical that Information and Communication Technology-enabled (ICT) devices lead to a non-negligible power consumption, e.g. about the quarter within a typical French household [1] (as shown in Figure 1.5), which causes some users to push forward the issue of energy efficiency of the overall home devices and particularly ICT devices, as an essential requirement for home-oriented solutions and products.

The analysis in [9] shows that 90% of wireless worldwide traffic will originate indoor (at home, at work...) by 2015, meaning that electromagnetic radiation emissions are becoming more and more ubiquitous within homes which might create fear likely to slow down future innovations. Meanwhile, costumers' concern regarding these radio-frequency emissions has been pinpointed through a set of European surveys [2]. Explicitly, the graph depicted in Figure 1.6 asseses the European public risk perception of EMFs.

<sup>3</sup>Term used in many research work like in [43], it means to make networks more energy efficient

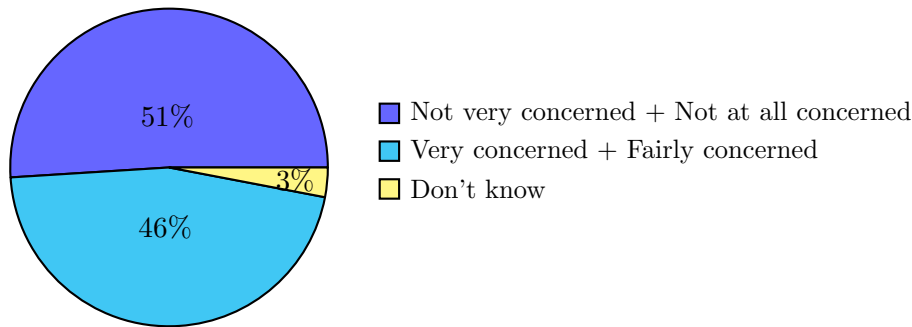


**Figure 1.6:** Risk perception of EMFs [2]

After giving a brief overview of the importance of ecological criteria for a user within home environment, we attempt in the sequel to survey the most relevant works that seek to meet these requirements. The goal of this approach is to highlight the need of designing a new innovative radiation-aware routing metric.

### 1.3.2 Energy Efficiency

Recently, the tendency is toward optimizing as much as possible the used energy. Low-power strategies can be incorporated at two different levels: hardware and software optimization. In hardware design of devices and components such as CPU, displays, disks, etc. However, gradual improvements in hardware technologies have not kept pace with the power consumption demands of the latest hand-held electronic devices. Recent multimedia mobile devices (e.g. smartphones) consume more power than ever. Recent and old research works are using advanced energy-efficient techniques in order to minimize integrated circuit and system power consumption [46, 47]. However, these techniques cannot ensure significant power saving without energy conservation software mechanisms to exploit them effectively like for instance the recent research area on cognitive radio [48]. In that regard, the literature bounds with energy-efficient solutions that enhance all transmission layers of the protocol stack, we describe herein only routing solutions.

Saving energy is an essential design issue for MANETs and Wireless Sensor Networks (WSNs), since equipments (e.g. sensors) in both networks are typically battery powered with a limited energy supply, unlike home network devices. Indeed, in some contexts such as in Figure 1.7, if the battery of the device A drains in a short period, that would lead to a potential network partition and then losing nodes connectivity which is the basic feature in a network. As a result, one of the most important objectives in routing solutions in MANETs and WSNs is how to save energy and maximize network or/and devices' lifetime. Feeney [49], and Stojmen-

ovic and Lin [50] gave good overviews of this topic. In this subsection, we describe routing metrics that have been proposed for this purpose.

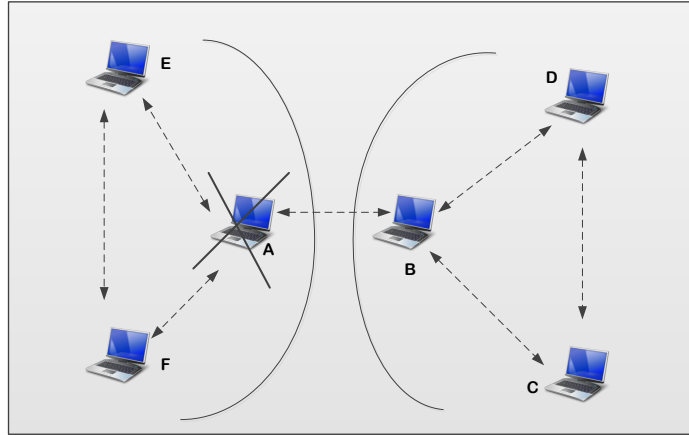


**Figure 1.7:** Wireless network partitioning because of a drained device (device A in this example)

According to the authors [51], the design of almost all energy-aware routing solutions meet two groups of goals:

1. Maximizing network lifetime: where the main goal is to distribute energy consumption over all network devices in balanced manner.
2. Active-energy saving: where the main goal is to find routing paths that minimize the energy consumption per packet which leads in most cases to minimize the overall energy consumption.

The common approach of protocols of the first group is to balance the energy consumption over the whole network. To do so, researchers have designed alternative metrics mainly based on the remaining node capacity such as Minimal Battery Cost Routing (MBCR) and its variants Min-Max Battery Cost Routing (MMBCR) [52], Conditional Max-Min Battery Capacity Routing (CMMBCR) [53] and Conditional Maximum Residual Packet Capacity (CMRPC) [54]. The main purpose of the mentioned works is to avoid that nodes' batteries drain so fast in MANET or WSN scenarios.

Since most of household devices are not battery-constrained, we lay more importance to the second category of protocols, more precisely we will focus on metrics' design in order to determine the most suitable candidate for our home network

routing scheme and, if any exist, to narrow modification to minimum under the assumption of a heterogeneous home network.

The Minimal Total Power metric (MTP) is the most basic formulation of energy-based routing metrics. It was first proposed by Scott and Bambos [55]. This metric was explicitly formulated later by Singh et al. [52], the goal is to minimize the energy  $\mathcal{E}$ , expressed in Equation (1.1), for every packet over a path  $\mathcal{P}$ .

$$\mathcal{E} = \sum_{u \rightarrow v \in \mathcal{P}} e(u, v) \quad (1.1)$$

Where  $e(u, v)$  represents the power usage for transmitting a packet from a node  $u$  to a node  $v$ . However, in both works [55, 52], authors did not mention how to measure or analytically calculate the transmission energy  $e(u, v)$ . Later, the authors in [56] and in [57] have started from the assumption that nodes can adjust their transmission power and then they have proposed a general model of energy consumption as a function of distance between two neighbors:  $e(u, v) = ad_{uv}^\alpha + c$ , where  $d_{uv}$  is the geographical distance between nodes  $u$  and  $v$ ,  $\alpha$  is the path loss exponent, and both  $a$  and  $c$  are constants.

This model is subsequently used by almost all routing protocols proposed for finding minimum energy consumption paths. For example, in [55], the authors have modified Dijkstra's algorithm and set the link cost to the transmission power  $e(u, v)$ . While in [58], the authors have used practically the same energy model to design their energy-aware link cost and then they have modified the Dynamic Source Routing (DSR) protocol to search the minimum cost path. Similarly, the Power-Aware Routing Optimization (PARO) protocol [59] used the transmission power as link cost, and because PARO assumes that a node could dynamically adjust its transmission power, PARO proposes to save energy consumption by selecting paths with larger number of short hops (in terms of distance), rather than using direct and longer paths that would need stronger signal i.e. higher level of transmission power.

Adaptations of the metric of transmission power,  $e(u, v)$ , keep succeeding. Michail and Ephremides [60] proposed a power and interference-aware metric that combines transmission energy and the call blocking probability. Another relevant approach of combining the traditional transmission energy with another metric is to additionally consider the energy consumption due to packets' retransmissions. Hence, the authors [61] have proposed to divide the transmission energy,  $e(u, v)$ , by the packet

loss information, and they have formulated a link cost between two nodes  $u$  and  $v$  as follows:

$$\frac{ad_{uv}^\alpha}{1 - Er_{uv}} \quad (1.2)$$

with  $Er_{uv}$  being the packet loss ratio on the link from node  $u$  to node  $v$  and  $ad_{uv}^\alpha$ , as already mentioned, is the energy needed to transfer a packet from  $u$  to  $v$ . This formula could readily be used with a Dijkstra-based algorithm in a reliable communication system (i.e. hop-by-hop retransmission model), but it does not hold for end-by-end retransmissions. To tackle this, the authors enhance their proposition in [62], by proposing Basic Algorithm for Minimum Energy Routing (BAMER) algorithm, for which they kept the same link cost formulation as expressed in Equation (1.2) while modifying how the path cost is concatenated with respect to a mixed retransmission model (i.e. hop-by-hop and end-to-end retransmission models).

Almost all minimum-energy routing protocols, previously mentioned [55, 52, 56, 57, 58, 59, 60, 61, 62], are based on the assumption that a node can dynamically adjust its transmission power corresponding to the distance from the next hop. Nevertheless, MAC layers of low cost wireless devices available for home network provide rarely this kind of transmission power control mechanism and certainly not in adaptive fashion [63, 64]. For this reason, we have assumed in the next chapters (more precisely in Section 2.4.1 and Section 5.3.3) that the transmission power remains fixed regardless the distance between the sender and the receiver, while taking into account the impact of the link conditions. More explicitly, we will consider the retransmissions' number in the formulation of our energy-aware link cost, combined with a fixed transmission power instead of a variable transmission power.

### 1.3.3 Electromagnetic Radiation Awareness

Whether from radio devices (Wi-Fi, 60 GHz) or from power lines or other objects that become indispensable within a home, electromagnetic waves are everywhere around us, and nobody intends to forego these new technologies.

When we talk about radio-frequency emission, the first thing that leaps to mind is the contribution of mobile networks; one of the reasons is that antennae of base stations transmit at higher level of power compared to the Wi-Fi Access Points (APs) (i.e. up to 20 dBm). In the same context, ITU-T Recommendation K.70 [4] defines techniques and calculation methods that could be used to assess the cumulative

exposure ratio, expressed in Equation (1.3), in the vicinity of transmitting base stations' antennae in order, on one hand to identify the source of radiation and on the hand to comply with exposure limits already defined by International Commission on Non-Ionizing Radiation Protection (ICNIRP) [65].

$$W_t = \sum_{i=100kHz}^{300GHz} \left( \frac{E_i}{E_{l,i}} \right)^2 \quad (1.3)$$

Where  $E_i$  is the electric field strength at the frequency  $i$ , and  $E_{l,i}$  is the reference limit at the frequency  $i$ .

In Equation (1.3), it is assumed that there are different sources radiating simultaneously at different frequencies which correspond to different radio-communication services (broadcasting, cellular systems, relay radios...) The main goal of ITU-T Recommendation K.70 [4] is to determine the compliance distances from which the field level is lower than the reference limits [65] (i.e.  $W_t \leq 1$ ). Whereas, for Wi-Fi frequencies (i.e. 2.4 GHz and 5 GHz) signals are transmitted at low power levels typically up to 20 dBm. In such case, radiated field will never exceed limits preconized by ICNIRP [65]. Thus, our goal is not to seek for compliance with reference limits. Instead, we want to reduce radiated energy within a specific area whenever it is possible.

PLC technology is an integral part of recent households, since it represents an effective way to build home network connectivity without requiring any new cable infrastructure. One particularity of this technology is that electrical wires were not initially designed to carry signals at high frequencies that could vary from 86 MHz to 2 MHz. At those frequencies, a power line behaves like an antenna and a part of the signal is radiated. Issues pertaining to electromagnetic emissions from PLC will be thoroughly discussed in Chapter 3.

Such involuntary emissions not only result in stronger signal attenuation at the receiver but also lead to ElectroMagnetic Compatibility (EMC) issues, as the radiated signal may interfere with other existing services, such as amateur radio or short wave broadcasting [66]. Hence, many researches, especially in the electrical and EMC fields, have shown particular interest on this matter [67, 68, 69, 70, 71]. These efforts have two main goals: First, modeling the phenomenon and then designing methods to mitigate its effects.

Regarding modeling work, Vukicevic [67] ascertained that the Method of Moments (MoM) is the best suited technique to the problem of EMFs' computation from PLC

networks. As to Mescco [68], he preferred to use the Finite Difference Time Domain (FDTD) method for the same purpose for a non-homogeneous domestic environment.

Since our goal is to design a radiation-aware metric, we need a straightforward model that provides a single value for each PLC link. This value has to characterize the electromagnetic radiation contribution of that link. Clearly, the presented methods (i.e. MoM and FDTD) are not appropriate for our problematic. We will address in details the issue of choosing the modeling method that best suits our needs in Subsection 3.3.2.

With respect to mitigation methods, a number of attempts have been presented in the literature to reduce emissions from PLC networks. They include, for example, the injection of an auxiliary PLC-like signal in order to cancel the resulting electromagnetic field on a specific point in space [69], the reduction of the common mode through adding a passive device between the wall outlet and PLC plug [70], and using time Reversal Technique (TR) to mitigate the ElectroMagnetic Interference (EMI) [71]. Most of solutions aiming to mitigate the level of electromagnetic radiation, address the signal itself either by intervening on forward power or on modulation techniques. Whilst for our contribution we have chosen to use a routing solution that carry data packet through links the further possible from a radiation-sensitive area.

## 1.4 Conclusion

In this chapter, we have surveyed the different aspects for smart homes or what we have called extended home networks. We have then presented and discussed different home network oriented solutions from a number of perspectives. In addition, we have focused on routing solutions in the light of green requirements, specifically energy efficiency and radio-frequency emissions.

We summarize in Table 1.1 the different proposals presented in this chapter and that, in some extent, treat issues pertaining to energy efficiency and mitigation of electromagnetic radiation. We want to highlight by this table the lack, in the literature, of a home network oriented routing solution that meets users' green requirements that we have already detailed in Section 1.3.

The present chapter concludes the background part of this thesis. In the next part we develop the necessary mathematical and physical tools for our models with the aim of designing a radiation-aware routing metric for home environment.

Table 1.1: Recapitulative table of surveyed works

Contribution/protocol/paper	Target platform	Routing	Power-awareness		Radiation-awareness	QoS
			Maximizing network lifetime	Minimizing transmission energy		
Maaser et al. [39]	Convergent Home Network					✓
Sahaly and Christin [40]	Convergent Home Network	✓				✓
Minimal Battery Cost Routing (MBCR) [52]	MANETs	✓	✓			
Min-Max Battery Cost Routing (MMBCR) [52]	MANETs	✓	✓			
Conditional Max-Min Battery Capacity Routing (CMNBCR) [53]	MANETs	✓	✓			
Conditional Maximum Residual Packet Capacity (CMRPPC) [54]	MANETs	✓	✓			
Scott and Bambos [55]	MANETs	✓		✓		
Doshi et al. [58]	MANETs	✓		✓		
Power-Aware Routing Optimization protocol (PARO) [59]	MANETs	✓		✓		✓
Michail and Ephremides [60]	MANETs	✓		✓		
Banerjee and Misra [61]	MANETs	✓		✓		
ITU-T Recommendation K.70 [4]	Mobile Networks					✓
Korovkin et al [69]	PLC Networks					✓
Mescoco et al [71]	PLC Networks					✓

## Part II

# Analytical Models of ElectroMagnetic Fields for Home Networks



# Modeling EMFs from Wi-Fi

## 2.1 Introduction

Radio-frequency emissions can result either from wireless devices (e.g. AP) as a functional aspect or from wired links and devices (e.g. power lines) as a side effect, we address only wireless links and radio devices in the scope of the present chapter.

At the onset, we argue the choice of the most appropriate measurement units that will be henceforth used for our routing issues. We review then the existing methods traditionally used to model such electromagnetic phenomenon with the aim of choosing the calculation method that most suits our goals.

Before any modeling work, we define a set of assumptions, definitions, and required models with respect to home environment. Subsequently, we model radiated energy stemming from Wi-Fi devices during data transmission. We therefore formulate our Radiant Exposure (RE) routing metric for Wi-Fi links. The goal of this metric is to select paths that guarantee minimum radiated energy level within a specific area.

Finally, we prove that our metric fulfills two properties: isotonicity and monotonicity, that are necessary and sufficient conditions for an optimal, consistent and loop free routing protocol as stated in [11].

We consider this modeling work as an essential step and one of the corner stones of the thesis.

## 2.2 Choice of Measurement Units

Keeping with our goal to make path selection based on electromagnetic radiation criteria, it has been a challenging task to glean the most appropriate physical quantity in order to evaluate this radiation level without using measurements, and relying only on computational techniques using a minimum number of parameters. Also, it would be timely to highlight the fact that such quantity will be used to formulate an additive routing metric and must exhibit the appropriate characteristics detailed in Subsection 2.6.1 and Subsection 2.6.3.

Radio-frequency signals used in wireless communication produce electrical, magnetic and electromagnetic fields. Depending upon the frequency range of the field, the physical quantities used to measure this electromagnetic radiation may be different. Examples include electric field ( $V.m^{-1}$ ), magnetic field ( $A.m^{-1}$ ), Specific Absorption Rate (SAR) ( $W.kg^{-1}$ ) and the power density ( $W.m^{-2}$ ). Only power density in air, under favorable conditions, can be readily formulated. We justify in this section the choice of the Radiant Exposure (RE) quantity.

### 2.2.1 Electric & Magnetic Fields

When it comes to electromagnetic waves, the electric field,  $\vec{E}$ , and the magnetic field,  $\vec{H}$ , are the first intuitive physical quantities that leap to mind to be used as routing metric in order to reduce radiated emissions. Electric fields are associated only with the presence of electric charge, whereas magnetic fields are the result of the physical movement of electric charge (electric current). Thus, the formulation of the electric and magnetic fields strength is intractable based on computational techniques. Besides, even though the electric and magnetic fields' vectors are additive according to the superposition principle, their strengths (vectors' modules) are not.

### 2.2.2 Specific Absorption Rate (SAR)

Specific Absorption Rate (SAR) is a measure of the rate at which radiated energy is absorbed by the human tissue per unit weight [72]. It is used to establish the maximum radio frequency energy level in Watts per kilogram ( $W.kg^{-1}$ ) that can be safely absorbed by people.

SAR definition incorporates the direct effects of human exposure to radio frequencies, but not necessarily the radiation itself which is the reason why it is often measured at one location of the human body. Furthermore, SAR is related to the electric field by:

$$SAR = \frac{\sigma|E|^2}{\rho}$$

where  $E$  is the induced electric field by the radiation ( $V.m^{-1}$ ),  $\rho$  is the tissue's density ( $Kg.m^{-3}$ ) and  $\sigma$  is the electrical conductivity ( $S.m^{-1}$ ).

Thus, on one hand the estimation of SAR requires the knowledge of electric field strength, which is complicated as previously mentioned, and on the other hand the parameter  $\rho$  depends on the sample that absorbs energy. Consequently, we will not rely on the SAR to quantify electromagnetic radiation from Wi-Fi devices.

### 2.2.3 Power Density

The power density,  $S$ , is defined as the amount of power per unit area of a radiated electromagnetic field [72]. Above 30MHz, the power density is usually expressed in milli- or micro-watts per square centimeter ( $mW.cm^{-2}$  or  $\mu W.cm^{-2}$ ). For a radiating source having a constant transmit power, the power density remains the same for a given point in the space over a given duration, meaning that it does not incorporate the time aspect of the radiation. That justifies the need of an *energy* quantity that provides the amount of radiated power over the transmission time. We will therefore rely on the power density to define the RE quantity (See Subsection 2.5.1).

## 2.3 Introduction to Different Modeling Methods

Transmitting antennae are the real source of intentional electromagnetic fields, not transmitters themselves, owing to the radiation patterns that define the electromagnetic fields distribution in the vicinity of the radio device. Literature abounds with work seeking for diligently modeling these radiation patterns for different purposes (e.g. enhancing antenna directivity). There are many methods for calculating the radiation levels and then the cumulative exposure in the vicinity of radiocommunication installations, especially in multiple sources environment [4, 73, 74]:

1. FDTD;
2. Multiple-Region Finite-Difference Time-Domain (MR/FDTD);
3. Ray tracing model;
4. Hybrid ray tracing/FDTD methods;
5. Near-field antenna models such as MoM;

6. Synthetic model;
7. Point source model;

In the aforementioned standards [4, 73, 74], these methods are used to determine compliance with exposure limits. Generally, selection of the appropriate modeling method depends on the following factors:

1. The field zone where the exposure evaluation is required (near-field or far-field zone);
2. The quantities being evaluated ( $E$ ,  $S$ , or SAR);
3. The topology of the environment where the exposure occurs (open, closed, presence or not of scatterers);
4. Accuracy level (low, medium or high);
5. Computational complexity (low, medium or high);

The following table compares the different methods according to the previously mentioned factors:

Table 2.1: Overview of electromagnetic radiation simulating methods [3, 4]

Method	Field zone	Quantity	Environment	Accuracy	Complexity
FDTD	Near-field	$E$ , SAR	Open	High	High
MR/FDTD	Near-field	SAR	Closed Multiple scatterers	High	Very high
Ray tracing	Far-field	$E$ , $S$	Open	High	Medium
MoM	Near-field	$E$	Open Closed Multiple scatterers	Very high	Very high
Synthetic	Far-field	$E$ , $S$	Open Closed Multiple scatterers	Medium	Medium
Point source	Far-field	$E$ , $S$	Open Closed Multiple scatterers	Low	Low

As we show later for home networks the appropriate fields' formulation is in the far-field zone<sup>1</sup>. Moreover, numerical methods are definitely the most accurate but their high complexity makes them less appropriate for our problematic, especially because a high accuracy is not of our goals.

<sup>1</sup>The perimeter of the far-field zone is calculated for Wi-Fi frequencies in Equation (2.2)

## 2.4 Modeling Assumptions

Wi-Fi antennae radiate energy delivered by a transmitter in the form of electromagnetic waves. Precise information regarding the radiating sources such as radiation pattern, antenna gain and transmit power are therefore required to estimate the radiated energy. Generally, it is difficult to obtain such information in real time, especially because they vary from one device to another.

In addition, as we will detail in Subsection 2.5.1, the definition of the RE relies on the power density caused by a radiating source so the accuracy of the radiated emissions calculation depends on the selected models. Thereby, we lay a great accent on radiating source and propagation environment characteristics. In radio-frequency transmission system, such as Wi-Fi, the power density and obviously the RE involve parameters intrinsically dependent on both emission/transmission system (antenna, amplifiers...) and propagation environment (path loss model, channel model). In order to simplify the design of the radiation-aware metric, we have made some assumptions regarding both systems and propagation environment characteristics; which are presented hereafter.

In Subsection 2.4.1, we justify the assumptions of isotropic antennae and constant transmit power for Wi-Fi devices. Then, we define in Subsection 2.4.2 a variety of models with respect to propagation conditions, these models will be used to formulate the RE metric. In our radiation-aware metric formulation, we will take into consideration the time that a packet takes to be successfully delivered. We exhibit therefore in Subsection 2.4.3 an appropriate packet time model. Since electromagnetic radiations are usually measured/calculated at a given point in the space, we define in Subsection 2.4.4 the concept of radiation-sensitive area that will be used interchangeably with the *hot spot* term for the rest of this thesis.

### 2.4.1 Emission/Transmission System

We assume that both the transmitter and the receiver have isotropic antennae, and that almost all Wi-Fi antennae are omnidirectional which have roughly the same behavior than isotropic ones. In this case, the isotropic antenna radiates energy equally in all directions; hence, the radiation pattern in any plane is circular as illustrated in Figure 2.1 where an isotropic antenna at point  $O$  radiates at power  $P$ . The power flows outwards from the origin and must flow through the spherical surface,  $s$ , of radius,  $r$ . The power density,  $S$ , at the point  $Q$  is defined as:

$$S = \frac{P}{s} = \frac{P}{4\pi r^2} \quad (2.1)$$

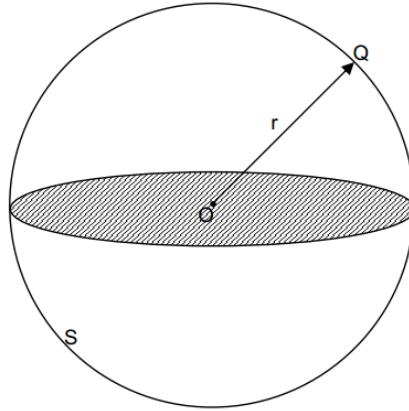


**Figure 2.1:** Isotropic antenna radiation assuming source model point

From a theoretical standpoint, transmit power depends on the modulation; it increases with higher coding rate and wider modulation bandwidth. However, in practice power amplifiers do not allow such adaptability. Hence, we assume that the transmit power remains constant for all Wi-Fi modulations [64].

## 2.4.2 Propagation Environment

In order to design an EMFs' model that provides a single value for each Wi-Fi link, we define, in this section, methods and models with respect to the propagation conditions in the home environment. First, we need a calculation method to estimate the radiated power from a Wi-Fi antenna at a given point in the space. To do so, we choose the Source Point Method from a set of existing methods that we have already reviewed in Section 2.3. Radio-frequency signals' propagation depends highly on the surrounding physical environment (e.g. indoor or outdoor, presence of physical barriers and their materials, etc.). It is then logical to define an appropriate propagation channel model for the home environment. Since radio-frequency signals and more precisely Wi-Fi signals undergo different physical phenomena (e.g. multi-path, reflection, diffraction, scattering) that themselves are depending on the structure of the surrounding environment. We define then in Subsection 2.4.2.3 the path loss model that best suits the propagation channel model of Subsection 2.4.2.2.

### 2.4.2.1 Source Point Method

Calculation related to propagation and electric field, in this chapter, are all made using the calculation model: Source Point model [4], in which the transmitting antenna is presented by one point source having a radiation pattern of the considered transmitting antenna. Such model is applicable only in the far-field region, i.e. for distances from the transmitting antenna bigger than:

$$d_r = \max\left(3\lambda, \frac{2D^2}{\lambda}\right)$$

Where  $d_r$  is the distance between the transmitting antenna and the point of measurement,  $D$  is the largest dimension of the antenna and  $\lambda$  is the signal wavelength. Given that almost all existing omnidirectional antennae are half-wave dipoles, we can easily conclude that, for home network use cases, electromagnetic radiation evaluation will be always in far-field region:

$$d_r = \max\left(3\lambda, \frac{2\left(\frac{\lambda}{2}\right)^2}{\lambda}\right) = \max\left(3\lambda, \frac{\lambda}{2}\right) = 3\lambda = \begin{cases} 37.5cm & \text{for } 2.4GHz \\ 18cm & \text{for } 5GHz \end{cases} \quad (2.2)$$

#### 2.4.2.2 Propagation Channel Model

The Additive White Gaussian Noise (AWGN) channel model is the most straightforward method to model a propagation channel since it does not account multi-path and fading phenomena. However, the residential environment is considered as an indoor environment; signals' propagation depends highly on walls and obstacles' placement. As a result, AWGN channel model is not adapted for such environment. We therefore assume the model B defined by the IEEE High Throughput Task Group (TGn) [75], and called for short TGnB. As stated in [5], the TGnB channel model is more appropriate for residential indoor environment.

The main contribution of this TGn is the definition of the path loss coefficients and parameters (e.g. shadow fading, loss exponent, etc.) for each environment [75]. We use these parameters' values hereafter to formulate our path loss equation.

#### 2.4.2.3 Path Loss Model

The path loss is one of the most important factors of the radio-frequency signals' attenuation. We assume here the path loss model defined in [5] which consists of the free space (FS) loss (slope of 2) up to a breakpoint distance, and a slope of 3.5 after the breakpoint distance. The path loss model is given as follows:

$$\begin{cases} PL(d) = PL_{FS}(d) + SF & d \leq d_{BP} \\ PL(d) = PL_{FS}(d_{BP}) + 35 \log\left(\frac{d}{d_{BP}}\right) + SF & d > d_{BP} \end{cases} \quad (2.3)$$

Where,  $d$  is the separation distance between the transmitter and the receiver in meters,  $PL_{FS}$  is the free space path loss in  $dB$ ,  $d_{BP}$  is the breakpoint distance in

meters and it is equal to  $5m$  for  $TGnB$ , and,  $SF$  is the shadow fading loss in  $dB$ , it is equal to  $4dB$ . The free space path loss is defined as follows:

$$PL_{FS}(d) = 20\log_{10}(d) + 20\log_{10}(f) - 147.5$$

Where  $PL_{FS}$  is in  $dB$  and  $f$  is the frequency in  $Hz$ .

### 2.4.3 Expected Packet Time (EPT) Model

We consider the time of successfully delivering a packet over a Wi-Fi link, including transmission and propagation times. The unreliability of wireless links (e.g. Wi-Fi links) may introduce packet transmission failures and hence several retransmissions. We assume the delay model introduced in [76] while neglecting the processing times (e.g. at routers). Let  $P_f$  denotes the probability of wireless link failure. The expected time of a packet of size,  $L$ , sent over the Wi-Fi link from a node  $u$  to a node  $v$  is expressed as follows:

$$\begin{aligned} EPT_{uv}(L) &= (\alpha_{uv}(L) + \beta_{uv}) \left( \frac{1}{1-P_f} \right) \\ &= \left( \frac{L}{BW_{uv}} + \beta_{uv} \right) \left( \frac{1}{1-P_f} \right) \end{aligned} \quad (2.4)$$

Where  $\alpha_{uv}(L)$  is the transmission duration,  $BW_{uv}$  is the Wi-Fi link bandwidth and  $\beta_{uv}$  is the propagation delay that will be henceforth neglected.

### 2.4.4 Radiation-Sensitive Area

The electromagnetic waves are characterized by their energy flux per unit area, which means also that the radiated emissions are distance dependent. In other words, they are always measured or calculated at a given point from the radiation source. For this reason, we introduce the concept of a radiation-sensitive area within home network wherein we want to reduce the delivered energy flux density (or the power density). Hence, nodes inside this region are avoided by the path selection algorithm (Illustrative examples are sketched in Figure 4.4).

The *hot spot* (radiation-sensitive area) concept introduced in this work, can be found in different context, but leading to similar routing problems. The authors in [77] distinct two categories, namely area *hot spot* (as our case) and link *hot spot* when a routing algorithm aims to avoid links suffering from congestion or saturation for instance. They present the Thermal-Aware Routing Algorithm (TARA) which avoids *hot spots* in human tissue wherein temperature is high due to implemented

sensor radiation and power dissipation. To the best of our knowledge, except TARA there are no other routing solutions that consider the *hot spot* concept.

## 2.5 Modeling EMFs from a Wi-Fi Link

Our goal is to limit electromagnetic radiations in a *hot spot* area over a given time. From a routing standpoint, the problem can be decomposed by taking into account the individual links and their contributions on the total amount of radiated energy within the area. In this section, we first give a general definition of the RE as a physical quantity, then we provide a precise formulation of the RE as a routing metric for Wi-Fi links. Finally, we exhibit the meaning of RE and our aim behind designing it as routing metric.

### 2.5.1 Radiant Exposure (RE) Definition

The radiant exposure is the power density ( $Wm^{-2}$ ) integrated over time, and has units of joule per square meter  $J.m^{-2}$ . A straightforward formula for the radiant exposure,  $RE$ , is given as follows:

$$RE = \int_0^T S^Q(t)dt \quad (2.5)$$

which simplifies to Equation (2.6) when  $S$  is constant over time.

$$RE = S^Q.T \quad (2.6)$$

Where  $S^Q$  is the power density at the investigation point  $Q$  and  $T$  is the radiation time (or the exposure time).

### 2.5.2 Formulation of the RE Metric for Wi-Fi Links

We formulate in Equation (2.7) the cost of a direct link,  $u \rightarrow v$ , as the radiant exposure in the radiation-sensitive area caused by transmitting a packet from node  $u$  to node  $v$  based on the formula 2.6:

$$w(u \rightarrow v) = S_u^Q.EPT_{uv} \quad (2.7)$$

Based on the source point model (Subsection 2.4.2), the power density  $S_u^Q$  at the

investigation point  $Q$ , is given as follows:

$$S_u^Q = \frac{P_{TX}^u}{4\pi r_{u,Q}^2} \quad (2.8)$$

Regarding the Expected Packet Time (EPT), we define it based on the delay model previously presented in Equation (2.4) and it is given as follows:

$$EPT_{uv}(L) = \left( \frac{L}{BW_{uv}} + \beta_{uv} \right) \left( \frac{1}{1 - P_{fuv}} \right) \quad (2.9)$$

The final link cost formula is then given by :

$$w(u \rightarrow v) = \frac{P_{TX}^u}{4\pi r_u^2} \cdot \left( \frac{L}{BW_{uv}} + \beta_{uv} \right) \left( \frac{1}{1 - P_{fuv}} \right) \quad (2.10)$$

A summary of all parameters used in Equation (2.10) and their units is provided in Table 2.2.

Table 2.2: Quantities and corresponding SI units of the parameters in Equation (2.10)

Symbol	Unit	Quantity
$S_u^Q$	$\frac{W}{m^2}$	Power density at the investigation point $Q$ within the radiation-sensitive area
$P_{TX}^u$	$W$	Transmit power of the node $u$
$r_{u,Q}$	$m$	Distance between the transmitter $u$ and the investigation point $Q$ within the radiation-sensitive area
$EPT_{uv}$	$s$	EPT over the link from $u$ to $v$
$L$	bits	Packet size
$BW_{uv}$	bits/s	Bandwidth of link $u \rightarrow v$
$\beta_{uv}$	$s$	Propagation delay
$P_{fuv}$		Failure probability of the link $u \rightarrow v$

For the sake of clarity, the notations  $S_u^Q$  and  $r_{u,Q}$  shall be replaced, in the sequel, by  $S_u$  and  $r_u$  respectively, meaning that there is by default an investigation point in the space (more precisely in the radiation-sensitive area) where the power density would be calculated.

### 2.5.3 RE Intuition

The intuition behind the RE metric is twofold: *i*) allowing us to have a link metric which helps the routing algorithm preferring paths that lead to smallest radiation amount in the *hot spot* area, *ii*) taking into account data transmission time, so that we deal with radiated energy instead of radiated power.

The goal of RE metric is to therefore find the minimum electromagnetic radiated energy routes. Essentially, we want the radiation-aware metric to increase in value as the link ends are near to a specific radiation-sensitive area. Hence, the minimum-radiation path is made up of nodes that are the furthest away possible from that area.

As the power density (Equation (2.1)) decreases with the distance, we can set the radiation-aware path cost to be the sum of power densities of all hops in the path, and then the minimum radiation property is fulfilled.

However, we also want that our metric reflects the *quality* of the path. Simply adding up the hops' power densities will not ensure this property, since we could select a very *slow* link while looking for minimum power density route. In order to reflect this property, we have to combine the power density which is a node-related metric to an additional link-related term. This additional term will be the expected packet time that depends on the link bandwidth and loss rate. The concept of radiant exposure arises then when multiplying the power density by the EPT. An exhaustive evaluation will be addressed in Subsection 2.7.

## 2.6 RE Routing Properties

As we have stated in Section 1.2, the design of a new routing protocol is usually based on the specificities of its target network's nature. A substantial part of any routing protocol/algorithm is the design of appropriate routing metrics. The authors of [11] have shown that the mathematical characteristics of the routing metrics have a great effect on the good operations of routing protocols. For this reason, we analyze, in this section, our RE metric properties. We prove first, in Subsection 2.6.1, that our RE metric is additive, which is a property of utmost importance since it implies that the RE metric could fit any shortest path algorithm (e.g. Dijkstra's algorithm). Furthermore, we show, in Subsection 2.6.3, that our RE metric fulfills the two properties recommended by the authors [11]: monotonicity and isotonicity, to guarantee loop-free, consistent and optimal routing protocol.

### 2.6.1 Additivity

Note that the RE is an additive quantity. Explicitly, this implies that the cost of transmitting a packet through a path is the sum of costs of links that make up this path. To prove this property we proceed by two steps: *i*) we first prove Lemma 2.6.1, then *ii*) we conclude Theorem 2.6.2 which ensues from Lemma 2.6.1.

**Lemma 2.6.1** *The power density generated from an isotropic antenna is additive to a close corrective term.*

**Proof** Let  $u$  and  $v$  be two isotropic antennae transmitting respectively with transmit power  $P_{TX}^u$  and  $P_{TX}^v$ . Let  $dP_r$  be the total radiated power from  $u$  and  $v$  delivered to the surface element  $dS$ .  $dP_r$  is then given by:

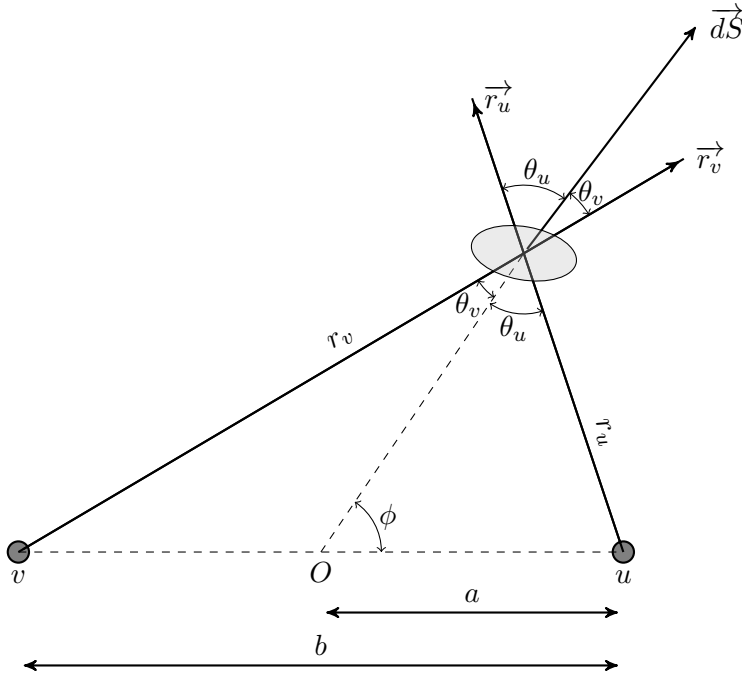


**Figure 2.2:** Illustration of the geometric parameters in Equations (2.13)–(2.20).

$$dP_r = \frac{P_{TX}^u}{4\pi r_u^3} \vec{r}_u \cdot \vec{dS} + \frac{P_{TX}^v}{4\pi r_v^3} \vec{r}_v \cdot \vec{dS} \quad (2.11)$$

$$= \left( \frac{P_{TX}^u}{4\pi r_u^2} \cos \theta_u + \frac{P_{TX}^v}{4\pi r_v^2} \cos \theta_v \right) dS \quad (2.12)$$

Based on the sine law we have Equation (2.13) and Equation (2.14). For more details, we sketch in Figure 2.2 all geometric parameters appearing in these equations.

$$\frac{a}{\sin \theta_u} = \frac{r_u}{\sin \phi} \quad (2.13)$$

$$\frac{(b-a)}{\sin \theta_v} = \frac{r_v}{\sin(\pi - \phi)} \quad (2.14)$$

Then

$$\sin \theta_u = \frac{a}{r_u} \sin \phi \quad (2.15)$$

$$\sin \theta_v = \frac{(b-a)}{r_v} \sin \phi \quad (2.16)$$

This implies that

$$\cos \theta_u = \left( 1 - \left( \frac{a}{r_u} \right)^2 \sin^2 \phi \right)^{\frac{1}{2}} \quad (2.17)$$

$$\cos \theta_v = \left( 1 - \left( \frac{b-a}{r_v} \right)^2 \sin^2 \phi \right)^{\frac{1}{2}} \quad (2.18)$$

And based on the limited development of the above formulae, we simplify them as follows:

$$\cos \theta_u = 1 - \frac{1}{2} \left( \frac{a}{r_u} \right)^2 \sin^2 \phi + o\left(\frac{1}{r_u^2}\right) \quad (2.19)$$

$$\cos \theta_v = 1 - \frac{1}{2} \left( \frac{b-a}{r_v} \right)^2 \sin^2 \phi + o\left(\frac{1}{r_v^2}\right) \quad (2.20)$$

By replacing  $\cos \theta_u$  and  $\cos \theta_v$  by their expressions (Equation (2.19) and Equation (2.20)) in Equation (2.12), we readily conclude the final expression of the total radiated power and it is given as follows:

$$dP_r = \{\xi(r_u, r_v) + \mathcal{L}(r_u, r_v, \phi)\} dS$$

Where

$$\begin{aligned}\xi(r_u, r_v) &= \frac{P_{TX}^u}{4\pi r_u^2} + \frac{P_{TX}^v}{4\pi r_v^2} \\ \mathcal{L}(r_u, r_v, \phi) &= \frac{P_{TX}^u a^2 \sin \phi}{8\pi r_u^4} + \frac{P_{TX}^v (b-a)^2 \sin \phi}{8\pi r_v^4} + o\left(\frac{1}{r_u^4}\right) + o\left(\frac{1}{r_v^4}\right)\end{aligned}$$

Note that  $\mathcal{L}(r_u, r_v, \phi)$  is the corrective term that could be neglected compared to  $\xi(r_u, r_v)$ . The final expression of the total radiated power generated from the two isotropic antennae  $u$  and  $v$  and delivered to the surface element  $dS$  is then given by:

$$dP_r \simeq \left(\frac{P_u}{4\pi r_u^2} + \frac{P_v}{4\pi r_v^2}\right).dS \quad (2.21)$$

By definition, the power density is the amount of radiated power over a surface element. So,  $\frac{dP_r}{dS}$  is the power density from both radiating sources,  $u$  and  $v$ . Then, from Equation (2.21),  $\frac{dP_r}{dS}$  is the sum of power densities of  $u$  and  $v$  (i.e.  $\frac{P_u}{4\pi r_u^2}$  and  $\frac{P_v}{4\pi r_v^2}$  respectively). Therefore, the power density radiated from two isotropic antennae is the sum of the power density generated from each of them to a close corrective term.  $\square$

We conclude then the following theorem:

**Theorem 2.6.2** *The radiant exposure as routing metric is additive.*

**Proof** Consider a node  $s$  having a packet for a node  $d$ , and this packet will be delivered through a path  $\mathcal{P}$  during an end-to-end delay  $T_{s,d}$ .

By definition, the total radiant exposure originating from all links  $u \rightarrow v$  that make up the path  $\mathcal{P}$  over a transmission time  $T_{s,d}$  is given by:

$$RE(\mathcal{P}) = \int_0^{T_{s,d}} S_{\mathcal{P}}.dt \quad (2.22)$$

Where  $S_{\mathcal{P}}$  is the total power density caused by the links that compose the path  $\mathcal{P}$ . According to Lemma 2.6.1, we have:

$$S_{\mathcal{P}} = \sum_{u \rightarrow v \in \mathcal{P}} S_{u \rightarrow v} \quad (2.23)$$

Where  $S_{u \rightarrow v}$  is the power density caused by the link  $u \rightarrow v$ . Then, from Equation (2.22) and Equation (2.23), the total radiant exposure of the path  $\mathcal{P}$  (over a transmission time  $T_{s,d}$ ) can be calculated as follows:

$$RE(\mathcal{P}) = \int_0^{T_{s,d}} \left( \sum_{u \rightarrow v \in \mathcal{P}} S_{u \rightarrow v} \right) dt \quad (2.24)$$

$$= \sum_{u \rightarrow v \in \mathcal{P}} \int_0^{T_{s,d}} S_{u \rightarrow v} dt \quad (2.25)$$

Assuming that power transmission occurs only when a packet is crossing a hop  $u \rightarrow v$ , which mean that the corresponding power density  $S_{u \rightarrow v}$  is equal to zero when  $t \notin [T_{ku}, T_{uv}]$ , where  $k$  is the immediate predecessor of  $u$  in the path  $\mathcal{P}$ .

Equation (2.25) implies then:

$$RE(\mathcal{P}) = \sum_{u \rightarrow v \in \mathcal{P}} \int_{T_{uv}} S_{u \rightarrow v} dt \quad (2.26)$$

$$= \sum_{u \rightarrow v \in \mathcal{P}} RE(u \rightarrow v) \quad (2.27)$$

Therefore, the total RE of the path  $\mathcal{P}$ , expressed in Equation (2.27), is exactly the sum the RE originating from links that make up this path.  $\square$

We can readily formulate this property in Equation (2.28), while respecting the chapter notation. Let  $\mathcal{C}(\mathcal{P})$  be the cost of the path  $\mathcal{P}$  and  $w(u \rightarrow v)$  be the cost of the link  $u \rightarrow v$  previously defined in Equation (2.10).

$$\mathcal{C}(\mathcal{P}) = \sum_{u \rightarrow v \in \mathcal{P}} w(u \rightarrow v) \quad (2.28)$$

### 2.6.2 Asymmetry

The RE asymmetry is twofold. Explicitly, the corresponding link cost (Equation (2.7)) consists of two terms. The first one,  $S_u$ , is the power density of signals stemming from the transmitter  $u$ . By definition, this quantity depends upon the distance between the radiation-sensitive area and the transmitter (Equation 2.8). As a result, power densities of both directions of a link are generally different (unless both link ends are at the same distance from the radiation-sensitive area). As an example, Figure 2.3 illustrates the difference between the cost of both directions of a Wi-Fi link.

Based on Equations (2.7) and (2.8), we have:

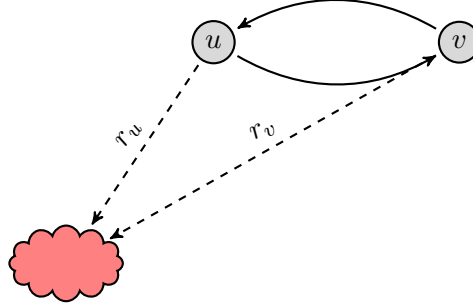


**Figure 2.3:** Different costs for both directions of the link between  $u$  and  $v$ .

$$\begin{cases} w(u \rightarrow v) = \frac{P_{TX}^u}{4\pi r_u^2} \cdot EPT_{uv} \\ \text{and} \\ w(v \rightarrow u) = \frac{P_{TX}^v}{4\pi r_v^2} \cdot EPT_{vu} \end{cases}$$

In most cases,  $u$  and  $v$  are not at the same distance from the radiation-sensitive area. Even with equal transmit powers,  $P_{TX}^u = P_{TX}^v$ , the cost of the direction  $u \rightarrow v$  is therefore different from the cost of the direction  $v \rightarrow u$ . This is expressed as follows:

$$r_u \neq r_v \Rightarrow S_u \neq S_v \Rightarrow w(u \rightarrow v) \neq w(v \rightarrow u)$$

Regarding the second term of Equation (2.7), the radiant exposure asymmetry is due to the asymmetric loss ratio. Indeed, the loss ratios in both directions of a link are likely different. That affects the percentage of packets received correctly and thus the probability that a packet would be successfully delivered (expressed by  $P_{f_{uv}}$  in Equation (2.9)). This can be expressed as follows:

$$P_{f_{uv}} \neq P_{f_{vu}} \Rightarrow EPT_{uv} \neq EPT_{vu} \Rightarrow w(u \rightarrow v) \neq w(v \rightarrow u)$$

Furthermore, receiver's noise might be different at each end of the link. In addition, for practical low-cost system, radio components are more likely different at each end of the link. For instance, although both sides might be set to use the same transmit power, manufacturing and calibration differences could be at the origin of different transmit powers. Consequently, this asymmetry in transmit powers affects data rates of both directions ( $(u \rightarrow v)$  and  $(v \rightarrow u)$  in the example of Figure 2.3), and then it affects the expected packet time according to Equation (2.9). This can

be expressed as follows:

$$P_{TX}^u \neq P_{TX}^v \Rightarrow BW_{uv} \neq BW_{vu} \Rightarrow w(u \rightarrow v) \neq w(v \rightarrow u)$$

Henceforth, when we talk about a link we implicitly mean the directed link from one end to another.

### 2.6.3 Isotonicity & Monotonicity

Following the routing algebra formalism in [10] and [11], authors have analytically proved that routing metrics have to hold the isotonicity and monotonicity properties in order to fulfill routing requirements: optimality, consistency and loop free-freeness. Explicitly, left and right monotonicity means that the path cost does not decrease when it is respectively prefixed or suffixed by another path or simply another link. Whereas, left and right isotonicity means that the relationship between the costs of two paths from the same source node holds when both paths are respectively prefixed and suffixed by a common third path or link. This being said, any additive routing metric is by definition monotonic and isotonic.

According to Yang and Wang [11], routing protocol convergence and loop-freeness are ensured when the routing metric is monotonic. Similarly, the isotonicity is a necessary and sufficient condition for convergence to optimal paths.

We have analytically proved that the RE metric is additive (see Section 2.6.1). Consequently, RE is monotonic and isotonic. We can therefore conclude that the RE metric can fit any Path Calculation Algorithm and Packet Forwarding Scheme reviewed in [11], and more specifically Dijkstra's algorithm in conjunction with hop-by-hop routing.

Note that the monotonicity and isotonicity issues turn out more critical for the multi-criteria routing algorithm discussed in Chapter 5.

## 2.7 RE Qualitative Evaluation

### 2.7.1 Interpretations

There are two possible ways to interpret the expression in Equation (2.7). First, since we are dealing with a physical phenomenon (i.e. electromagnetic radiation) it would be timely to mention the physical interpretation of the RE metric. Basically, keeping or removing the second term (i.e. EPT) is what actually makes the difference

between radiated energy and radiated power. If we set the routing metric to be merely the power density, we will evaluate in this case an instantaneous value which reflects only the intensity of radiated field over an area. Nevertheless, waves are spread out in space and time. So, by integrating the power density over time, the radiant exposure measures the effective amount of energy delivered per unit area in a specific time interval of interest.

Second, we can view Equation (2.7) as a tradeoff between radiated power and throughput. Interestingly, the RE of a link  $u \rightarrow v$  can be viewed as the radiation generated from the node  $u$ , weighted by the link delay. Accordingly, the slower a link is, the higher is its radiation level.

A last observation about the RE formulation is that the first term,  $S_u$ , can be seen as a node-related metric since according to its expression in Equation (2.8), the power density depends solely upon node  $u$  parameters. This been said, all outgoing links from node  $u$  will have the same value. As to the second term, it is obvious that the expected packet time is a link-related metric since it depends on the link *quality*.

### 2.7.2 Impact of Distance from Radiating Source

The power density decreases exponentially as function of  $\frac{1}{r^2}$  (Equation (2.8)), it is then worth to determine how far from the radiating source the radiant exposure remains significant. To do so, we sketch in Figure 2.4 the variation of the radiant exposure (Equation (2.10)) as function of distance from the radiation source, and for different IEEE 802.11n modulation schemes. We set the following values for the RE formula (2.10) parameters:

- Transmit power:  $P_{TX} = 100mW (= 20dB)$
- Packet size:  $p = 1500$  bytes
- Transmission failure probability:  $P_f = 10\%$
- Data rates for 802.11n modulation schemes for two spatial streams are given in the Table 2.3

As shown in Figure 2.4, time average of radiated emissions expressed by the radiant exposure quantity is larger at distances below  $10m$ , but cannot be neglected even for farther distances. Figure 2.4 clearly demonstrates as well the effect of the increasing distance between transmitter and receiver reflected by the increasing expected time to deliver a packet.

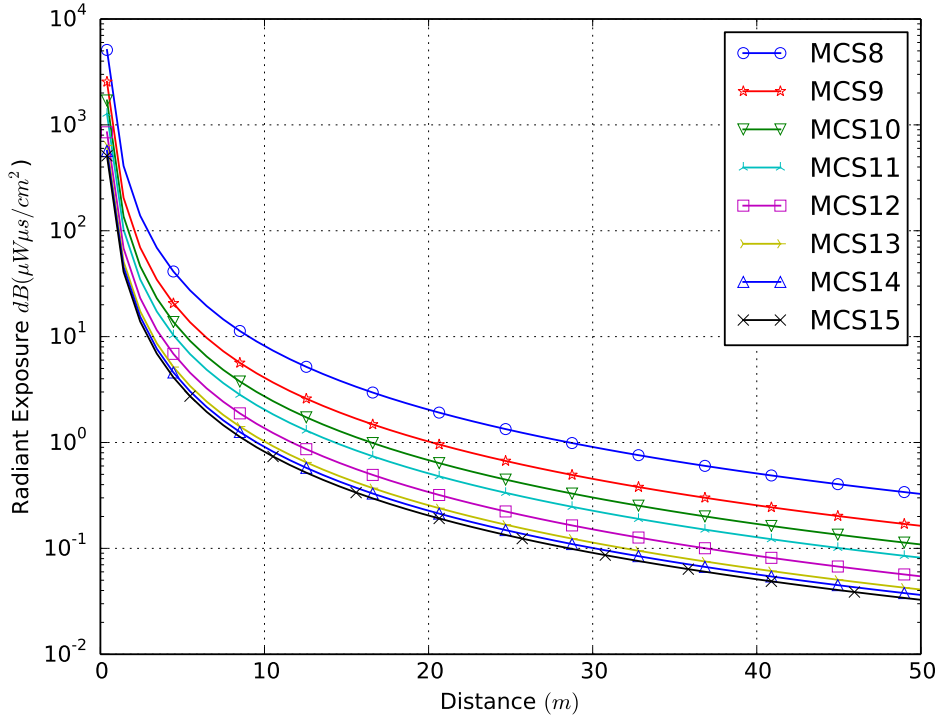


**Figure 2.4:** Radiant Exposure versus distance from radiating source for different modulation schemes of IEEE 802.11n

Table 2.3: Data rates for 802.11n modulation schemes [5]

MCSs index	Modulation	Code rate	Data rate (Mbps)
8	BPSK	1/2	13
9	QPSK	1/2	26
10	QPSK	3/4	39
11	16-QAM	1/2	52
12	16-QAM	3/4	78
13	64-QAM	2/3	104
14	64-QAM	3/4	117
14	64-QAM	5/6	130

### 2.7.3 Impact of Link Capacity

We show here the impact of the link capacity expressed by the distance between transmitter and receiver. For our analysis, we move the receiver away from the transmitter so as to degrade the link quality, namely the throughput. Subsequently, and based on Equation (2.10) we calculate the radiant exposure value to successively

deliver a packet of size 1024 bytes from one node to another and depict results in Figure 2.5.

NS3 incorporates a detailed MAC and physical layer implementation of IEEE 802.11n standard. We have implemented the path loss model presented in Subsection 2.4.2.3. We have used a constant bit rate UDP-based traffic with a sending rate of 23 Mbps. We have measured the average time of a 1024 bytes packet based on the model presented in Subsection 4.3.4. In Figure 2.5, the X-axis indicates the distance between the transmitter and the receiver (1-hop link), as to Y-axis shows the calculated radiant exposure corresponding to 1024 bytes packet. We show results for different distance from the radiation-sensitive area: 0.5m, 1m, 5m and 10m.

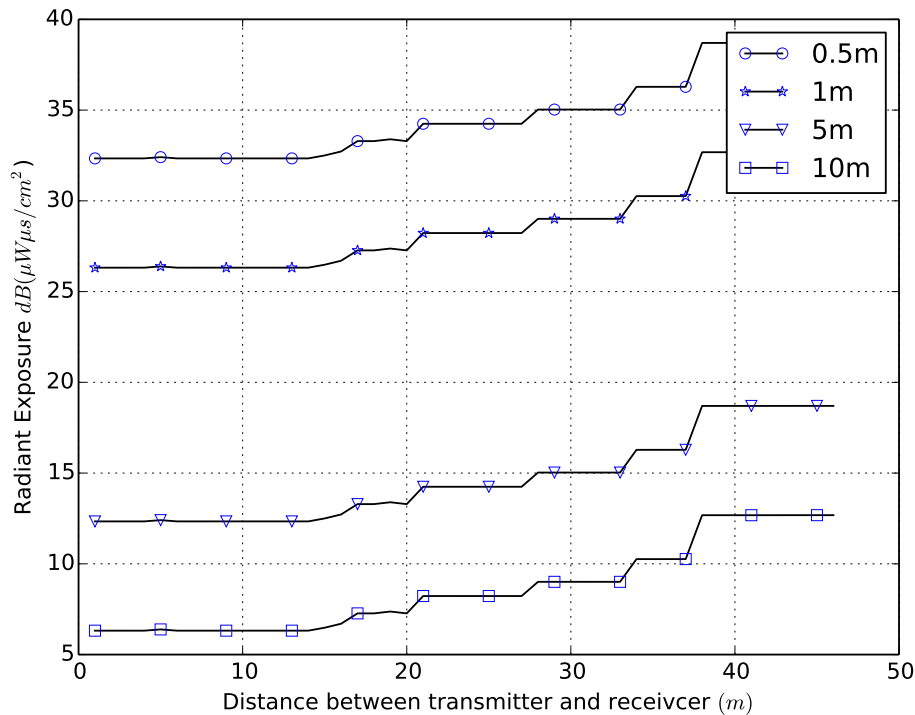


**Figure 2.5:** Radiant Exposure versus an IEEE 802.11n link capacity expressed by distance between transmitter and receiver for different distance from the radiation-sensitive area.

Basically, the further the receiver from the transmitter is the higher is the transmission duration and therefore the higher is the radiated energy. Indeed, as the receiver moves farther from the transmitter, owing to the path loss attenuation the received signal power level declines gradually, which forces the communication link to pick *less complicated* modulation to operate at successively lower data rates, and

as a consequence longer packet times. This in turn leads to more radiated energy expressed by the increasing trend of the radiant exposure metric with lower link capacity.

## 2.8 Model Inaccuracies

The premise behind the model detailed above, is to find a single value for each Wi-Fi link that characterizes radiated emissions during data transmission time. Subsequently, this value is used to design a radiation-aware routing metric for Wi-Fi links. To do so, we have assumed a set of simplifying assumptions leading to some model inaccuracies.

Indeed, we have assumed that Wi-Fi antennae are isotropic. However, almost all Wi-Fi antennae are half wave dipoles, which mean that they are omnidirectional. An isotropic antenna radiates equally in all directions, horizontally and vertically whereas an omnidirectional antenna radiates equally in all horizontal directions. The radiation pattern of the former would be a sphere and of the latter would be a torus (donut-shaped). Specifically, the power density in omnidirectional antenna case is as follows [73]:

$$S_{half-wave} = \frac{EIRP}{4\pi r^2} F(\theta, \phi) = \frac{G_{max} P_{TX}}{4\pi r^2} F(\theta, \phi)$$

Where:

- $S_{half-wave}$  is the plane-wave power density ( $Wm^{-2}$ ) of a half wave dipole in a given direction
- $S_{isotropic}$  is the power density ( $Wm^{-2}$ ) of an isotropic antenna
- $EIRP$  is the equivalent isotropically radiated power ( $W$ )
- $r$  is the distance (m) from the radiation source
- $P_{TX}$  is the transmit power ( $W$ )
- $G_{max}$  is the maximum gain of the transmitting antenna, in the case of half wave antenna,  $G_{max} = 1.64$
- $F(\theta, \phi)$  is the antenna numeric gain (normalized gain),  $\phi$ - azimuth angle,  $\theta$ - zenith angle.

We express the error relatively to the power density of an isotropic antenna. The error is then given as follows:

$$\begin{aligned}
Error &= \frac{S_{half-wave} - S_{isotropic}}{P_{isotropic}} \\
&= \frac{\frac{G_{max} P_{TX}}{4\pi r^2} F(\theta, \phi) - \frac{P_{TX}}{4\pi r^2}}{\frac{P_{TX}}{4\pi r^2}} \\
&= G_{max} F(\theta, \phi) - 1
\end{aligned}$$

The normalized gain of a half wave antenna (omnidirectional) is given by [73]:

$$F(\theta, \phi) = \left[ \frac{\cos(\frac{\pi}{2} \cos(\theta))}{\sin(\theta)} \right]^2$$

Therefore, the final expression of the error becomes as follows:

$$Error = 1.64 \left[ \frac{\cos(\frac{\pi}{2} \cos(\theta))}{\sin(\theta)} \right]^2 - 1; \quad \theta \in [0, \pi] \quad (2.29)$$

According to the power density error expression (Equation (2.29)), we can readily notice that the probability that the power density of the isotropic antenna exceeds the power density of a real omnidirectional antenna (i.e.  $Error \leq 0$ ) is almost 63%. The assumption of an isotropic antenna (see section 2.4.1) holds appropriate since we are considering the worst case of radiation for most positions.

Note that this error can reach a maximum value of  $-1$  for the vertical direction along the antenna (i.e.  $\theta = 0, \pi$ ). As expected, since the radiation of the half wave antenna drops off as we approach the vertical direction, unlike radiation from an isotropic antenna that in turn remains the same even along the antenna.

Finally, although the isotropic antenna concept exists only in theory, it guarantees a good approximation while simplifying substantially radiation model design.

We have assumed in our model that radiation could stem exclusively from transmitters' antennae. However, at reception, antennas are also radiating, but with much lower levels in the range of  $pW$  to  $nW$ .

## 2.9 Summary

In this chapter we have first discussed some issues related to modeling electromagnetic radiation originating from Wi-Fi devices. We have as well briefly presented a set of methods used in practice for this purpose.

Finding a single value for each Wi-Fi link that characterizes the contribution of its endpoints to the cumulative radiated energy, was not an a straightforward task. We had to consider a set of simplifying assumptions. This lead to the formulation of a radiation-aware routing metric that we call Radiant Exposure and formulated as follows (see Subsection 2.5.2) :

$$w(u \rightarrow v) = \frac{P_{TX}^u}{4\pi r_u^2} \cdot \left( \frac{L}{BW_{uv}} + \beta_{uv} \right) \left( \frac{1}{1 - P_{f_{uv}}} \right)$$

We have then studied four of our metric properties: additivity, asymmetry, isotonicity and monotonicity that could influence the routing protocol performances. Furthermore, we have derived a qualitative evaluation of our metric, first by interpreting the different trade-offs and second by showing the impact of the two main parameters: distance from the radiation-sensitive area and the link bandwidth.

Finally, we have discussed some inaccuracies of our radiation model, and showed that although some assumptions are theoretical, they can meet our requirements.



# Modeling EMFs from Power Line Communication (PLC)

## 3.1 Introduction

Power Line Communication (PLC) has emerged and became more and more attractive in the last few years given the low installation cost. The home network is the best environment to benefit from the advantages of this technology, thanks to the availability of an existing electrical wires. This technological improvement does not come for free. In fact, using a channel designed originally for other purposes means that it is not optimized for the frequencies and applications of interest for broadband transmission. So that some concerns about emissions could arise. Indeed, communication signals are lost as radiation emissions while traveling over power lines at high frequencies.

Hence, this chapter seeks to model such electromagnetic fields generated from power lines while carrying data at high frequencies. We study in the scope of this chapter only the indoor segment. Then, before describing the radiated fields model and formulating the radiation-aware routing metric, we justify our method choice and show the different existing in-home wiring topologies. At the end of the chapter, we show radiated energy cartography for different topologies and finally we discuss some model inaccuracies.

PLC shall mean throughout this chapter power lines that carry communication signals at high frequencies.

## 3.2 Fundamentals of PLC Technology

### 3.2.1 Operating Principle

#### 3.2.1.1 Physical Medium

PLC technology works by coupling to the existing electrical phase a modulated signal that could occupy the extended frequency band 2 – 100MHz according to the specifications IEEE 1901 [31]. Hence, the PLC technology uses the power network as a support medium.

#### 3.2.1.2 Channel Characterization

Power lines were not initially designed to propagate broadband communication signals, so that they were never intended for carrying data at frequencies above 1kHz. As a result, the communication channel does not ease propagation. Indoor channel modeling represents therefore one of the most interesting challenges in PLC systems, from engineering point of view. There are several reasons for this and we mention hereafter few of them. The characteristic impedance of a power line displays a high variability in the MHz region; numerous reflections of the High Frequency (HF) signals are therefore caused by such impedance discontinuity of in-home cables [78]. The result is multi-path signal propagation with frequency selective fading [79]. In addition, the propagating signals are affected by attenuation increasing with length and frequency leading to a limited channel capacity. A better understanding of this channel characteristics and the determination of the most influencing parameters allow the optimization of the PHY layer and the maximization of the data rate.

A number of approaches for the PLC transmission channel characteristics and noise scenarios have been studied [80, 81, 82]. In [80], PLC channel model has been derived from multipath propagation behavior. There have also been attempts to statistically characterize the PLC channel [81, 82, 83]. Moreover, more sophisticated proposals have been implemented into simulators [84, 82, 85]. We will rely on these characterization models to calculate the throughput for simulations in the following chapters.

In summary, the purpose of most channel characterization work is to model the signal propagation along the power line and do not take into account the signals' dissipation through those lines which cause radiated emissions in their surroundings.

### 3.2.2 EMFs Related Features

#### 3.2.2.1 EMFs Issues Related to PLC

The in-home electromagnetic emissions do not emanates solely from radio devices, but also involuntarily from power lines. Clearly, the particularity of PLC technology is that power lines were initially designed and optimized for power transmission at frequencies of  $50/60Hz$  so they represent a hostile medium for transmission at higher frequencies. Hence, when superimposing a higher frequency signal over the existing electrical circuit, signal is lost through electromagnetic radiation [86].

The source of these emissions is the differential and the common mode currents. The data signals injected by PLC modems are differential mode signals. The differential mode contributes very poorly to the radiated emissions. As to the common mode is the main radiator, since it is characterized by currents in each of the conductors being in phase [87].

Clearly, ElectroMagnetic Compatibility (EMC) is an important and non-trivial item for the development and operation of PLC systems. Furthermore, the radiated emissions represent only one aspect of the EMC considerations.

#### 3.2.2.2 Standardization Context

In order to ensure the coexistence of communication systems and standardize products, companies have created PLC standards in the framework of, for instance, the HomePlug PowerLine Alliance or the Universal Power Line Association. Since PLC devices are seen as Information Technology Equipment (ITE), they have therefore to comply with the current standard of International Special Committee on Radio Interference (CISPR) [88] pertaining to radio-electric interferences.

Limits and methods of measurement with respect to EMC of ITEs are exhaustively described in [88].

Although the currently used PLC frequency range is below 30MHz, upcoming standards plan to extend this band. It was already proposed in the standard IEEE 1901 [31] the use of an optional band from 30MHz to 50MHz, also the technology HomeplugAV2 [89] uses additional frequency spectrum from  $30MHz$  to  $86MHz$  beyond frequencies used previously by HomePlug AV [89]. Hence, limits related to frequencies upper to 30MHz are shown in the Table 3.1.

Table 3.1: Limits of radiated emissions at a distance of 10m

Frequency Range	Requirement
30 MHz to 230 MHz	30 dB $\mu$ V/m
230 MHz to 1000 MHz	37 dB $\mu$ V/m

### 3.3 Modeling EMFs from a PLC Link

#### 3.3.1 EMFs Modeling Issues

The way electromagnetic radiation actually occurs in PLC networks is currently partially understood, in part given the vast variety of network types and configurations, which has made it complicated to extract the fundamental influencing factors, and in other part, given the strong variability of the impedance and attenuation characteristics in the MHz region used for broadband PLC. Thus, the understanding of PLC-related electromagnetic emissions characterization is a tedious issue. We try to summarize herein the most important issues that underlie the assessment of EMF from PLC:

- High variability of networks types and configurations;
- High variability of electrical load from one home to another and for different times of the day;
- Strong variation of network characteristics (power lines impedance and attenuation) as functions of time since new appliances can be plugged in and out or turned on and off at any time and they present, in the general case, nonlinear impedance to the network;
- Lack of consensus on an exact definition of measuring methods;
- PLC regulation affects many sectors: electricity, telecommunication and electromagnetic compatibility;
- Electromagnetic context is closely linked to the existing tools of radiation modeling. Such tools, however, are highly dependent on propagation area: close or far from radiation source;

#### 3.3.2 Introduction to Different Modeling Methods

Attempts to analytically model EMFs or also to use numerical tools in order to estimate the radiation due to data transmission in power networks have been performed in several countries and relying on different methods [67, 70]. Investigating

the power lines radiation could be conventionally carried out by applying four families of methods:

1. Circuit theory
2. Transmission line theory
3. Formal solutions of Maxwell equations
4. Antenna theory

### **Circuit Theory**

In this approach, voltages and currents are calculated using lumped circuit elements such as resistances, inductances and capacitances. Propagation phenomena are not considered, since this method assumes that the wavelengths of signals injected over the electrical line are much longer than the length of this line. For instance, for a frequency of 30 MHz, this method can be applied for power lines whose dimensions do not exceed 1m (ten times smaller than the wavelength) which is not necessarily the case for indoor PLC systems. Therefore, the application of the circuit theory appears to be unsuitable for too expanded configurations, PLC systems in particular.

### **Transmission Line Approach**

One of the basic assumptions of the Transmission Line (TL) theory is that the cross sectional dimension is small enough to neglect all propagations except those occurring along the line axis [90]. As a result, line transmission theory is ideally suited to the 'transmission line mode' (differential-mode) electric current assumption but not necessarily in line with the EMC behaviors because it does not assume the common-mode (also so-called 'antenna-mode') current distribution which is the primary source of radiation. Although the differential mode is responsible for part of the radiation, the common mode can be designated as the main culprit when it comes to emissions from PLC networks [87, 91]. Besides, the TL theorem is leading to roughly determine the induced voltages and currents at any point of the line, however the resolution of the equations system mandates the knowledge of the excitation and the end loads, meaning the knowledge of impedance and linear admittance matrices of each line, which is onerous to calculate (given the high variability of such parameters in the context of home environment).

### **Full-Wave Approaches**

Generally, all numerical tools that have been developed to model the electromagnetic issues, typically aspire to resolve Maxwell equations in frequency or time domain. We

mention for instance the Finite Element Method (FEM), the FDTD, the MoM and many others that have each their own advantages and specified applications. These methods are actually implemented in many commercial packages such as Numerical Electromagnetics Code (NEC) [92] or Computer Simulation Technology (CST) [93]. However, it turns out that using such software to treat expanded geometrical configurations (e.g. PLC systems) requires experience in electromagnetism and very detailed input data together with huge computer resources.

### Antenna Theory

The goal of this theory is to decompose a linear power line into elementary segments and then assume that each section is a radiating source. According to the superposition principle, the electric and magnetic field vectors can be therefore calculated at any point in the space, by summing up electric and magnetic field vectors originating from each elementary segment. This applies only under the assumption of thin lines, which means that the conductor radius can be neglected compared to signals wavelength propagating through that cable.

The EMC issues are still the main and the unique motivation of all the previously mentioned methods. All these tools aim to assess, measure and model the induced currents and voltages which are at the origin of the radiation. A complementary method is then needed to estimate the radiated energy at a given point in the space (more likely in the far region).

When it comes to electromagnetic emissions from PLC systems, the common-mode current is the main culprit. Antenna theory is the unique tool to take this current in consideration. This need is perfectly justified in the particular case of PLC systems where the radiation can mainly come from the common mode current due to the proximity of the conductors carrying data signals from each other. Finally, given that a highest accuracy is not of our goals, we will rely on the antenna theory in order to model radiated emissions from PLC systems.

### 3.3.3 EMFs' Model for a PLC link

#### 3.3.3.1 Simplified Approach

For most electric linear systems such as PLC, the electromagnetic field strength at any given point in the space is linearly proportional to the power level of the injected PLC signal. Meaning that the relation between the radiated energy (and the electromagnetic field) and the input signal can be expressed as a frequency dependent factor. For a given network and at a given point in the space, this factor

could be measured. Nevertheless, it has been experimentally observed that it varies remarkably from one configuration to another [67]. As a conclusion, we cannot rely on measurement methods to calculate radiated field at a given point of the power line surrounding.

We do not aim herein to thoroughly calculate the radiated field generated by power lines while carrying data at high frequencies, the issue is much more complicated, but the goal is to find a simple and basic mathematical model that provides one single value characterizing the radiated energy for each virtual PLC link, in other words, to formulate a radiation-aware additive routing metric<sup>1</sup>.

As previously mentioned, the calculation of the radiated field emanating from an electric system requires the identification of the currents distribution of this system. The traditional numerical methods mandate very fine mesh of the propagation medium, the surrounding space or both.

Thus, the calculation of the electromagnetic fields involves two steps:

- the estimation of the currents and
- the use of the currents for the computation of the associated electromagnetic fields.

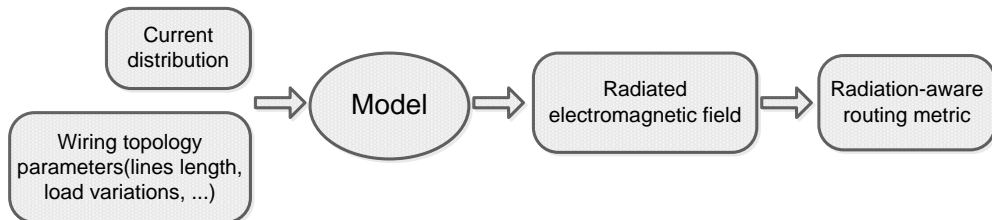


**Figure 3.1:** Block diagram of modeling procedure

In the following study, we consider that this resolution is accomplished and the current distribution is known.

The block diagram depicted in Figure 3.1 shows the procedure of evaluating electromagnetic fields and then formulating the radiation-aware routing metric.

<sup>1</sup>We mean by virtual PLC link, a link between two network nodes which is not necessarily linear and may be composed by multiple segments

### 3.3.3.2 Introduction to In-Home Wiring Topologies

It has been proved in [67] that common-mode current, which is the main source of radiation, is a strong function of the wiring topology. The topology of in-house PLC systems is less homogeneous than the outdoor Low-Voltage (LV) network making the channel behavior more unpredictable. Moreover, the electrical topology of a single home is complex because of the multitude of branches of wires, which vary in length, change direction and have different electric load attached to them. The radiation can thus be expected to vary from a house to another, even in the same neighborhood. Tree-like and star-like configurations are almost universally used in most countries. Devices are fed from the service panel by means of several branch circuits that reach the outlets in a non-specified manner, as depicted in Figure 3.2. In most cases, the layout of such circuits, the number of wires in each branch and their lengths are unknown. Moreover, there are devices with quite different characteristics that influence the end charges and then the current as a time function.

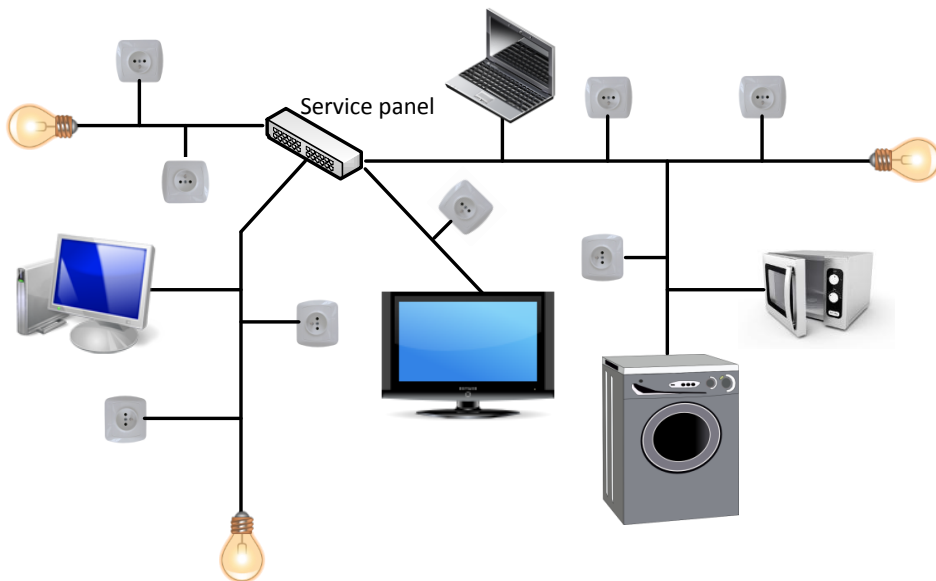


**Figure 3.2:** An example of in-home PLC network

For tackling the aforementioned constraints, it is crucial to make some assumptions in order to yield a basic in-home wiring topology schematic. Literature abounds with bottom-up modeling solutions that for defining the channel behavior, they start from the physical network features and above all the in-home wiring topology [94, 84, 95]

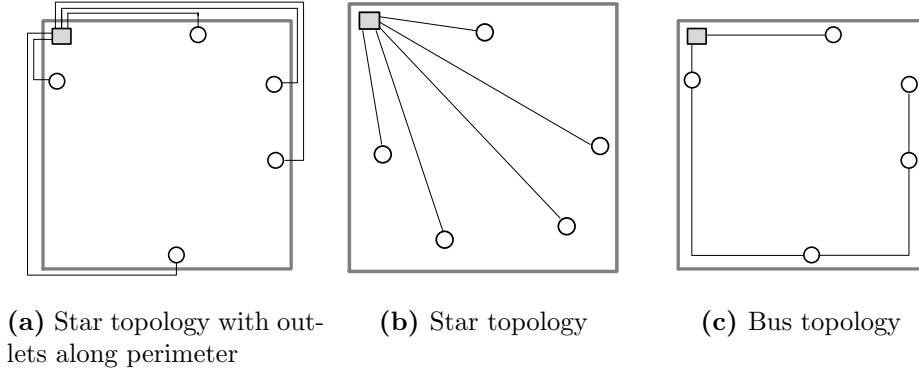


**Figure 3.3:** Three most conventional in-home wiring topologies

The authors in [94] state that it can be seen from the analysis of the European norms and wiring practices that the in-home wiring deployment could be regular and structured. Furthermore, they proposed a random indoor wiring topology generator derived from the observations of regulations and common practices in real scenarios. Each generated wiring infrastructure fulfills some rules. First, the number of outlets inside each room is a Poisson variable, in other words outlets are placed according to a Poisson arrival process, and then they are uniformly distributed along the area perimeter, which is the most conceivable configuration. Secondly, they distinguished the three most usual practices that outlets can be connected according to them, namely star structure that fulfills the minimum distance between outlets and the root (derivation box) (Figure 3.3b), a star topology with outlets placed along the sides only (Figure 3.3a), and finally a bus topology (Figure 3.3c).

### 3.3.3.3 Electric Current Distribution

The imperfect symmetry of indoor power grid leads to conversion of the desired symmetric (differential mode) signals into asymmetric (common mode) signals. It has been proved that the common-mode current is the main cause of radiated emissions at distances larger than 1 meter [87]. In particular, common-mode currents of noticeably less magnitude than differential-mode currents can have the same or often higher level of radiated fields associated to them. So, a particular attention should be paid to this mode in order to predict the way electromagnetic waves radiate from PLC systems. Seeking for further simplicity, we assume solely the contribution of the common-mode currents.

Depending on the current distribution, waves are either standing or traveling. And according to line transmission theory, electric current distribution can be one

or the other of the following distributions:

- Sinusoidal variation of the current amplitude along the power line implies standing waves;
- Constant or exponentially decreasing amplitude along the power line implies traveling waves.

We assume in the sequel that it is hypothesized:

- A power is not loaded in the extremity;
- An alternating electric current.

The current formula used hereafter is given by:

$$I(z) = I_{max} \sin(k(\frac{L}{2} - |z|)) \quad (3.1)$$

### 3.3.3.4 Radiated Emissions from a Power Line Using Antenna Theory

The antenna theory is built upon the extrapolation of the obtained results for a radiating dipole in order to find the radiated electromagnetic components from a power line (seen as wire antenna).

We assume first that a power line is thin enough that its radius is much lower than the smallest wavelength in the frequency range. This assumption is verified for the PLC frequency range from 2MHz to 100 MHz.

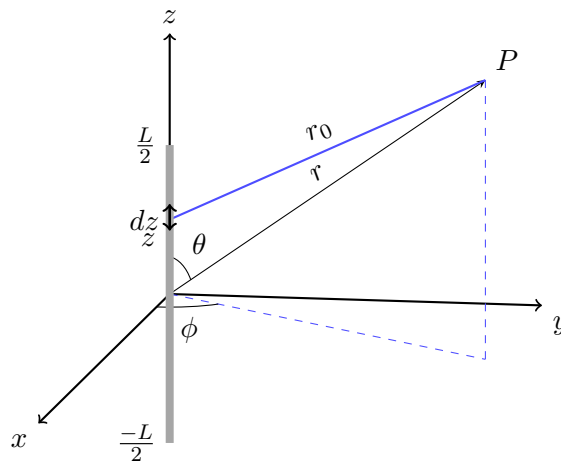


**Figure 3.4:** Illustration of antenna theory applied for linear PLC line

An electric line is herein seen as the juxtaposition of elementary dipoles, in such way that the total electric field is obtained by integrating the elementary fields. Explicitly, the power line of length,  $L$ , through which the current,  $I(z)$  flows, is positioned on the  $z$  axis of the coordinate system  $(x, y, z)$  as depicted in Figure 3.4. Clearly, the radiated electromagnetic components from an infinitesimal dipole have been described in most antenna books, and we can basically state that the electric and magnetic field radiated by a small dipole,  $dz$ , in the different space regions depend upon the current in that dipole,  $I(z)$ , the electric field is given by:

$$\begin{cases} dE_r = \frac{I(z)e^{-jkr}}{4\pi} \left( \frac{2\eta_0}{r^2} + \frac{2}{j\omega\epsilon r^3} \right) \cos(\theta) dz \\ dE_\theta = \frac{I(z)e^{-jkr}}{4\pi} \left( \frac{j\omega\mu}{r} + \frac{\eta_0}{r^2} + \frac{1}{j\omega\epsilon r^3} \right) \sin(\theta) dz \\ dE_\varphi = 0 \end{cases}$$

Where  $\eta_0 = \sqrt{\frac{\mu}{\epsilon}}$  is the air impedance and  $k = \frac{2\pi}{\lambda}$ . And regarding magnetic field:

$$dH = dH_\varphi = \frac{I(z)}{4\pi} \left( jk + \frac{1}{r} \right) \frac{e^{-jkr}}{r} \sin(\theta) dz$$

For the frequency range  $[2MHz, 100MHz]$ , wavelength varies from  $150m$  to  $3m$ . Within a home environment, we would need to estimate radiation for distances far from the power line varying from some centimeters to a dozen meters. Hence, the far zone assumption does not hold for all frequencies. It would then be timely to simplify field expressions according to propagation regions (close and far):

**Immediate proximity zone:**  $r \ll \lambda$

$$\begin{aligned} \vec{dE} : dE_r &= \frac{I(z)\eta_0 e^{-jkr}}{2\pi jkr^3} \cos(\theta) dz \\ dE_\theta &= \frac{I(z)\eta_0 e^{-jkr}}{4\pi jkr^3} \sin(\theta) dz \end{aligned} \quad (3.2)$$

$$\vec{dH} : dH_\varphi = \frac{I(z)e^{-jkr}}{4\pi r^2} \sin(\theta) dz \quad (3.3)$$

**Far zone:**  $r \gg \lambda$

$$\vec{dE} : dE_\theta = \frac{jk\eta_0 I(z)}{4\pi r} e^{-jkr} \sin(\theta) dz \quad (3.4)$$

$$\vec{dH} : dH_\varphi = \frac{jkI(z)}{4\pi r} e^{-jkr} \sin(\theta) dz \quad (3.5)$$

Interestingly, from Equations (3.2) and (3.3), we note that the electric and the magnetic fields expressions within the close zone are generated from electrostatics. In other words, since  $\vec{E}$  and  $\vec{H}$  are in quadrature-phase within the close region, there is no active energy exchange between the dipole and the space (only reactive energy), which means that there is no radiation in the near region; it should be stressed that we can therefore assume electromagnetic radiation calculation in the far zone only, meaning only equations (3.4) and (3.5).

We can readily generalize the expression of the total electric field radiated from a power line of length,  $L$ , is given by integrating between  $-\frac{L}{2}$  and  $\frac{L}{2}$  the electric field created by a dipole of length  $dz$  expressed in Equation (3.4). The electric field is then given by Equation (3.6):

$$\begin{aligned} \vec{E} &= \int_{-\frac{L}{2}}^{\frac{L}{2}} dE_\theta \vec{e}_\theta \\ \vec{E} &= \left( \frac{jk30}{r} e^{jkr} \sin \theta \int_{-\frac{L}{2}}^{\frac{L}{2}} I(z) e^{jkz \cos \theta} dz \right) \vec{e}_\theta \end{aligned} \quad (3.6)$$

According to the general equation (3.6), it appears that radiated field and current are closely tied. Then, to calculate the total electric field radiated from a power line, we need the corresponding current distribution that will affect as well the radiated power. Using the current expression given in equation (3.1) we have developed calculation of Equation (3.6), then electric field generated by a power line of length,  $L$ , and radiated at the point at a distance  $r$ , from the line middle is given as follows:

$$E = j60I_{max} \left\{ \frac{\cos(k\frac{L}{2} \cos \theta) - \cos(k\frac{L}{2})}{\sin \theta} \right\} \frac{e^{jkr}}{r} \quad (3.7)$$

To design a routing metric that can fit any shortest path algorithm, we need an additive physical quantity. It has been proved in the Theorem 2.6.2 in Chapter 2 that the Radiant Exposure is additive. We need now to develop the expression of the total radiated power for the case of PLC links. By definition, the total radiated power is determined by integrating the Poynting vector over a closed surface,  $S$ , of

a sphere of radius  $r$ . the conventional expression is given by:

$$P_r = \frac{1}{2} \text{Re} \left( \oint_S \vec{E} \wedge \vec{H} \cdot d\vec{S} \right) = \frac{1}{2} \oint_S \frac{|E|^2}{\eta_0} dS \quad (3.8)$$

Then, from equations (3.7) and (3.8), we can readily conclude the total radiated power from a linear power line of length  $L$ :

$$\begin{aligned} P_r &= \frac{1}{2} \left( \int_0^{2\pi} \int_0^\pi \frac{|E|^2}{\eta_0} r^2 \sin\theta d\theta d\varphi \right) \\ &= 30 I_{max}^2 \Upsilon \end{aligned}$$

Where

$$\Upsilon = \int_0^\pi \frac{\left\{ \cos\left(k\frac{L}{2}\cos(\theta)\right) - \cos\left(k\frac{L}{2}\right) \right\}^2}{\sin\theta} d\theta \quad (3.9)$$

The main objective of our work is to reduce the level of electromagnetic radiation within a specific area and not to give exact values of this level. Our goal is then not to have a very fine degree of accuracy, this is why we choose to approximate the integral  $\Upsilon$  (Equation (3.9)) using one of the most basic method among the interpolating functions, namely the midpoint method or the rectangle method.

The rectangle method consists of letting the interpolating function to be a constant function (a polynomial of degree zero) which passes through the point  $\left(\frac{a+b}{2}, f\left(\frac{a+b}{2}\right)\right)$ . Hence, the integral of a given function can be approximated as follows:

$$\int_a^b f(x) dx \approx (b-a) f\left(\frac{a+b}{2}\right) \quad (3.10)$$

The integral  $\Upsilon$  can therefore be calculated as follow:

$$\Upsilon \approx \pi \left(1 - \cos\left(k\frac{L}{2}\right)\right)^2 \implies P_r = 30\pi I_{max}^2 \left(1 - \cos\left(\pi\frac{L}{\lambda}\right)\right)^2$$

For this integrated function,  $f(x) = \frac{\left\{ \cos\left(k\frac{L}{2}\cos(x)\right) - \cos\left(k\frac{L}{2}\right) \right\}^2}{\sin(x)}$ , the midpoint coincides with its maximum, meaning that we are considering the worst case when

the radiated energy reaches its maximum level in all space directions. Such approximation shall certainly overestimate radiation evaluation, but it is of less importance, given that, as already mentioned, our goal is to select one path from several alternatives that minimize the level of radiation expressed hereafter by the RE quantity.

For this model, it is assumed that the power line radiates equally in all space directions. We can then calculate the power density by dividing the total radiated power by the sphere surface,  $4\pi r^2$  :

$$S = 7.5 \frac{I_{max}^2}{r^2} \left( 1 - \cos\left(\pi \frac{L}{\lambda}\right) \right)^2 \quad (3.11)$$

All parameters are depicted in Figure 3.4 and summarized in the Table 3.2.

Table 3.2: Electric and magnetic quantities and corresponding SI units.

Symbol	Unit	Quantity
$E$	$V.m^{-1}$	Electric field strength
$H$	$A.m^{-1}$	Magnetic field strength
$P_r$	$W$	Radiated power
$S$	$W.m^{-2}$	Power density
$I(z)$	$A$	Electric current at the point $z$ through the power line
$I_{max}$	$A$	Maximum electric current through a power line
$k$	$m^{-1}$	Wave number
$\lambda$	$m$	Wave length
$w$	$rad.s^{-1}$	Angular frequency
$\epsilon$	$F.m^{-1}$	Air permittivity
$\mu$	$H.m^{-1}$	Air magnetic permeability
$\eta_0$	$\Omega$	Air impedance
$r$	$m$	Distance between the middle of the power line and the investigation point $P$
$L$	$m$	Length of the power line

### 3.3.3.5 Formulation of the RE metric for a PLC Link

It is recalled here, as stated in Chapter 2, that we rely on the RE definition to design our radiation-aware routing metric for PLC links. The same issue pertaining to Wi-Fi links has been exhaustively treated in Subsection 2.5.2. Explicitly, the radiant exposure is a time integral of the power density  $S(Wm^{-2})$ , and has units of joule per square meters  $Jm^{-2}$ . A straightforward radiant exposure,  $H$ , formula is given by:  $S.t$ , where  $S$  is the power density usually in  $Wm^{-2}$  and  $t$  is the exposure time in seconds. As already mentioned in previous chapters, the premise behind using such physical quality is to assess the accumulated amount of radiated energy during data transmission within a given area rather than using instantaneous values. Power

line adapter plugs are used to connect a device to the network. These adapters have usually one end into device's Ethernet interface and the other end into an electric wall outlet. In real installation, power lines are usually laid over walls (see Figure 3.5). Consequently, the virtual link ( $u \rightarrow v$ ) (sketched by dashed line in Figure 3.5) is more often not straight, it is instead composed of several branches of conductors.

Consequently, we define the weight of the PLC link,  $w(u \rightarrow v)$ , to be the sum of the radiant exposure values generated from conductor branches that compose this link,  $B_n$ ;  $n \in 1, \dots, N$ . Where  $N$  is the total number of linear segments. A generalized formula is given as follow:

$$w(u \rightarrow v) = \sum_{n=1}^N S(B_n) \cdot EPT_{uv} \quad (3.12)$$

Where  $S(B_n)$  is the power density generated by the segment  $B_n$  carrying an alternating current having a maximum value of  $I_{max}^{B_n}$  and finally  $r_{B_n}$  is the distance from the middle of the linear conductor segment and the area wherein we want to reduce the electromagnetic radiation level. Using the radiation model of a power line, previously demonstrated in Section 3.3.3.4 and from Equation (3.11), we can readily conclude the general expression of the link cost  $w(u \rightarrow v)$ :

$$w(u \rightarrow v) = \sum_{k=1}^N 7.5 \frac{I_{max}^{B_n}{}^2}{r_{B_n}^2} \left(1 - \cos\left(\pi \frac{B_n}{\lambda}\right)\right)^2 \cdot EPT_{uv} \quad (3.13)$$

### Calculation example

We illustrate here a calculation example of a PLC link weight. In this example we adopt the bus topology with conductors along the perimeter. A typical arrangement is sketched in Figure 3.5. We assign the identifiers 1 and 2 respectively to each of the two nodes. Clearly, the PLC link is not linear but composed of three segments  $B_1$ ,  $B_2$  and  $B_3$ . Consequently, the cost of the link ( $1 \rightarrow 2$ ) is the sum of the radiant exposure values generated from the three segments within the radiation-sensitive area, sketched in Figure 3.5 by a red cloud. We assume that all nodes are stationary and their positions are predefined, so as we can easily find the distances  $R_1$ ,  $R_2$  and  $R_3$  from the middle of each segment and the red area. The cost link is therefore given as:

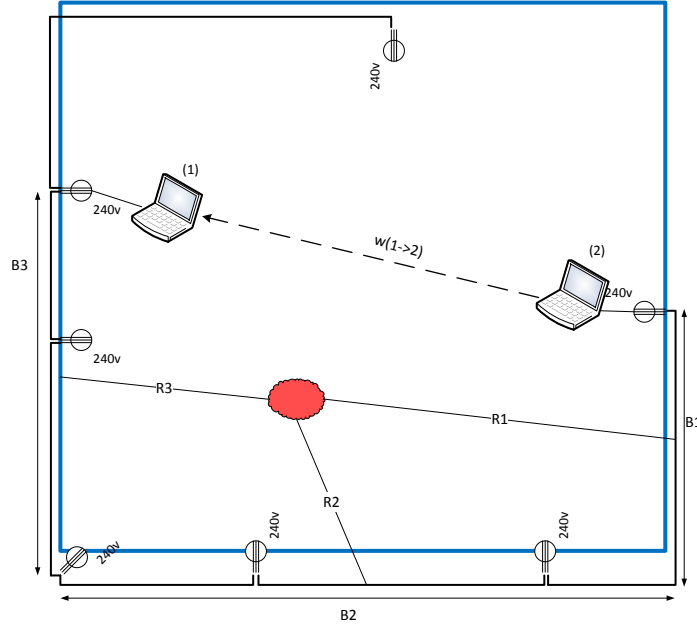


**Figure 3.5:** Metric calculation example for a typical wiring topology: Bus topology (Figure 3.3c) with conductors along the perimeter

$$w(1 \rightarrow 2) = 7.5 \left\{ \frac{I_{max}^{B1}}{R_{B1}^2} (1 - \cos(\pi \frac{B1}{\lambda}))^2 + \frac{I_{max}^{B2}}{R_{B2}^2} (1 - \cos(\pi \frac{B2}{\lambda}))^2 + \frac{I_{max}^{B3}}{R_{B3}^2} (1 - \cos(\pi \frac{B3}{\lambda}))^2 \right\} .EPT_{12}$$

### 3.3.4 Radiated Energy Cartography

In order to analyze the effect of frequency, the electric current and the power lines arrangement (wiring topology), we consider the bus configuration example sketched in Figure 3.6 with the corresponding dimensions. We calculate relying on the model described in Section 3.3.3.4, the radiated field over an area of  $15m \times 15m$ , which corresponds to the contribution of all power lines existing in the room. We have therefore performed a set of simulations with different frequencies of PLC band and different values of electric current.

The purpose of such radiated field cartography is to pinpoint the main influencing factors and then to be able to explain simulation results of the radiation-aware selection path algorithm in the following chapters.

Figures 3.7 show examples of radiated energy cartography for the network configuration depicted in Figure 3.6.

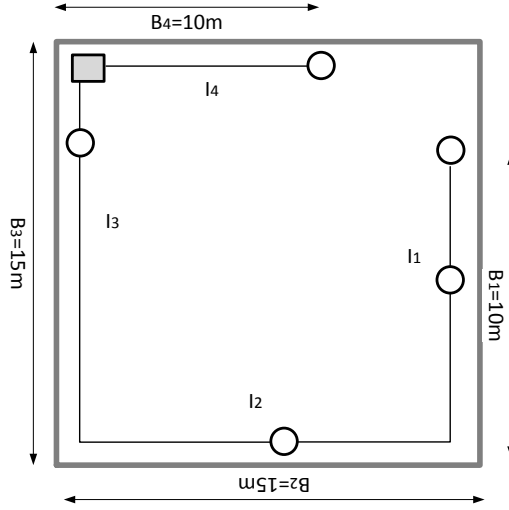


**Figure 3.6:** Bus configuration example with corresponding dimensions

### Effect of frequency ( $\frac{B_i}{\lambda}$ )

According to Equation (3.11), the second term  $\alpha(B_i) = (1 - \cos(\pi \frac{B_i}{\lambda}))$  could cancel the contribution of a line if the condition (3.14) is fulfilled.

$$\frac{B_i}{\lambda} = 2k\pi, \quad \text{where } k \in \mathbb{N} \quad (3.14)$$

$$\frac{B_i}{\lambda} = (2k + 1)\pi, \quad \text{where } k \in \mathbb{N} \quad (3.15)$$

As we see in Figure 3.7b, only lines  $B_1$  and  $B_4$  which contribute to the power density since  $\frac{B_2}{\lambda} = \frac{B_3}{\lambda} = 4$  and then  $(1 - \cos(\pi \frac{B_2}{\lambda})) = (1 - \cos(\pi \frac{B_3}{\lambda})) = 0$ . Nevertheless, this contribution would reach the maximum in case the ratio power line to wavelength verifies the condition (3.15), for instance, for the frequency 60MHz (Figure 3.7a), the radiated energy from segments  $B_1$  and  $B_4$  is equal to zero in all space because of  $\alpha(B_1)$  and  $\alpha(B_4)$ , whereas the contributions of  $B_1$  and  $B_2$  are maximum.

For a general case at frequency 96MHz, we can notice, as plotted in Figure 3.7c, that the four power lines are generating radiated energy.

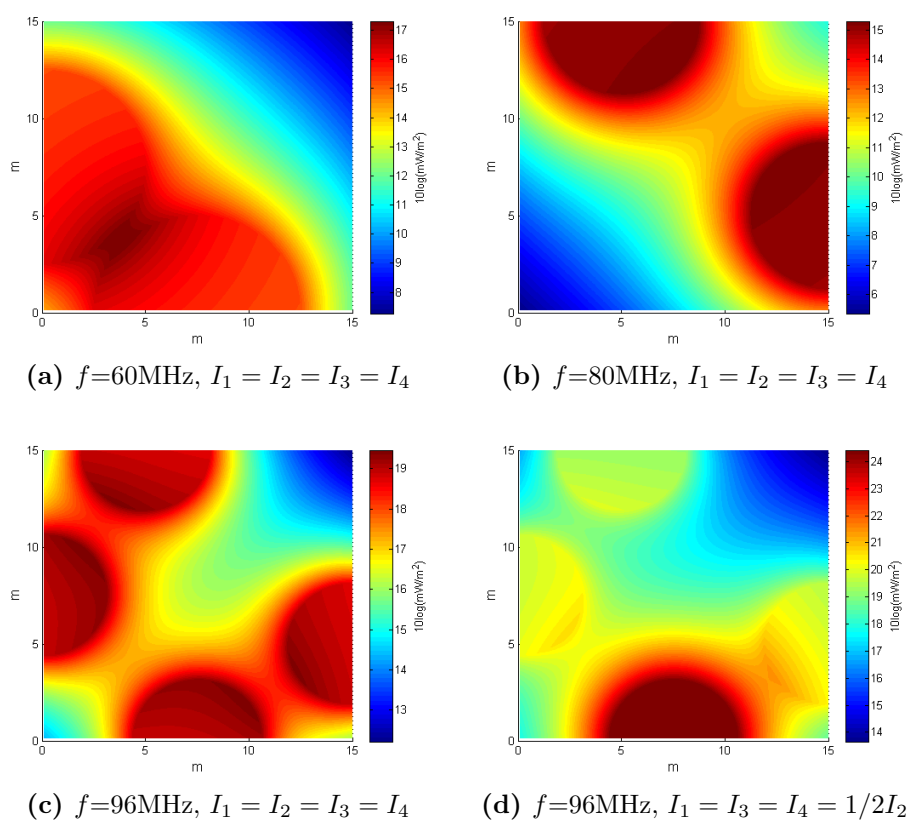


**Figure 3.7:** Power density cartography for bus topology example in Figure 3.6

### Effect of electric current strength

In Figure 3.7d, we kept the same configuration as Figure 3.7c except for the electric current that we changed the maximum value for the segment at the bottom. As we see, by increasing the electric current strength through the segment  $B_2$  from  $5mA$  to  $10mA$ , the radiated energy in the immediate surroundings of that segment has increased.

### 3.3.5 Model Inaccuracies

With the aim of finding a single value for each PLC link between two nodes that characterizes the radiated energy originating from that link, we have assumed a set of simplifying assumptions leading to a basic model with some inaccuracies. Indeed, regarding electric current, we have neglected the contribution of the differential-mode current which might underestimate the evaluated strength of the radiated field. We have also considered a perfect electric current distribution (Equation (3.1)) which is not always the case in real life scenarios.

It was hypothesized that a power line is not loaded at its ends which leads to Equation (3.1). Otherwise, the electric current expression would be as follows:

$$I(z) = I_{max} \sin k(a - |z|)$$

, where  $a - L$  is equivalent to the additional charge (capacitive or resistive) In such a case, it could be necessary to frequently identify impedances at the line ends given that different appliances would be plugged in and out at any time. Such assumption turns out relevant due to the onerous task of identifying load characteristics at the line ends. Furthermore, we have used a basic approximation method, i.e. the midpoint method (Equation (3.10)) in order to calculate the radiated energy at any point of the space. Although it is less accurate than many of other approximating methods (e.g. Simpson's rule), it guarantees a good error-to-complexity tradeoff. The error of such method is estimated to:

$$Error \leq \frac{(b-a)^3}{24} f''(\xi) \text{ for some } \xi \in [a, b]$$

We have compared it with errors of two other well-known approximating methods for  $L = 5m$  and  $f = 30MHz$ , and we showed results in Table 3.3.

This slight difference between different errors could be justified by the number of subintervals which is here equal to 1. Such a choice has been motivated by

Table 3.3: Error examples of three integral approximating methods

Midpoint Rule	Trapezoid Rule	Simpsons Rule
$\frac{(b-a)^3}{24} f''(\xi)$	$\frac{-(b-a)^3}{12} f''(\xi)$	$\frac{-(b-a)^5}{2880} f^{(4)}(\xi)$
5,074	10,1480	4,6473

our readiness of decreasing the calculation complexity while minimizing as much as possible the radiated energy within a specific area.

### 3.4 Conclusions

The support medium for in-home PLC systems is the electric grid. The unbalanced nature of this network combined with the use of high frequencies is at the origin of electromagnetic radiation phenomenon. Basically, the power lines used for transmitting the useful signal act as an antenna, and a part of the transmitted power is radiated.

In this chapter, we studied the problem of modeling electromagnetic fields stemming from power lines while carrying data signal at high frequencies which is not obvious without using any sophisticated tool (MoM or FDTD based).

In this chapter, some fundamentals of the PLC technology have been presented. Antenna theory has been chosen to model radiated field from a linear power line. Then, we assumed the midpoint approximation method in order to formulate the radiated energy. Besides, we have studied some calculation inaccuracies that could overestimate the radiated energy.

The most challenging task is to design a model that yields a single value for each PLC-link that characterizes its contribution of radiation. Following the same philosophy of Chapter 2, this leads to the formulation of the RE routing metric expressed as follows (see Section 3.3.3.5):

$$w(u \rightarrow v) = \sum_{k=1}^N 7.5 \frac{I_{max}^{B_n}}{r_{B_n}^2} \left( 1 - \cos\left(\pi \frac{B_n}{\lambda}\right) \right)^2 .EPT_{uv}$$

Hence, this value could be used subsequently by a shortest path algorithm in the next chapters.

## **Part III**

# **Green Home Network Routing Solutions**



# ElectroMagnetic Radiation-Aware Routing Algorithms

## 4.1 Introduction

In the previous chapters, we have proposed two EMF models for both Wi-Fi and PLC technologies. We have as well pointed out how we have designed radiation-aware routing metrics based on those models.

In this chapter, we first underline how to calculate and then implement the proposed metrics in conjunction with shortest path routing algorithms for two types of networks: fully wireless and heterogeneous multi-hop networks. We introduce herein a new link-adaptive path cost expression to tackle the different radiation behavior of wireless and wired technologies for the case of heterogeneous network.

Finally, we evaluate and analyze our proposals in comparison to other existing routing algorithms.

## 4.2 Preliminaries

### 4.2.1 Overview

The authors of [96] state that a link-state routing protocol involves four components that fulfill the following questions:

1. How to discover neighbors of a node?

2. How to calculate and assign metrics to direct links?
3. How a node propagates metrics of links that it has with its neighbors?
4. How these links' weights are used to make the best path for a given destination?

We notice that the four components mentioned above could be split into two independent clusters. The first one refers to the *algorithmic* aspects; it comprises link metric calculation and the path calculation algorithm which correspond respectively to the second and the fourth components. As to the second one, it refers to the *communication* aspects of routing, in other words, the mechanisms of exchanging routing information between nodes in the network (e.g. using LSAs for OSPF, RREQ and RREP for DSR ...), this cluster consists of the neighbors discovery mechanisms and the packet forwarding scheme (source-based, hop-by-hop ...) which correspond respectively to the first and the third components.

We synthesize in Figure 4.1 general interactions between different components for each node. Accordingly, we do not mention, in the scope of the our work, required mechanisms and interactions when a link is broken, topology information change or more generally when updating routing tables is needed to maintain network connectivity.

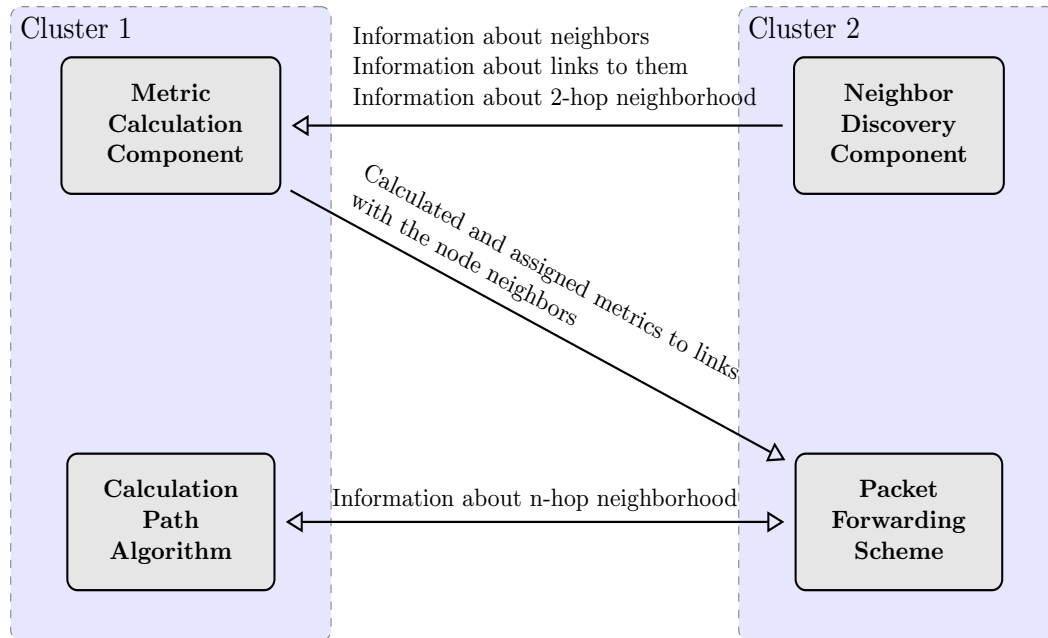


**Figure 4.1:** Semantic schematic of general interactions between different components of a link-state routing protocol for one node.

### 4.2.2 Chapter Scope

We will not implement in the scope of this chapter elements of the second cluster. We will focus on the algorithms aspects. In other words, we will treat how the RE routing metric (that we have exhaustively defined in Chapter 2 and Chapter 3) is calculated and assigned to directed links and how these metric values are subsequently combined to form a path cost for both wireless and heterogeneous environment.

We propose novel computation algorithms that combine Dijkstra’s algorithm and the hop-by-hop scheme. This algorithm must be fed with information about the network state and topology.

## 4.3 ElectroMagnetic Radiation-Aware Routing Algorithm (EMRARA) for Wireless Multi-Hop Networks

### 4.3.1 Network Assumptions

In this section, a home network is considered as a wireless network that can host few radio devices, 100 at most, and which has a single egress to Internet that we call here Home Gateway (HG). We assume that all nodes are stationary and their positions are predefined as well as the radiation-sensitive area location. Moreover, we assume that each node is equipped with one 802.11n radio with an equal number of antennae for all nodes. It is important to underline here the point that we differentiate two categories of nodes; User Equipment (UE) and routers or access points (APs). UEs consist of traffic senders or receivers to or from the HG whereas APs consist of relay nodes. The intuitive impact of this differentiation is that we cannot turn off a UE even if it is in the vicinity of the radiation-sensitive area unlike relay nodes that can be turned off if necessary.

### 4.3.2 Network Model

We model our wireless network of nodes connected by bidirectional links as a connected directed graph  $G = (V, E)$ , where  $V$  is the set of nodes and  $E$  is the set of edges representing directed wireless links. We assign to each node a unique identifier  $u = 1, 2, \dots, |V|$ , with has a maximum transmit power,  $P_{TX}^u$ . Each directed link,  $u \rightarrow v$  from node  $u$  to node  $v$ , has a non-negative edge cost,  $w(u \rightarrow v)$ . For more generality, we assume an asymmetric case where  $w(u \rightarrow v)$  is not the same as  $w(v \rightarrow u)$ . A path,  $\mathcal{P}$ , from a source,  $s$ , to a destination,  $d$ , is denoted by  $\mathcal{P}_{s,d}$  with

a global cost,  $\mathcal{C}(\mathcal{P}_{s,d})$  ( $\mathcal{C}(\mathcal{P})$  for short). The problem to be solved is then presented in Equation (4.1) and it consists of finding the best path  $\mathcal{P}_{s,d}^*$ :

$$\mathcal{C}(\mathcal{P}_{s,d}^*) = \min_{\mathcal{P}_{s,d}} \mathcal{C}(\mathcal{P}_{s,d}) \quad (4.1)$$

### 4.3.3 Algorithm Description

Thanks to its isotonicity and monotonicity, the RE metric (for exhaustive definition, refer to Section 2.6.3) can fit the combination Dijkstra's algorithm and the hop-by-hop scheme as proved by authors in [11] while guaranteeing optimality, consistency and loop-freeness in routing.

In contrast with the traditional Internet routing protocols, our electromagnetic radiation-aware algorithm finds the minimum radiation path, expressed in Equation (4.1), where the cost associated with each link is a function of the level of the radiated energy within a given area caused by transmitting data through that link. Using the RE definition (Equation (2.10)) as pairwise link weight, the routing algorithm's job is to compute the shortest path from a source to a destination which minimizes the sum of the RE costs of constituent links.

Unlike most of metrics used in traditional routing protocols that mainly assess link quality in terms of inherently system-related criteria, such as delay, bandwidth or throughput, RE as routing metric presents the specificity of influencing routing decisions by external environment changes. In the example depicted in Figure 4.2, each link ( $u \rightarrow v$ ) is labeled with the RE value generated at the radiation-sensitive area sketched by a red cloud.

It is clear from Figure 4.2 that outbound links from node 5 have the highest values of RE. This can simply be explained since node 5 is the closest node to the radiation-sensitive area. For instance, when node 1 has a packet for node 7, the EMRARA chooses node 3 and then node 6 instead of 5, since node 6 is further from the radiation-sensitive area than node 5. In fact, electromagnetic signals radiated from node 6 are more attenuated than those emitted from node 5. The minimum electromagnetic radiated energy path is indicated by the dashed links. When the 1500 bytes packet reaches node 7 through the path  $1 \rightarrow 3 \rightarrow 6 \rightarrow 7$ , the expected radiant exposure at the radiation-sensitive area is  $2.574 \frac{W\mu s}{m^2}$ . While considering the hop count metric, Dijkstra's algorithm will choose the path  $1 \rightarrow 5 \rightarrow 7$ , incurring a radiant exposure of  $12.831 \frac{W\mu s}{m^2}$  at the radiation-sensitive area.

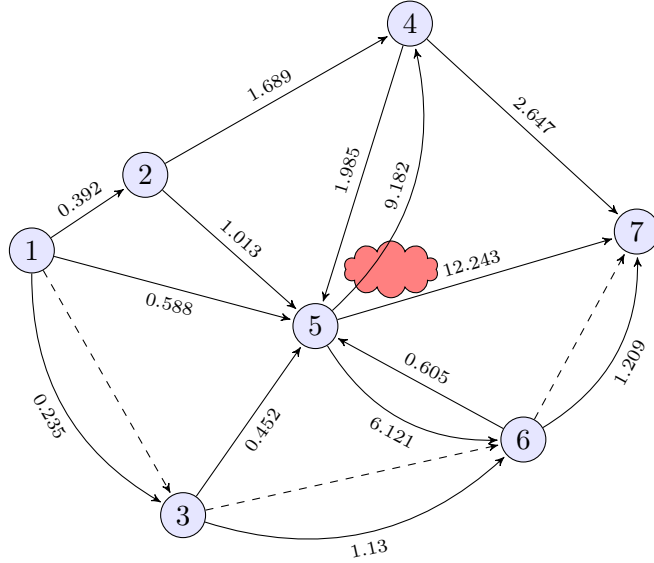


Figure 4.2: Illustration of EMRARA

#### 4.3.4 Computing EPT

We have previously defined in Section 2.4.3 the Expected Packet Time (EPT) of a link and formalized it in Equation (2.4). This definition incorporates the link bandwidth to obtain the time spent in transmitting the packet, as well as the failure probability in order to take into consideration the expected retransmissions number.

To calculate the EPT according Equation (2.4), we need to know the failure probability of the corresponding link. The value of  $P_{f_{uv}}$  is generally defined as follows:

$$P_{f_{uv}} = 1 - (1 - p_r)(1 - p_f) \quad (4.2)$$

De Couto described in [97] how to approximate the loss probability in both forward and reverse directions,  $p_f$  and  $p_r$  respectively, by using the broadcast packet technique. Since we are not using, in the scope of this chapter, a discrete-event network simulator, we choose to use a fixed value of  $P_{f_{uv}}$  equal to 10%.

In the rest of the thesis, we use interchangeably the two terms *bandwidth* and *nominal data rate* to refer to the same thing. The problem of determining the bandwidth of each link is not easy. One possibility is to fix the bandwidth of each IEEE 802.11 radio to a given value. For instance, in order to show the ETX metric

performances, De Couto *et al.* [98] have restricted the bandwidth of their IEEE 802.11b radios to 1 Mbps.

Another possibility is to allow the radios to automatically select the rate for every packet. This mechanism is known as Rate Control Algorithm, Rate Selection Algorithm or Rate Adaptation Algorithm. Although even most recent IEEE 802.11 standards do not specify the algorithm for setting the rate, most of IEEE 802.11 radios support it, and hence each constructor has its proprietary solution.

In summary, the rate adaptation algorithm consists of a set of rules on how to select the preferred rate for outgoing data taking into account the wireless channel conditions. These conditions can be determined using the physical characteristics of the channel, or using link layer information such as packet-loss or ACK failures.

We propose an *ideal* sender-based rate selection algorithm using the physical characteristics of the wireless channel to determine the best suited Modulation and Coding Scheme (MCS). The main idea in this algorithm is to select the rate of an outgoing packet based only on distance between transmitter and receiver, meaning that the sender takes as input, the distance from the receiver to provide the corresponding rate. In summary, we illustrate through Algorithm 1 the rate selection by the sender of an outgoing packet. One has to mention that for this algorithm we assume IEEE 802.11n radios transmitting over two antennae which mean eight possible data rates using two spatial streams.

To accomplish Step 6, we need to determine the set of transmission ranges, *Ranges*, corresponding to the modulation schemes, MCS. Herein, a transmission range,  $d_{MCS_k}$ , is seen as the maximum distance that a packet could travel along with the modulation scheme MCS k. To calculate  $d_{MCS_k}$ , we rely on the link budget formula given as follows:

$$RecSens(MCS_k) = P_{TX}^u - PL(d_{MCS_k}) \quad (4.3)$$

Where  $RecSens(MCS_k)$  is the receiver sensitivity (or also reception threshold) that denotes the minimum power level of a received signal modulated with MCS k.  $P_{TX}^u$  is the transmit power in dBm of the sender. As to  $PL(d_{MCS_k})$  is the TGnB path loss at the distance  $d_{MCS_k}$  from transmitter. Based on the model presented in

---

**Algorithm 1:** Selection of the most suited link rate.

---

<b>Data:</b>	{	MCS	=	[MCS <sub>8</sub> , MCS <sub>9</sub> , ..., MCS <sub>15</sub> ]
		Rates	=	[R <sub>MCS<sub>8</sub></sub> , R <sub>MCS<sub>9</sub></sub> , ..., R <sub>MCS<sub>15</sub></sub> ]
		Ranges	=	[d <sub>MCS<sub>8</sub></sub> , d <sub>MCS<sub>9</sub></sub> , ..., d <sub>MCS<sub>15</sub></sub> ]
		MCS/Range/Rate	=	database

**Result:** Most suited rate to send a packet from transmitter  $u$  to receiver  $v$  ;

```

1 if  $d_{uv} > Ranges[0]$  then
2   | There is no direct link between  $u$  and  $v$ ;
3   | return 0
4 else
5   |  $i = 0$ ;
6   | while  $i < length(Ranges)$  and  $Ranges[i] \geq d_{uv}$  do
7     | Look on MCS/Ranges/Rates database for corresponding MCS of
8     | Ranges[i];
9     |  $bestMCS = MCS[i]$ ;
10    |  $i ++$  ;
11  | Look on MCS/Range/Rate database for the corresponding rate of
12  |  $bestMCS$ ;
13  |  $bestRate = Rates[i]$ ;
14  | return  $bestRate$ ;

```

---

Section 2.4.2.3, the path loss then is formulated as follows:

$$PL(d_{MCS_k}) = 35 \log_{10}(d_{MCS_k}) + 20 \log_{10}(f) - 154 \quad (4.4)$$

According to Equation (4.3) and Equation (4.4), the latter distance,  $d_{MCS_k}$ , is therefore calculated in the absence of any interference and it is given by:

$$d_{MCS_k} = 10^{\frac{P_{TX}^u - RecSens(MCS_k) - 20 \log_{10}(f) + 148}{35}} \quad (4.5)$$

A summary of the MCSs as they map to the minimum receiver sensitivity measured for a Packet Error Rate (PER) of 10%, and their corresponding rate has been specified by the standard [33] and given in the Table 4.1.

Accordingly, from Table 4.1 and Equation (4.5), we summarized information needed for Steps 7 and 8 of Algorithm 1 in Table 4.2. We show in this table a calculation example for 2.4 GHz band, a spacing channel of 20 MHz and for a transmit power of 17 dBm.

Table 4.1: Receiver sensitivity corresponding to IEEE 802.11n modulation schemes [5].

MCSs indices for 2 spatial streams	Modulation	Code rate	Receiver sensitivity (dBm) (20MHz channel spacing)	Receiver sensitivity (dBm) (40MHz channel spacing)
8	BPSK	1/2	-82	-79
9	QPSK	1/2	-79	-76
10	QPSK	3/4	-77	-74
11	16-QAM	1/2	-74	-71
12	16-QAM	3/4	-70	-67
13	64-QAM	2/3	-66	-63
14	64-QAM	3/4	-65	-62
14	64-QAM	5/6	-64	-61

Note that the distance  $d_{MCS_k}$ , expressed in Equation (4.5), depends on the frequency and the channel spacing (20MHz or 40MHz for IEEE 802.11n), we illustrate the impact of these parameters on the transmission ranges in Figure 4.3. In the same context and seeking for more details of how Algorithm 1 works, a transmission range to MCSs mapping is sketched in Figure 4.3.

Thus, knowing the distance between the transmitter and the receiver we can expect which modulation will be used and then the expected packet duration based on the data rate. While assuming that the transmitter uses always the most robust MCS for the given channel conditions.

Table 4.2: Transmission ranges and data rates corresponding to 802.11n MCSs indices.

MCSs indices for 2 spatial streams	Transmission range (m)	Data rate (Mbps)
8	49.63	13
9	40.74	26
10	35.72	39
11	29.32	52
12	22.54	78
13	17.32	104
14	16.22	117
14	15.19	130

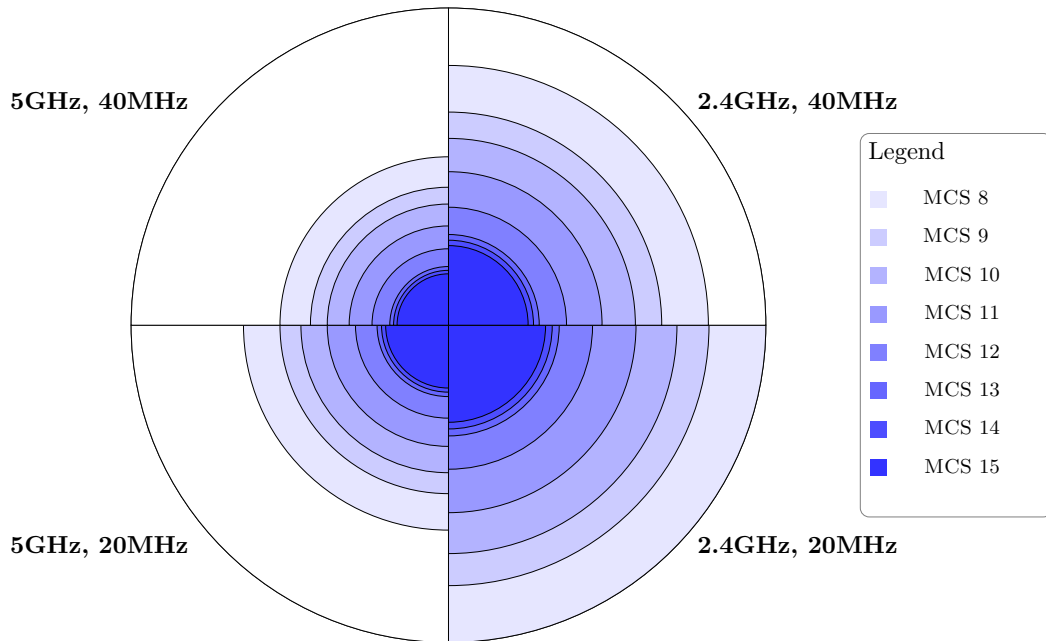


Figure 4.3: Transmission ranges to MCSs mapping

## 4.4 EleetroMagnetic Radiation-Aware Routing Algorithm for Heterogeneous multi-hop networks (EMRARA-H)

### 4.4.1 Network Assumptions

Unlike Section 4.3.1, a home network herein is considered as a heterogeneous network hosting four categories of nodes that we call: *Wi-Fi nodes*, *PLC nodes*, *UE* and *relay nodes* (also called routers). Explicitly, a PLC node (e.g. Wi-Fi Powerline Bridge) has both PLC and IEEE 802.11n interfaces but we assume that only one interface could be active at a time, whereas, a Wi-Fi node has only an IEEE 802.11n interface. Regarding UE and routers, we have already clarified the distinction in Section 4.3.1, we need just to substitute AP by router.

Thus in our heterogeneous network, a node can either be Wi-Fi or PLC node, whereas a UE could be selected as relay node. Moreover, we assume that all nodes are stationary and their positions are predefined.

### 4.4.2 Network Model

According to the previously mentioned assumptions, we model our heterogeneous network as a connected and multidirected graph

$G(V_{Wi-Fi} \cup V_{PLC}, E_{Wi-Fi} \cup E_{PLC})$  that allow to have multiple edges between the same source and target nodes. Where  $V_{Wi-Fi}$  represents the set of Wi-Fi nodes and  $V_{PLC}$  is the set of PLC nodes, as to  $E_{Wi-Fi}$  and  $E_{PLC}$ , they are the sets of Wi-Fi and PLC direct links respectively. We assign to each node a unique identifier  $u = 0, 1, \dots, |V|$ . Moreover, each link  $u \rightarrow v$  has non-negative edge cost,  $w_k(i \rightarrow j)$ , the index  $k \in 1, 2$  is used to designate the RE value according to the link nature, Wi-Fi and PLC respectively. Note that  $k = 1$  if  $u \rightarrow v \in E_{Wi-Fi}$  and  $k = 2$  if  $u \rightarrow v \in E_{PLC}$ .

#### 4.4.3 Link-Adaptive RE Path Cost

We present herein an extended routing metric that takes into consideration electromagnetic radiation from both Wi-Fi and PLC links. Based on the aforementioned radiation models detailed in Chapter 2 and Chapter 3, we formulate in Equation (4.6) a link-adaptive path cost to assess the amount of radiant exposure within the radiation-sensitive area caused by a packet transmission through a path  $\mathcal{P}_{s,d}$  from a source  $s$  to a destination  $d$ .

$$\mathcal{C}(\mathcal{P}_{s,d}) = \sum_{u \rightarrow v \in \mathcal{P}_{s,d}} (\alpha_{u,v} w_1(u \rightarrow v) + \beta_{u,v} w_2(u \rightarrow v)) \quad (4.6)$$

,where

$$w_1(u \rightarrow v) = \frac{P_{TX}^u}{4\pi r_i^2} \cdot EPT_{uv} \quad (4.7)$$

$$w_2(u \rightarrow v) = \sum_{B_n \in u \rightarrow v} \frac{30\pi I_{max}^{B_n}{}^2}{4\pi r_{B_n}^2} \cdot EPT_{uv} \left(1 - \cos\left(\pi \frac{B_n}{\lambda}\right)\right)^2 \quad (4.8)$$

$$\alpha_{u,v} = \begin{cases} 1 & \text{if } u \rightarrow v \in E_{Wi-Fi} \\ 0 & \text{otherwise} \end{cases} \quad (4.9)$$

$$\beta_{u,v} = \begin{cases} 1 & \text{if } u \rightarrow v \in E_{PLC} \\ 0 & \text{otherwise} \end{cases} \quad (4.10)$$

The objective function formulated in Equation (4.6) provides the total cost of the path  $\mathcal{P}_{s,d}$  from a source,  $s$ , to a destination,  $d$ , in terms of radiant exposure.

Equations (4.7) and (4.8) derive from the RE metric formulation of a Wi-Fi and a PLC link previously presented in Subsection 2.5.2 and subsection 3.3.3.5 respectively. As regards Equations (4.9) and (4.10), they are constraints that ensure that a given link  $u \rightarrow v$  belonging to the optimal path  $\mathcal{P}_{s,d}^*$  is either Wi-Fi or PLC and allow to assign the corresponding RE metric value to that link.

#### 4.4.4 Computing EPT

Following the same logic as Section 4.3.4, we present herein how to calculate the EPT based on the link nature. To do so, we extend Algorithm 1 as follows:

---

**Algorithm 2:** Selection of the most suited link rate for heterogeneous network.

---

<b>Data:</b>	{	MCS	=	$[MCS_8, MCS_9, \dots, MCS_{15}]$
		Rates	=	$[R_{MCS_8}, R_{MCS_9}, \dots, R_{MCS_{15}}]$
		Ranges	=	$[d_{MCS_8}, d_{MCS_9}, \dots, d_{MCS_{15}}]$
		MCS/Range/Rate		database
		Set of Wi-Fi nodes		$E_{Wi-Fi}$
		Set of PLC nodes		$E_{PLC}$
		Peak rate of PLC technology		PeakRate

**Result:** Most suited rate to send a packet from transmitter  $u$  to receiver  $v$  based on link nature;

```

1 if  $u$  and  $v \in V_{PLC}$  then
  | {
  |    $(u \rightarrow v) \in E_{Wi-Fi}$  then do Algorithm 1
  |    $(u \rightarrow v)' \in E_{PLC}$  then bestRate = PeakRate
2 | }
3 else
4 |  $(u \rightarrow v) \in E_{Wi-Fi}$  then do Algorithm 1
5 return bestRate;

```

---

At Step 1 of Algorithm 2, we check whether nodes  $u$  and  $v$  are PLC nodes, i.e. have both Wi-Fi and PLC interfaces. Hence, the connection between them might be accomplished by two possible links, which we expressed in Line 2. In the case of a Wi-Fi connection (i.e.  $(u \rightarrow v) \in E_{Wi-Fi}$ ) we simply execute Algorithm 2 in order to calculate the best transmission rate. Regarding the PLC link (i.e.  $(u \rightarrow v) \in E_{PLC}$ ), and given that the rate depends on many time-variant factors, we assume the maximum value proposed by the used technology. Otherwise, if the transmitter is a Wi-Fi node, the connection is guaranteed by Wi-Fi regardless the receiver node nature; this has been expressed on Line 3.

## 4.5 Implementation

We have designed a software simulator based on the graph library NetworkX [99]. NetworkX is a Python package that provides classes and generators to create standard graphs as well as algorithms to treat and analyze resulting networks, in addition to many visualization tools.

We have first implemented the propagation model presented in Section 2.4.2.3, the generalized rate selection algorithm presented in Algorithm 2 and operations for calculating links metrics.

Regarding path selection operations, we need at the onset to distinguish two different approaches: When the network is fully wireless, we implement EMRARA while considering the well-known Dijkstra’s algorithm and assigning to each directed edge the corresponding value of the RE metric (Equation (2.10)). Whereas when the network is heterogeneous (Section 4.4), it could happen that two nodes are connected by two different links, we therefore implement a generalized Dijkstra’s algorithm to find the shortest path in a multigraph.

To do so, we propose to upgrade the *edge relaxation* step. Accordingly, we implement the pseudo-code presented in Algorithm 3 which enables to choose out the minimum value of the two weights corresponding to the Wi-Fi and PLC links between two PLC nodes.

---

**Algorithm 3:** ‘Relaxation’ pseudo-code for parallel edges

---

```

1 for each neighbor v of u do
2   if v ∈ VPLC then
3     minweight(u, v) = min( (u → v)Wi-Fi, (u → v)PLC )
4     if dist[u] + minweight(u, v) < dist[v] then
5       dist[v] = dist[u] + minweight(u, v)

```

---

Since throughout our work the fully wireless network is a special case of the heterogeneous network (more generally a classical directed graph is as well a special case of a multigraph), we use in simulations the generalized Dijkstra’s algorithm that will works as well for both use cases.

## 4.6 Results and Evaluations

In this section, we underline how using EMRARA and EMRARA-H algorithms mitigate the radio-frequency emissions drawn from fully-wireless and heterogeneous networks respectively, compared to other routing schemes.

### 4.6.1 Performance Metrics

In order to bring out the performances of the proposed routing algorithm, we lay a particular stress on *ecological* effects; we then use three different evaluation metrics: Cumulative Radiant Exposure (CRE), Cumulative Radiated Power (CRP) and Cumulative Consumed Energy (CCE).

- **Cumulative Radiant Exposure (CRE):** Is the sum of the radiant exposure during the transmission of a packet through shortest paths from all UEs to the egress router (HG) and inversely from the egress router to all UEs which we refer to *UP* and *DOWN* flow respectively. CRE is expressed as follows:

$$\text{CRE}_{\text{UP}} = \sum_{\forall \text{UE}} \sum_{\mathcal{P}_{\text{UE, HG}}} \sum_{(u \rightarrow v) \in \mathcal{P}_{\text{UE, HG}}} \text{RE}(u \rightarrow v) \quad (4.11)$$

$$\text{CRE}_{\text{DOWN}} = \sum_{\forall \text{UE}} \sum_{\mathcal{P}_{\text{HG, UE}}} \sum_{(u \rightarrow v) \in \mathcal{P}_{\text{HG, UE}}} \text{RE}(u \rightarrow v) \quad (4.12)$$

- **Cumulative Radiated Power (CRP):** Similarly, is the sum of the power density caused by transmitting simultaneously a packet through shortest paths from all user equipment to the GW and inversely. CRP is expressed as follows:

$$\text{CRP}_{\text{UP}} = \sum_{\forall \text{UE}} \sum_{\mathcal{P}_{\text{UE, HG}}} \sum_{(u \rightarrow v) \in \mathcal{P}_{\text{UE, HG}}} \frac{\text{RE}(u \rightarrow v)}{\text{EPT}_{uv}} \quad (4.13)$$

$$\text{CRP}_{\text{DOWN}} = \sum_{\forall \text{UE}} \sum_{\mathcal{P}_{\text{HG, UE}}} \sum_{(u \rightarrow v) \in \mathcal{P}_{\text{HG, UE}}} \frac{\text{RE}(u \rightarrow v)}{\text{EPT}_{uv}} \quad (4.14)$$

- **Cumulative Energy Consumption (CEC):** Is the sum of the energy consumed by UEs and only *ON* routers while all UEs are transmitting or receiving, assuming that nodes were turned off before starting to transmit.

### 4.6.2 Experimental Methodology

We conduct simulations in our empirical study, based on the implementation described in Section 4.5, in order on one hand, to prove the effectiveness of our link-adaptive path cost for both wireless and heterogeneous environment, and on the other hand, to answer the following questions. *Compared to some traditional known schemes, how effectively can our algorithm reduce the radiated energy caused by radio-frequency emissions within a given area? What is the cost in terms of energy consumption? How network parameters influence our algorithms?* Network parameters could include:

1. Network size, **N**: or in other words nodes population.
2. User Equipment population, **UEP**: percentage of user equipment among the total number of network nodes.
3. Routers population, **RP**: percentage of routers among the total number of network nodes.
4. Wi-Fi nodes population, **WP**: percentage of Wi-Fi nodes among the total number of network nodes.
5. PLC nodes population, **PP**: percentage of PLC nodes among the total number of network nodes.

We vary the aforementioned parameters during simulations in order to analyze their effects on the performance results.

Note that network nodes are by default Wi-Fi nodes, meaning that when there is no PLC node in the network (i.e. **PP**=0%), we consider a fully wireless network (i.e. **WP**=100%). In this case, it is the EMRARA implementation that will be used. Otherwise, when the **PP** is set up to a given value, it is the EMRARA-H corresponding implementation that will be used (refer to Section 4.5).

Unless otherwise noted, our simulations are run with the following fixed parameters. The bus topology (Figure 3.3c) is used for outlets arrangement. The transmit power is the same for all Wi-Fi interfaces and it is equal to 17 dBm. The peak rate of each PLC link is 100Mbps which corresponds to the rate of Qualcomm QCA7450 chipset supporting the HomePlug AV/AV2 technologies. Finally, **N** nodes of the same transmission range are randomly distributed into a  $200m \times 200m$  square field. For each parameter setting, 500 trial networks are generated.

Explicitly, for each trial, a new topology is generated, and then for each topology we randomly pick a set of nodes, **PP**, that have PLC interface in addition to Wi-Fi interface and a set of user equipment (UE), **UEP**, that we could not turn off regardless of their positions relative to the electromagnetic radiation-sensitive area. Since the down-link traffic in home network is higher than the up-link traffic, we only assume the down-link traffic sent from the HG (which is the unique egress to the Internet in our model) to all users. Then, the average of the different performance metrics of the best paths computed in all 500 trials are calculated for the individual algorithms, respectively, as well as the corresponding standard deviations.

### 4.6.3 Numerical Results

In order to study the performance of our suggested schemes, we implemented and observed four separate routing algorithms:

1. Hop-Count: The minimum hop-count routing algorithm, where the cost of all links is identical and independent from both the radiated power at the radiation-sensitive area and the data rate. The cost of each link is equal to 1. We will henceforth designate it by *Hop-Count* algorithm.
2. Bandwidth: The maximum bandwidth routing algorithm, where the cost of a link is calculated by dividing a reference bandwidth by the nominal data rate of that link. For all simulations, this reference bandwidth is equal to the maximum data rate provided by the IEEE 802.11n standard (refer to the Table 4.2), namely 130Mbps. In such a way, a link which has a bigger data rate will have a smaller link cost. This algorithm will be designated by *Bandwidth*.
3. RPA: The Radiated Power-Aware algorithm, where the cost associated with each link is the power density stemmed from the transmitter and radiated at the radiation-sensitive area (without considering the transmission time across that link). We use the link cost of Equation (2.8) or Equation (3.11) according to the link nature whether Wi-Fi or PLC. It is designated in the sequel by *RPA* for short.
4. EMRARA: Our EletecroMagnetic Radiation-Aware Routing Algorithm (EMRARA), where the link cost includes the packet duration, and thus it considers the radiated energy instead of radiated power. The interpretation of such combination has been already detailed in Section 2.7.1. In the case of heterogeneous network we will talk about EMRARA-H.

Since the Hop-Count is the most used algorithm for routing packet, we define a *normalized* value of each performance metric with respect to each algorithm to be the ratio of its average to that of Hop-Count algorithm.

We have conducted simulations for different radiation-sensitive area positions. Figure 4.4 presents plots of a network example of 100 Wi-Fi nodes, 30 among them are UEs, and five topologies with respect to radiation-sensitive area. We plot all UEs and only powered APs (including the HG) positions. UEs are designated by blue circles while APs are designated by red ones. Directed lines (arrow at one end or at both ends of each link) between UEs or between UEs and APs highlight that RE cost may be different according to the packet direction, and then the outward path could be different from the return path. Figures 4.4a, 4.4b, 4.4c, 4.4d, 4.4e depict shortest paths, in terms of radiation exposure in different positions of the hot spot, from all UEs to the HG and shortest paths from HG to all UEs. For further details, we plot in Figure 4.4f Hop-Count shortest paths. Clearly, five different positions of sensitive area lead to different results, accordingly the selected relay APs for the network topology shown in Figure 4.4c are exactly in the opposite side for the topology depicted in Figure 4.4d.

#### For wireless network

For results shown in Figures 4.5a, 4.5b, we kept the same topology for each trial since UEs positions influence greatly the final results. We present results for only one position of the radiation-sensitive area which is depicted in Figure 4.4a.

We can readily notice the huge gap between results values between UP (Figure 4.5b) and DOWN (Figure 4.5a) flow, which points out the asymmetric behavior of radiant exposure metric. Indeed, for DOWN flow when all UEs are receiving from HG, electromagnetic signals are much more attenuated than when they are transmitting since radiation-sensitive area is further from the gateway than from UEs (see Figure 4.4a).

Moreover, Figure 4.5 captures the effectiveness of our routing algorithm to direct data away from the sensitive area (situated, for this example, in the center of simulations domain), since the EMRARA outperforms the "Hop-count", "Bandwidth" and "RPA" algorithms.

It is also noticeable that the Hop Count algorithm causes more than ten times the CRE compared to EMRARA as it picks paths composed by a minimum number of links even if they are long which amounts to be exposed to electromagnetic emissions for a longer time.

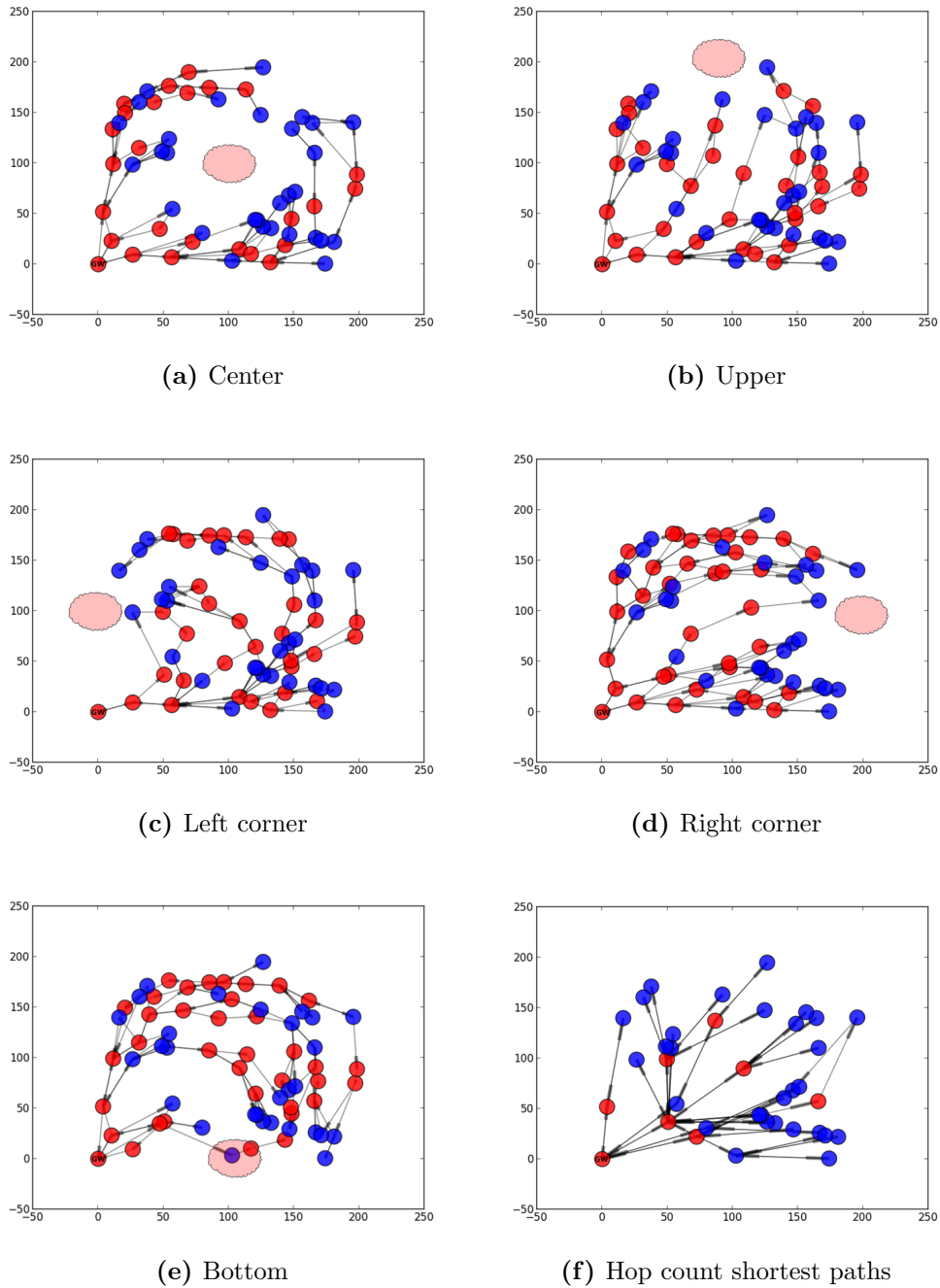
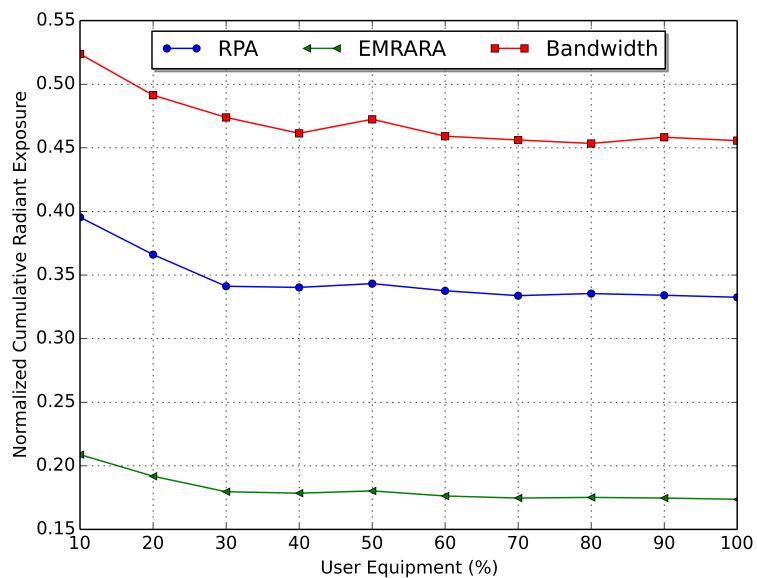
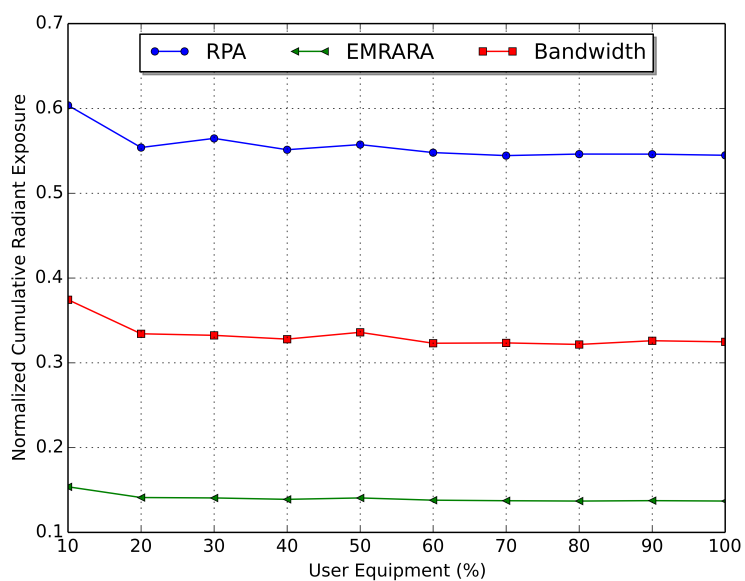


**Figure 4.4:** Network topologies examples showing all shortest paths from/to UEs with respect to four radiation-sensitive area positions that EMRARA avoids.

Even with 100% of **UEP**, EMRARA can hold down the least level of radiation within the radiation-sensitive area. Another clear message from Figure 4.5, is that



(a) Downlink flow



(b) Uplink flow

**Figure 4.5:** Normalized CRE within the radiant-sensitive area depicted in Figure 4.4a for  $N=100$  and  $PP=0\%$

CRE variations for both Bandwidth algorithm and EMRARA follow roughly the same trend. It is owing to the compliance of the expected packet time's definition with link capacity.

Regarding energy consumption (Figure 4.6), the Hop-Count algorithm outperforms the other ones, since the packet is carried through the least number of intermediate nodes as shown in Figure 4.7. Explicitly, we define the metric cumulative relay nodes to be the sum of relay nodes crossed by a packet from a source to a destination of all shortest paths calculated from HG to all UEs, as formulated in Equation (4.15). We show the variations for each algorithm in Figure 4.7.

$$\sum_{\forall \text{UE}} \sum_{\mathcal{P}_{\text{GW,UE}}} \text{Relay Node} \in \mathcal{P}_{\text{GW,UE}} \quad (4.15)$$

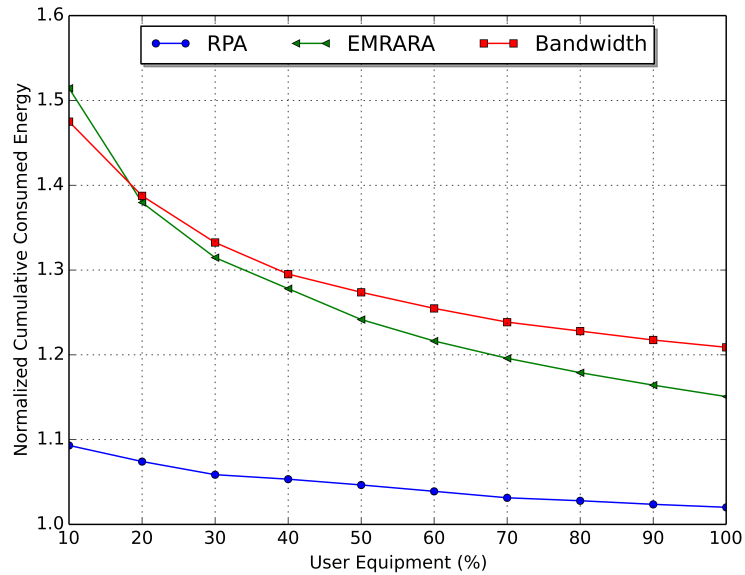


**Figure 4.6:** Normalized CEC when all UEs are receiving

#### For heterogeneous network

For simulations of heterogeneous network, we randomly pick, for each trial, a set of PLC nodes that have both PLC and Wi-Fi interfaces, with interface selection based on Algorithm 2. For consistency, we assume for each trial 70% of nodes to be UEs (which is likely the case in a real home network scenario).

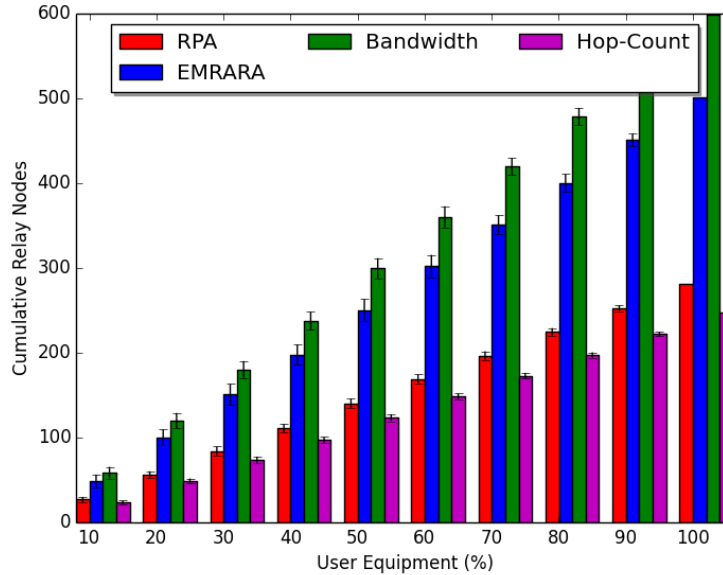


**Figure 4.7:** Cumulative relay nodes when all UEs are receiving

We conduct simulations for different values of network size and PLC nodes population. Similarly, results are normalized with respect to the Hop-Count algorithm.

As general finding, Figure 4.8 captures the effectiveness of our algorithm to direct data away from the sensitive area since EMRARA-H outperforms Hop-Count, Bandwidth and RPA algorithms, for all network sizes and different **PP** values.

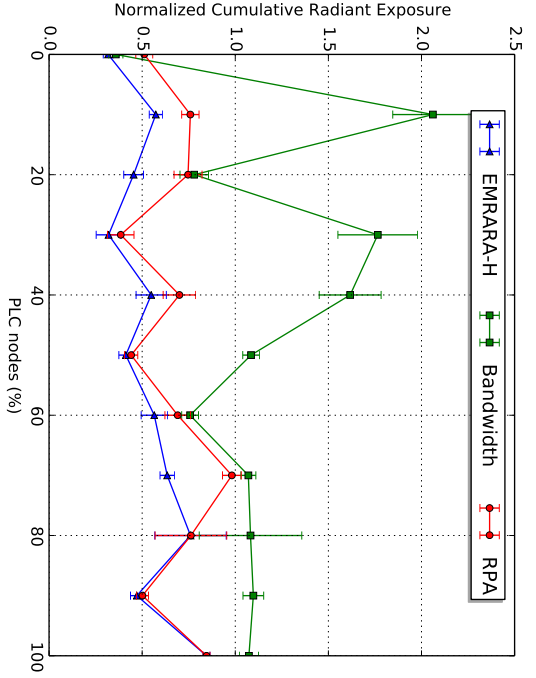
Meanwhile, it is noticeable from Figure 4.8, that increasing the network size results in a higher efficiency of EMRARA-H algorithm with respect to Hop-Count algorithm in terms of radiant exposure. For example, when we have 100 nodes in the network (Figure 4.8), EMRARA-H generates 3 times less cumulative radiant exposure (also called cumulative radiated energy) than Hop-Count algorithm in 54% cases (even 5 times less for the configuration **PP**=0% ( see also Figure 4.5a), and the configuration **PP**=10%). While, when we have 60 and 20 nodes, EMRARA-H generates 3 times less cumulative radiant exposure in 27% and 18% cases respectively. Explicitly, since we kept the same simulation domain of  $200m \times 200m$  for different network sizes, small number of nodes leads to less alternative paths than bigger networks, then both algorithms may pick the same optimal paths for small networks.

Regarding the cumulative radiated power, from Figure 4.9, we can notice that all compared algorithms keep the same variation trend as for the cumulative radiant

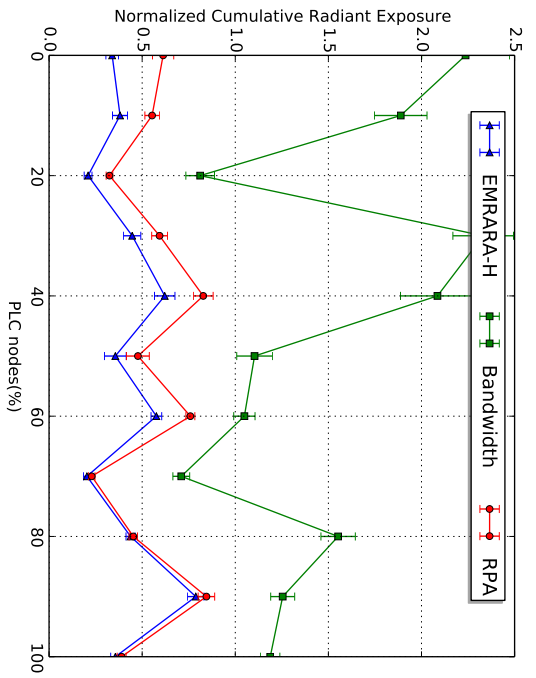
exposure. The Bandwidth algorithm is the worst in terms of radiated power, even worse than the Hop-Count algorithm since while looking for the best paths in terms of links capacity, the Bandwidth algorithm may select paths composed by more links than Hop-Count algorithm and then more radiating sources.

Regarding energy consumption, paths selected by the EMRARA-H algorithm consume always more than Hop-Count algorithm, such an increase can reach in the worst cases 13%, 16% and 17% more than energy consumed by paths selected by minimum hop count algorithm, for networks of 20, 60 and 100 nodes respectively (Figure 4.10). We can then underline that our algorithm guarantees an acceptable compromise between energy consumption and radio-frequency emissions within a given area. Another clear message from Figure 4.10, is that the energy consumption decreases remarkably when PLC nodes number increases, it is obvious since a PLC interface consumes less than a Wi-Fi interface while assuming that a PLC interface consumes as much energy as an Ethernet interface.

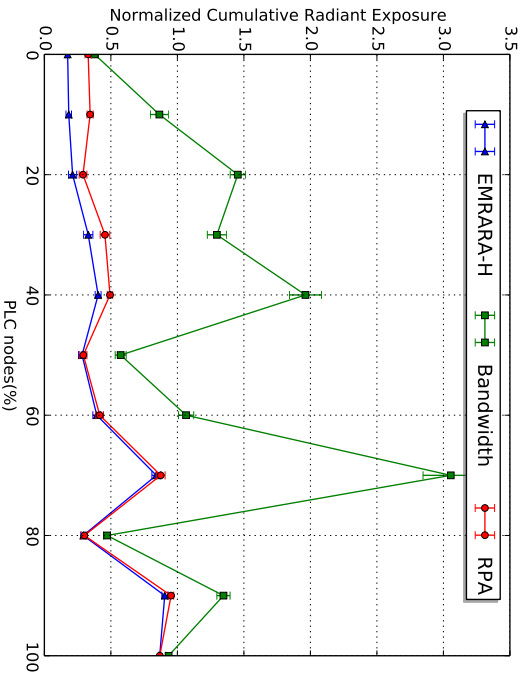
Bars in Figures 4.11 are split in two parts, the dashed ones represent the cumulative number of PLC links, and the second ones represent the cumulative number of Wi-Fi links that make up all shortest paths from the HG to all UEs. We point out from Figures 4.11 that the overall energy consumption is closely linked to the cumulative number and the nature (whether it is PLC or Wi-Fi) of links that make up the shortest paths from the HG to all UEs whereas it is not necessarily the case to explain the cumulative radiant exposure variations, because radio-frequency emissions depend upon the distance between the radiating sources and the sensitive area. Concretely, in Figure 4.11a for instance, for a network of 50% of PLC nodes EMRARA-H uses more Wi-Fi links than a network of 70% of PLC nodes, and as a consequence the first one produce less radiant exposure and radiated power emissions than the second one (see Figure 4.8a and Figure 4.11a).



(a) 20 Nodes

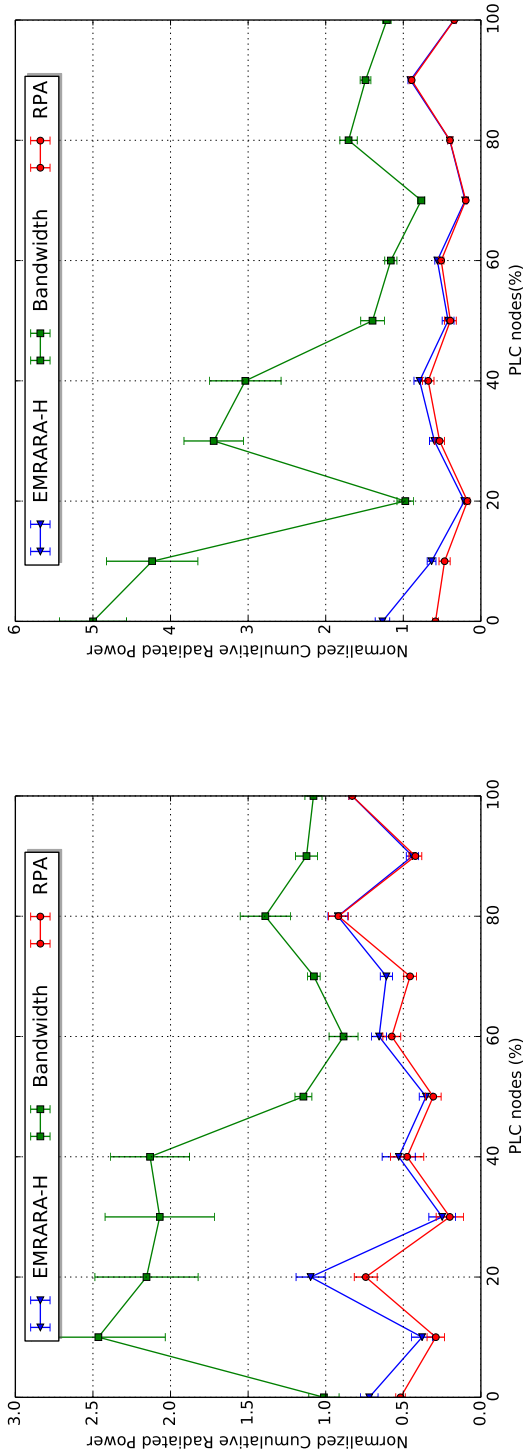


(b) 60 Nodes



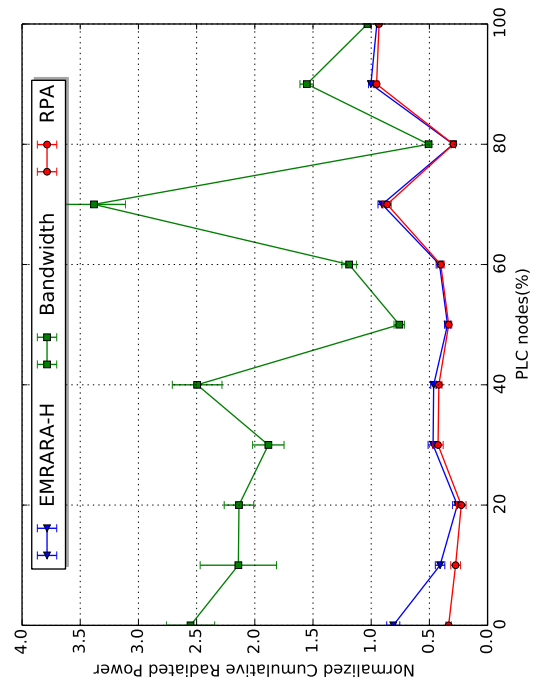
(c) 100 Nodes

Figure 4.8: Normalized cumulative radiant exposure within the radiant-sensitive area depicted in Figure 4.4a for  $UEP = 70\%$ . Figures represent 20, 60, 100 nodes, respectively.



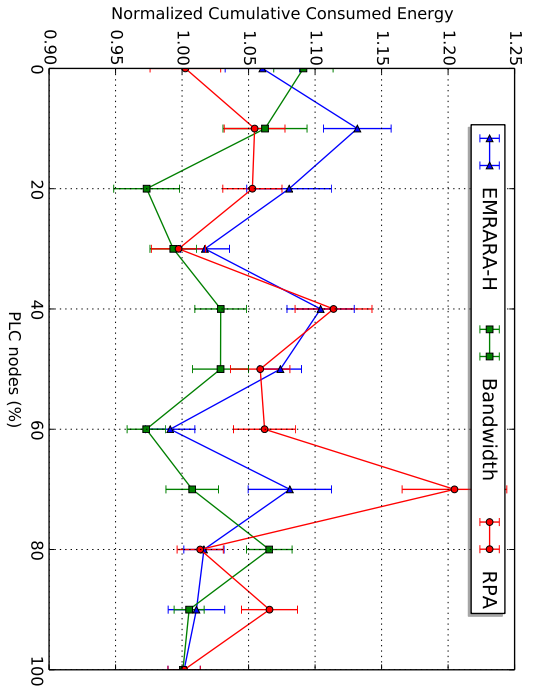
(a) 20 Nodes

(b) 60 Nodes

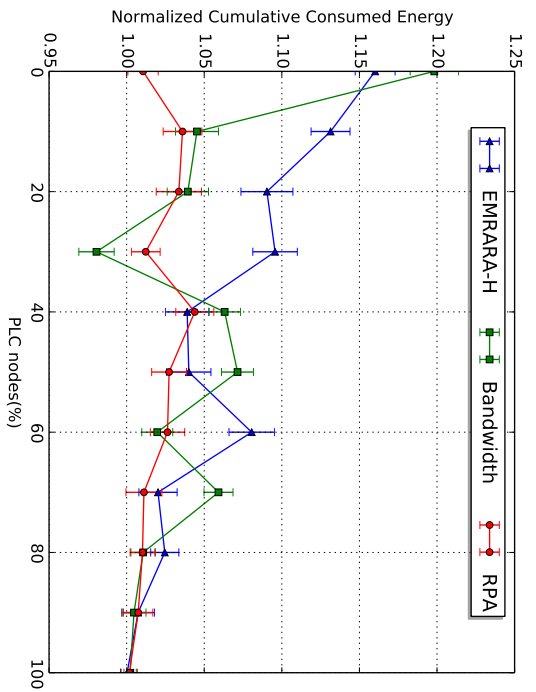


(c) 100 Nodes

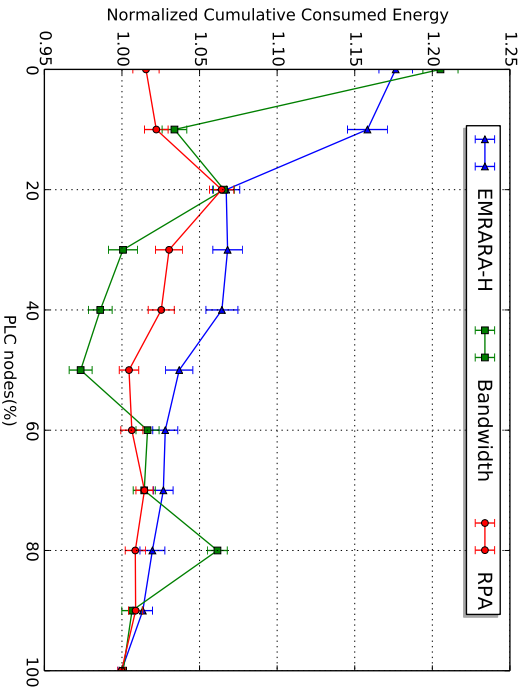
**Figure 4.9:** Normalized cumulative radiated power within the radiant-sensitive area depicted in Figure 4.4a for **UEP= 70%**. Figures represent 20, 60, 100 nodes, respectively.



(a) 20 Nodes

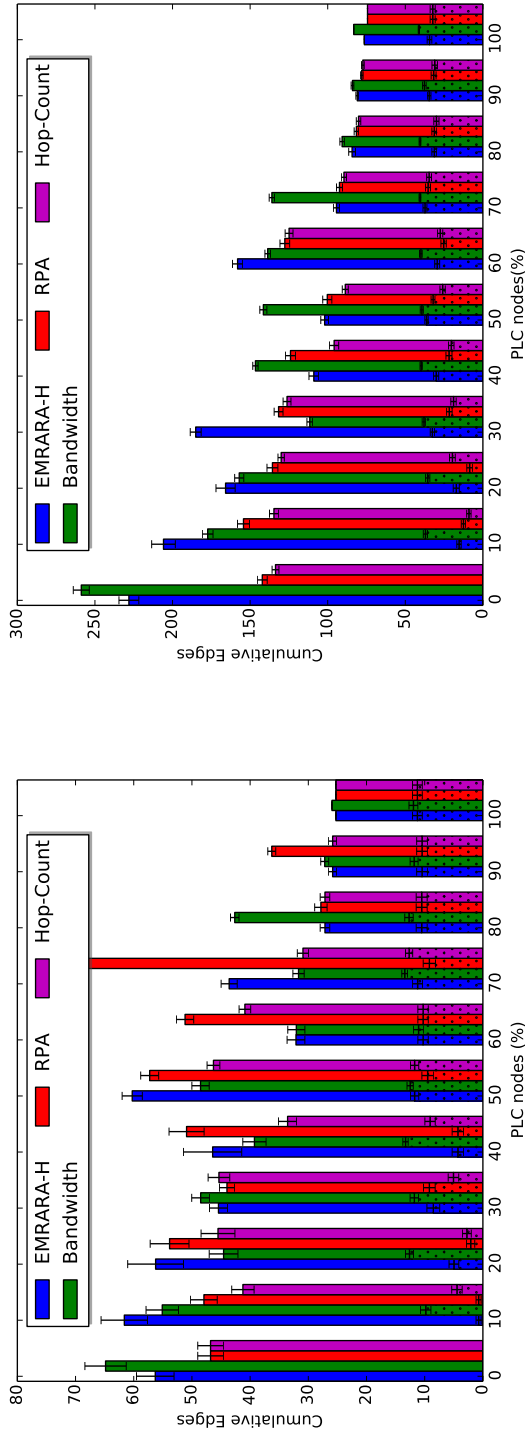


(b) 60 Nodes

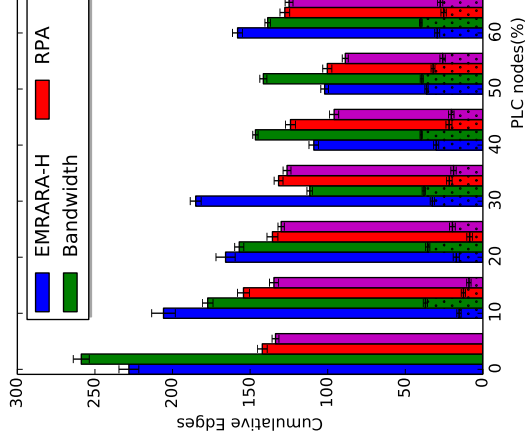


(c) 100 Nodes

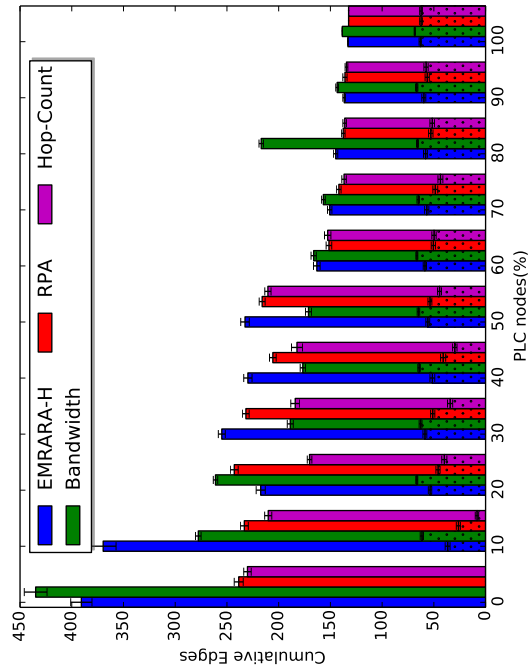
Figure 4.10: Normalized cumulative energy consumption variations with changes in network size. Figures represents 20, 60, 100 nodes, respectively



(a) 20 Nodes



(b) 60 Nodes



(c) 100 Nodes

**Figure 4.11:** Cumulative Wi-Fi and PLC (dotted bars) links number variations with changes in network size. Figures represent 20, 60 and 100 nodes respectively.

## 4.7 Conclusions

In this chapter, we have carried out numerical evaluations in order to bring out the effectiveness of our proposals on reducing radio-frequency emissions compared to other well-known routing solutions based on widely accepted metrics.

We have considered three different *green* analyses in terms of radiated energy, radiated power and energy consumption. We have investigated the impact of different parameters (network size, UE population, Wi-Fi/PLC nodes ratio). As a result, we list the most relevant conclusions:

- As a general observation, EMRARA-H is able to reduce radiated energy within a specific area with a factor of 2 with respect to Hop-Count in 80% of network configurations.
- The higher is the network density; the more effective is EMRARA-H on reducing radiated energy within the radiation-sensitive area. Clearly, owing to lack of alternative paths in small networks (e.g. 20 nodes spread in 200m\*200m square field), EMRARA can likely select the same best paths as Hop-Count algorithm.
- The nature and the number of links that make up a path from a source to a destination have definitely a direct impact on the radiated energy. Nevertheless, we have noticed that there is no linear relationship between both of them. Explicitly, let's consider two different topologies with the same network size. It may happen that a packet is crossing less hops (then less links) to reach the destination in the first configuration than in the second one, while producing more radiated energy. This is mainly due to the relative position of UEs with respect to the radiation-sensitive area.

Finally, we can mention two challenges of the proposed solution. The first is the impact on quality-of-service of making routing decisions based on minimum radiant exposure path cost. A priori our proposal will not be worse than Bandwidth algorithm since the RE metric definition incorporates in some extent link's data rate. The second is the cost in terms of energy consumption. We have noticed that EMRARA-H may lead to up to 17% more energy consumption than Hop-Count in worst cases. In order to tackle this challenge, it is necessary to investigate the possibility of eventual trade-off. This issue is the core of the next chapter.

# Multi-Criteria ElectroMagnetic Radiation-Aware Routing Algorithms

## 5.1 Introduction

In Chapter 4, we proposed and analyzed EMRARA and EMRARA-H for computing the minimum radiation exposure path in multi-hop wireless and heterogeneous networks, respectively.

In this chapter we point out that in some cases a multi-objective optimization is required. Traditionally, conventional routing algorithms find the best path from a source to a destination while considering a single QoS criterion. For home network, however, user might require additional requirements as stated in the Chapter 1, such as saving energy or reducing electromagnetic radiation for instance. Intuitively, improved data rate and radiation exposure come at the cost of more energy consumption due to the use of higher number of nodes as shown by simulations in Chapter 4. As a result, we attempt to investigate in the present chapter the possibility to reach a better compromise between required user objectives according to her/his preferences.

In the following, we present the selected multi-objective method, namely the Normalized Weighting Function, as well as some promising initial results.

## 5.2 Preliminaries

### 5.2.1 Overview & Chapter Scope

The Multi-Constrained Path (MCP) and Multi-Criteria Routing (MCR) problems are often confused although they differ significantly. They are both integral parts of the broad field of multi-objective optimization [100, 101] since they consider several conflicting criteria and seek to find an optimal solution that minimize (or maximize) these criteria. Nevertheless, the MCP problem is a sub-category of the multi-criteria routing problems and is considered in the literature as the most common formulation of them especially in QoS routing. More specifically, in the MCP problem the aim is obtain feasible path(s) that satisfy constraints related to several metrics. This routing technique is relevant mainly in multi-service Internet networks. Many attempts have been made to achieve the MCP problem resolution either using heuristics [102, 103, 104] or with exact algorithms [105, 106].

In this chapter, we treat the multi-criteria problem without any specific constraints on the routing metrics. This having said, existing solutions of the MCP problem are not necessarily in line with our assumptions and objectives.

### 5.2.2 From Multi-Criteria to Mono-Criterion Optimization

The literature abounds with several techniques that have been developed to transform multi-criteria optimization problem to single-criterion problem [105, 107]. A general formulation of finding best path is usually called the least-cost path problem. We specify this concept for the MCR problem as well as the network model and notations as follows:

**Problem 1** *Given a source  $s$  and a destination  $d$  in a directed graph  $G(V, E)$ , a weights<sup>1</sup> vector  $\vec{w} = (w_1, w_2, \dots, w_m)^T$  for each edge with respect to different criteria, the  $k$ th cost,  $k \in [1, \dots, m]$ , of a path  $\mathcal{P}_{s,d}$  is given by  $\mathcal{C}_k = \sum_{u \rightarrow v \in \mathcal{P}_{s,d}} w_k(u \rightarrow v)$  and finally a path-length function  $\mathcal{C}$  defined by:*

$$\begin{aligned} \mathcal{C} : \quad \mathbb{R}^m &\rightarrow \mathbb{R} \\ (\mathcal{C}_1, \dots, \mathcal{C}_m) &\rightarrow \mathcal{C} \end{aligned} \tag{5.1}$$

*Find a path  $\mathcal{P}_{s,d}^*$ <sup>2</sup> such that for every path  $\mathcal{P}_{s,d}$ ,*

$$\mathcal{C}(\mathcal{P}_{s,d}^*) \leq \mathcal{C}(\mathcal{P}_{s,d}) \tag{5.2}$$

---

<sup>1</sup>To not to be confused with the preference weights that will be used later in Section 5.3.1 to express the user preferences

<sup>2</sup>Same notation has been used in Section 4.3.2 and Section 4.4.3

This method allows path computation algorithms to consider a single objective function, which combines relative path costs on single *overall cost*; this objective function is called *path-length* function<sup>3</sup>.

Solving Problem 1 is based on the specification of two crucial elements:

1. Definition of the path-length function (see Equation (5.1))
2. Computation processes leading to Inequality (5.2) for every path  $\mathcal{P}_{s,d}$

The choice of the path-length function is fundamental and depends on the application field. Therefore, many researchers have combined different mechanisms corresponding to the above mentioned components. For example, interesting contributions on linear path-length functions have been proposed in [102, 107, 108]. Whereas, authors in [106, 109, 105] defined non-linear path length functions to summarize many costs in a single scalar. Regarding mechanisms to find the least cost path, the authors in [102, 104] assume centralized computations with link-state routing, a source routing is used in [103]. Yuan [110] incorporated bi-criteria optimization technique for OSPF routing to minimize network congestion and the impact of link failures. SAMCRA [105] and HMCOP [106] use centralized computations with extended Dijkstra and Bellman-Ford algorithms. And finally, Malakooti and Thomas [107] have implemented a different routing approach, consisting in a distributed solution that stores all alternative paths and before ranking them in order to choose the optimal one.

None of these solutions, however, consider the impact of optimizing electromagnetic radiation-aware criteria simultaneously with other energy and QoS criteria. Authors in [111] have proved that routing with two or more additive metrics, if simultaneously optimized, is NP hard problem. Consequently, our approach is to solve the least cost path problem (Problem 1) while considering the Normalized Weithing Function as path-length function and a Dijkstra's algorithm extension as path computation algorithm.

## 5.3 Composite Multi-Criteria Routing Algorithm

### 5.3.1 Weighting Function

We rely and adapt on one of the most used methods of Multi-Criteria Decision Making (MCDM) problem, namely, the weighting method. Introduced initially by Gass [112] and Zadeh [113], such method transforms multi-objective problem into

<sup>3</sup>A widespread term used in most papers dealing with MCR, for example [105]

a mono-objective problem while aggregating several criteria into one global cost by multiplying each objective function by a weighting factor and summing up all the weighted criteria, which amounts to minimizing (or maximizing) a single objective function (Equation (5.3)) instead of optimizing several objectives. The weighting function to be used as the path-length function is given as:

$$\mathcal{C}(\mathcal{P}_{s,d}) = \sum_{k=1}^m \gamma_k \mathcal{C}_k(\mathcal{P}_{s,d}) \quad (5.3)$$

Where  $(\gamma_1, \gamma_2, \dots, \gamma_m)$  is the set of weights of importance for each objective and  $\gamma_k \geq 0 \forall k \in [1, \dots, m]$  and, typically,  $\sum_{k=1}^m \gamma_k = 1$ . And  $\mathcal{C}_1, \mathcal{C}_2, \dots, \mathcal{C}_m$  refer to the objective functions, or in other words the path costs with respect to different independent routing criteria under consideration.

We assume here that the user is involved in the process of selecting the best path from a source to a destination in an a priori fashion; in other words, preference information,  $(\gamma_1, \gamma_2, \dots, \gamma_m)$ , is beforehand defined by from the user.

### 5.3.2 Normalization

The magnitudes of the objective functions might be different which could confuse the method. Consequently, it is much more meaningful to set the weights of importance  $(\gamma_1, \dots, \gamma_m)$  when all metrics are normalized with some scaling (e.g. 1 for the best, 0 for the worst). In this way, weights fit best to the significance of each objective. We propose thereby to normalize the edge costs while dividing  $w_k$  by the highest value,  $w_{k_{max}}$ , over the whole network. An edge cost will be noted henceforth by  $W_k$  and is given by:

$$W_k(u \rightarrow v) = \frac{w_k(u \rightarrow v)}{w_{k_{max}}} \quad (5.4)$$

Where

$$\forall k \in \{1, 2, 3\} \quad w_{k_{max}} = \max \{w_k(u \rightarrow v) \mid \forall u, v \in |V|\} \quad (5.5)$$

### 5.3.3 Objective Functions

In this case, the objective functions are defined as path sub-lengths according to each routing metric (which is the  $k$ th edge weight  $w_k$  in the Problem 1). For instance, if we consider a bi-criteria problem, namely delay and bandwidth, the first objective

function will be the sum of delay values through all links forming a path from a source to a destination. As for bandwidth the objective function will be the minimum value through that path. Our objectives are:

1. Minimize the total radiated energy within the radiation-sensitive area when transmitting data packets from a source,  $s$ , to a destination,  $d$ . This goal objective is expressed by the objective function  $\mathcal{C}_1$ , expressed in Equation (5.6).
2. Minimize the total radiated power within the radiation-sensitive area when transmitting data packets from a source,  $s$ , to a destination  $d$ . This goal objective is expressed by the objective function  $\mathcal{C}'_1$  expressed in Equation (5.7).
3. Minimize the total expected energy consumption from a source,  $s$ , to a destination,  $d$ . This goal objective is expressed by the objective function  $\mathcal{C}_2$ , expressed in Equation (5.8).
4. Maximize the end-to-end bandwidth from a source,  $s$ , to a destination,  $d$ . This goal objective is expressed by the objective function  $\mathcal{C}_3$ , expressed in Equation (5.10).

We formulate the sub-length  $\mathcal{C}_1$  of a path  $\mathcal{P}_{s,d}$  with respect to the first objective as the sum of the normalized costs of edges that make up this path expressed in Equation (5.4) and Equation (5.5):

$$\mathcal{C}_1(\mathcal{P}_{s,d}) = \sum_{(u \rightarrow v) \in \mathcal{P}_{s,d}} W_1(u \rightarrow v) = \sum_{(u \rightarrow v) \in \mathcal{P}_{s,d}} \frac{w_1(u \rightarrow v)}{w_{1max}} \quad (5.6)$$

For  $w_1$ , we chose the same formula (Equation (2.10)) described in Subsection 2.5.2 for the case of fully wireless network<sup>4</sup>. As to  $w_{1max}$ , it is calculated based on the expression presented in Equation (5.5):

$$w_1(u \rightarrow v) = \frac{P_{TX}^u}{4\pi r_u^2} \cdot \left( \frac{p}{BW_{uv}} + \beta_{uv} \right) \left( \frac{1}{1 - P_{f_{uv}}} \right)$$

We define  $\mathcal{C}'_1$  to study the impact of correlated criteria. This approach is detailed in Section 5.6. Thereby, we use alternately  $\mathcal{C}'_1$  and  $\mathcal{C}_1$  to assess electromagnetic

---

<sup>4</sup>All parameters are given in Table 2.2.

radiation.  $\mathcal{C}'_1$  is then formulated as follows:

$$\mathcal{C}'_1(\mathcal{P}_{s,d}) = \sum_{(u \rightarrow v) \in \mathcal{P}_{s,d}} W'_1(u \rightarrow v) = \sum_{(u \rightarrow v) \in \mathcal{P}_{s,d}} \frac{w'_1(u \rightarrow v)}{w'_{1max}} \quad (5.7)$$

$w'_1$  is defined in such a way that the correlation term,  $\left(\frac{p}{BW_{uv}} + \beta_{uv}\right) \left(\frac{1}{1-P_{fuv}}\right)$ , from the bandwidth definition cancels out. It is given by:

$$w'_1(u \rightarrow v) = \frac{P_{TX}^u}{4\pi r_u^2}$$

Even under perfect conditions, packets can be lost through wireless links due to various factors, such as fading, interference, multi-path effects and collisions. Hence, a packet may likely be transmitted more than once. Assuming a hop-by-hop retransmission model [61], we formulate  $\mathcal{C}_2$  as follows:

$$\mathcal{C}_2(\mathcal{P}_{s,d}) = \sum_{(u \rightarrow v) \in \mathcal{P}_{s,d}} W_2(u \rightarrow v) = \sum_{(u \rightarrow v) \in \mathcal{P}_{s,d}} \frac{w_2(u \rightarrow v)}{w_{2max}} \quad (5.8)$$

Where

$$w_2(u \rightarrow v) = N(u, v) \cdot P_{TX}^u \quad (5.9)$$

is the expected energy consumption of successfully delivering a packet over the link  $u \rightarrow v$ , and  $N(u, v)$ <sup>5</sup> denotes the expected number of transmissions for a packet to be successfully delivered over that link.

Regarding  $\mathcal{C}_3$ , the purpose is to maximize the end-to-end bandwidth. Nevertheless, to be in line with the global problem (Problem 1) we define a suitable link cost:

$$w_3(u \rightarrow v) = \frac{1}{BW(u \rightarrow v)}$$

Where  $BW(u \rightarrow v)$  is the capacity of the link  $u \rightarrow v$ , and similarly the objective

---

<sup>5</sup>Similar to ETX definition [97].

function is then expressed as follows:

$$\mathcal{C}_3(\mathcal{P}_{s,d}) = \sum_{(u \rightarrow v) \in \mathcal{P}_{s,d}} W_3(u \rightarrow v) = \sum_{(u \rightarrow v) \in \mathcal{P}_{s,d}} \frac{w_3(u \rightarrow v)}{w_{3max}} \quad (5.10)$$

## 5.4 Implementation

Similarly to the previous chapter, we have designed a software simulator based on the graph library NetworkX [99]. We made the same network assumptions as in Subsection 4.3.1 (i.e. a fully wireless network). Moreover, we assume a global routing scheme, which means that each node possesses complete knowledge of the entire network topology and the link costs.

Regarding path selection operations, we need first to assign to each edge a vector of normalized costs  $\vec{W} = (W_1, W_2, \dots, W_m) = (\frac{w_1}{w_{1max}}, \frac{w_2}{w_{2max}}, \dots, \frac{w_m}{w_{mmax}})$ . This is implemented as a separate routing table with respect to each criterion (also metric). Then, a shortest path corresponding to a given combination of preference weights and the normalized criteria (i.e.  $\sum_{k=1}^m \gamma_k W_k$ ) is calculated using a modified version of Dijkstra's algorithm. We propose in Algorithm 5 only the *edge relaxation step*. Moreover, we need at the onset to normalize links' costs. This is has been accomplished by the pseudo-code presented by Algorithm 4

---

**Algorithm 4:** Pseudo-code for normalizing the cost of the edge  $(u \rightarrow v)$  with respect to the  $k$ th criterion

---

```

1 Normalize( $G, k, u, v$ )
2 maxvalue = None
3 for each  $(x \rightarrow y) \in E$  do
4   if maxvalue  $\leq w_k(x \rightarrow y)$  then
5     maxvalue =  $w_k(x \rightarrow y)$ 
6 norm-metric =  $\frac{w_k(x \rightarrow y)}{\text{maxvalue}}$ 
7 return norm-metric
```

---

---

**Algorithm 5:** 'Relaxation' pseudo-code for multi-criteria edge cost

---

```

1 for each neighbor  $v$  of  $u$  do
2   for each  $k$  in  $[1, m]$  do
3      $W_k = \text{Normalize}(G, k, u, v)$ 
4      $\text{newlength}(u, v) = \gamma_1.W_1 + \dots + \gamma_m.W_m$ 
5     if  $\text{dist}[u] + \text{newlength}(u, v) < \text{dist}[v]$  then
6        $\text{dist}[v] = \text{dist}[u] + \text{newlength}(u, v)$ 

```

---

More specifically, each node measures individual-level metrics and uses an extended version of Dijkstra's algorithm to calculate best paths to all other nodes by assessing the composite cost, which is the normalized weighted sum of the separated metric values. Finally, each  $m$ -tuple of preference weights  $(\gamma_1, \gamma_2, \dots, \gamma_m)$  corresponds to a new execution of the algorithm. This has been presented in Subsection 5.5.3.

## 5.5 Evaluations & Results

### 5.5.1 Experimental Methodology

We conduct simulations in our empirical study based on the implementation described in Section 5.4, in order to answer the question: *There is a direct implication between the preference weights and simulations outcomes?* In addition, we wanted to study the effectiveness of the composite path costs compared to single metrics optimized individually.

Similarly as in Subsection 4.6.2,  $N$  nodes of the same transmission range are randomly distributed into a  $200m \times 200m$  square field. 500 trial networks are then generated. For each trial we randomly pick a set of nodes to be UE<sup>6</sup>, and from this set we randomly pick again a single UE that will receive the traffic from the HG. Then, the average of the different performance metrics of the best paths from the HG to a UE computed in all 500 trials are calculated for the different algorithms to be compared.

### 5.5.2 Evaluation Metrics

In the previous chapter we used cumulative performance metrics for all shortest paths from HG to all UE, and normalized them with respect to the Hop-Count (See

---

<sup>6</sup>Previously defined in Subsection 4.3.1.

Subsection 4.6.1 and Subsection 4.6.3). In this chapter, we calculate the performance for a single path between the HG and a randomly picked UE. We then use three different evaluation metrics:

- Radiant Exposure: The average over  $M$  trials of the cost of the shortest path from the HG to a given UE,  $\mathcal{P}_{HG,UE}^*$ , in terms of radiant exposure. We express this as follows:

$$\text{Radiant Exposure} = \frac{1}{M} \sum_{i=1}^M \sum_{(u \rightarrow v) \in (\mathcal{P}_{HG,UE}^*)^i} w_1(u \rightarrow v)$$

- Radiated Power: The average over  $M$  trials of the cost of the shortest path from the HG to a given UE,  $\mathcal{P}_{HG,UE}^*$ , in terms of power density. We express this as follows:

$$\text{Radiated Power} = \frac{1}{M} \sum_{i=1}^M \sum_{(u \rightarrow v) \in (\mathcal{P}_{HG,UE}^*)^i} w'_1(u \rightarrow v)$$

- energy consumption: The average over  $M$  trials of the cost of the shortest path from the HG to a given UE,  $\mathcal{P}_{HG,UE}^*$ , in terms of expected energy consumption (see Equation (5.9)). In the same way, we express this as follows:

$$\text{energy consumption} = \frac{1}{M} \sum_{i=1}^M \sum_{(u \rightarrow v) \in (\mathcal{P}_{HG,UE}^*)^i} w_2(u \rightarrow v)$$

In our study we performed  $M = 500$  trials for the evaluation of each metric.

### 5.5.3 Numerical Results

Our goal is to analyze how a Dijkstra-based shortest path algorithm behaves in the context of conflicting routing criteria weighted by user preferences. We chose to depict simulation results for the three following user-oriented preference groups:

1.  $\mathcal{G}_1$ : All criteria are important:  $(\frac{1}{3}\mathcal{C}_1 + \frac{1}{3}\mathcal{C}_2 + \frac{1}{3}\mathcal{C}_3)$ ,  $(\frac{1}{3}\mathcal{C}'_1 + \frac{1}{3}\mathcal{C}_2 + \frac{1}{3}\mathcal{C}_3)$
2.  $\mathcal{G}_2$ : Energy does not matter:  $(\frac{1}{3}\mathcal{C}_1 + \frac{1}{3}\mathcal{C}_3)$ ,  $(\frac{1}{3}\mathcal{C}'_1 + \frac{1}{3}\mathcal{C}_3)$
3.  $\mathcal{G}_3$ : Bandwidth does not matter:  $(\frac{1}{3}\mathcal{C}_1 + \frac{1}{3}\mathcal{C}_2)$ ,  $(\frac{1}{3}\mathcal{C}'_1 + \frac{1}{3}\mathcal{C}_2)$

We present here results for  $M = 500$  trials, run each time on  $\mathbf{N}$  wireless network nodes, in order to highlight how selecting different weight combinations according to users' preferences will lead to different outcomes. The results in Figure 5.1, Figure 5.2 and Figure 5.3 show that averages of expected energy consumption, radiant exposure, and radiated power vary in accordance to weights assigned for each criterion.

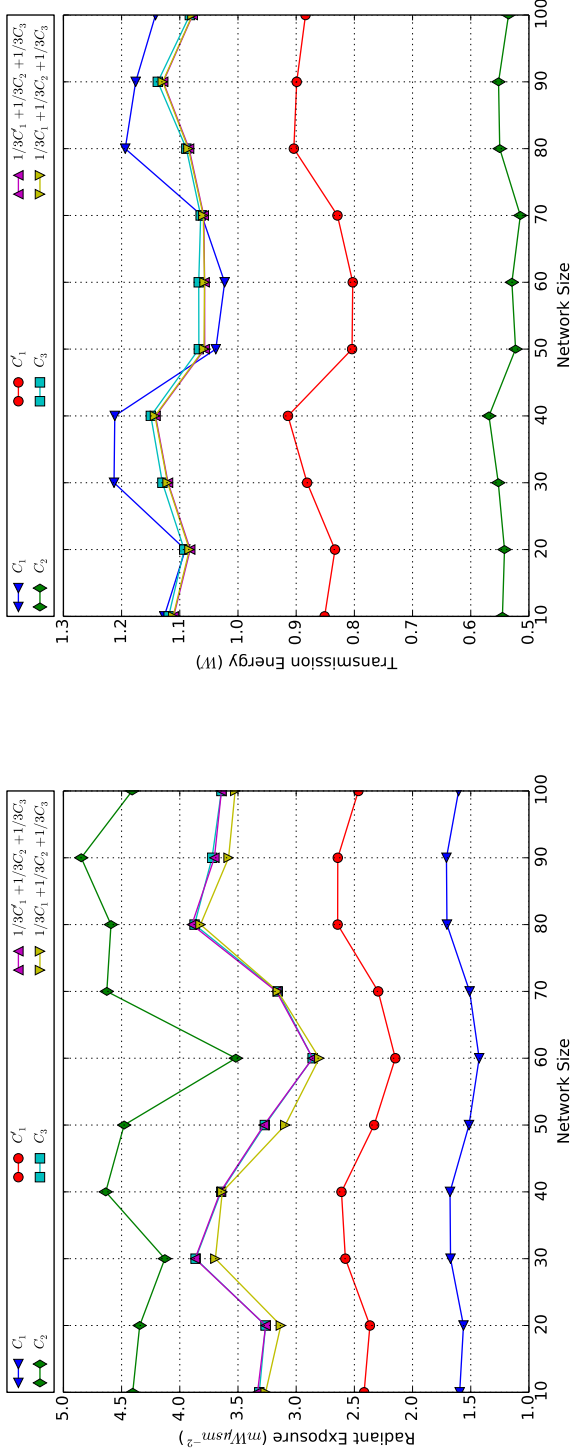
**Results for  $\mathcal{G}_1$ :** From Figure 5.1a, both combinations  $(\frac{1}{3}\mathcal{C}_1 + \frac{1}{3}\mathcal{C}_2 + \frac{1}{3}\mathcal{C}_3)$  and  $(\frac{1}{3}\mathcal{C}'_1 + \frac{1}{3}\mathcal{C}_2 + \frac{1}{3}\mathcal{C}_3)$  lead to less amount of radiant exposure than  $\mathcal{C}_2$  and  $\mathcal{C}_3$  optimized individually while conserving almost the same amount of energy consumption as  $\mathcal{C}_3$ , as depicted in Figure 5.1b.

The combinations  $(\frac{1}{3}\mathcal{C}_1 + \frac{1}{3}\mathcal{C}_2 + \frac{1}{3}\mathcal{C}_3)$  and  $(\frac{1}{3}\mathcal{C}'_1 + \frac{1}{3}\mathcal{C}_2 + \frac{1}{3}\mathcal{C}_3)$  generate significantly more radiant exposure than  $\mathcal{C}_1$  and  $\mathcal{C}'_1$  respectively (Figure 5.1a). However they outperform them in most cases in terms of energy consumption (Figure 5.1b).

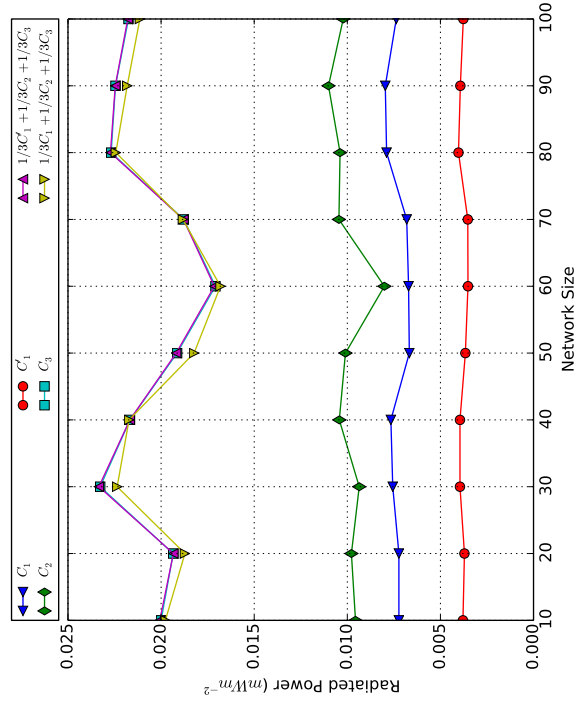
Unlike what was expected, the shortest path algorithm with the combination  $(\frac{1}{3}\mathcal{C}_1 + \frac{1}{3}\mathcal{C}_2 + \frac{1}{3}\mathcal{C}_3)$  outperforms the algorithm with the combination  $(\frac{1}{3}\mathcal{C}'_1 + \frac{1}{3}\mathcal{C}_2 + \frac{1}{3}\mathcal{C}_3)$  in terms of radiated power as depicted in Figure 5.1c. Indeed, it is evident from Figure 5.1c that it is the bandwidth criterion ( $\mathcal{C}_3$ ) which prevailed over the other criteria. As already explained in Subsection 2.7.1, radiated power is an instantaneous quantity, which depends only on the number of radiating sources and their distances from the radiation-sensitive area. Hence, while looking for better paths in terms of link capacity,  $\mathcal{C}_3$  and thus  $(\frac{1}{3}\mathcal{C}'_1 + \frac{1}{3}\mathcal{C}_2 + \frac{1}{3}\mathcal{C}_3)$  may select paths composed by more links and then more radiating sources, which justifies their higher amount of radiated power.

**Results for  $\mathcal{G}_2$ :** It is noticeable from Figure 5.2a and Figure 5.2c, that both combinations  $(\frac{1}{2}\mathcal{C}_1 + \frac{1}{2}\mathcal{C}_3)$  and  $(\frac{1}{2}\mathcal{C}'_1 + \frac{1}{2}\mathcal{C}_3)$  outperform  $\mathcal{C}_3$  in terms of radiant exposure and radiated power while interestingly consuming the same amount of energy consumption as shown in Figure 5.2b.

There are two clear messages from Figure 5.2b. On one hand, even though the combination  $(\frac{1}{3}\mathcal{C}_1 + \frac{1}{3}\mathcal{C}_3)$  radiates more energy than  $\mathcal{C}_1$  (Figure 5.2a), it clearly consumes less energy consumption. On the other hand, since energy consumption is not taken into account in this cluster, we can notice the important gap between  $\mathcal{C}_2$  and  $(\frac{1}{2}\mathcal{C}_1 + \frac{1}{2}\mathcal{C}_3)$ .

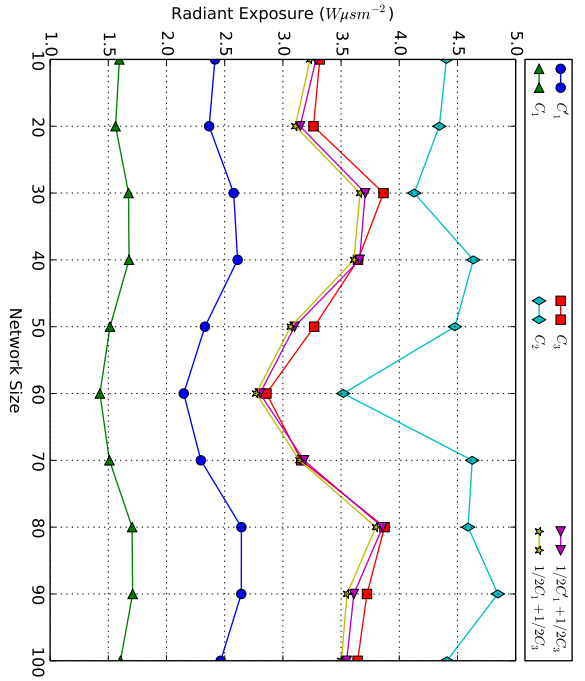


(a) Average Radiant Exposure for the shortest path between the HG and a UE. (b) Average Expected energy consumption for the shortest path between the HG and a UE.

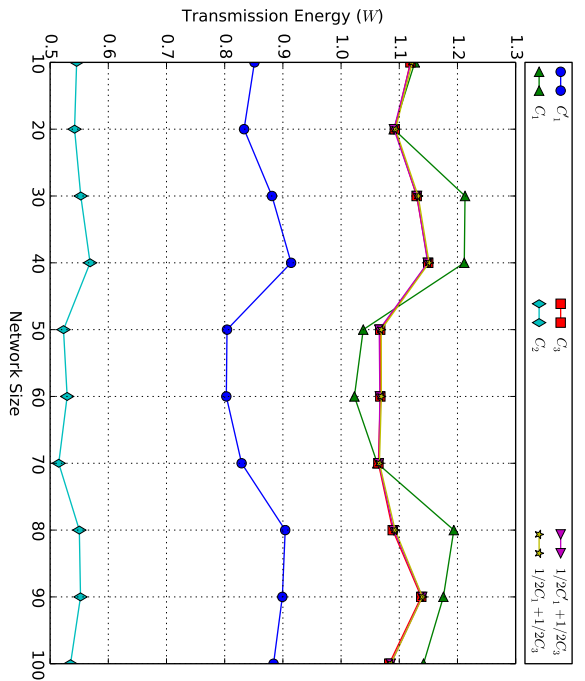


(c) Average Radiated Power for the shortest path between the HG and a UE.

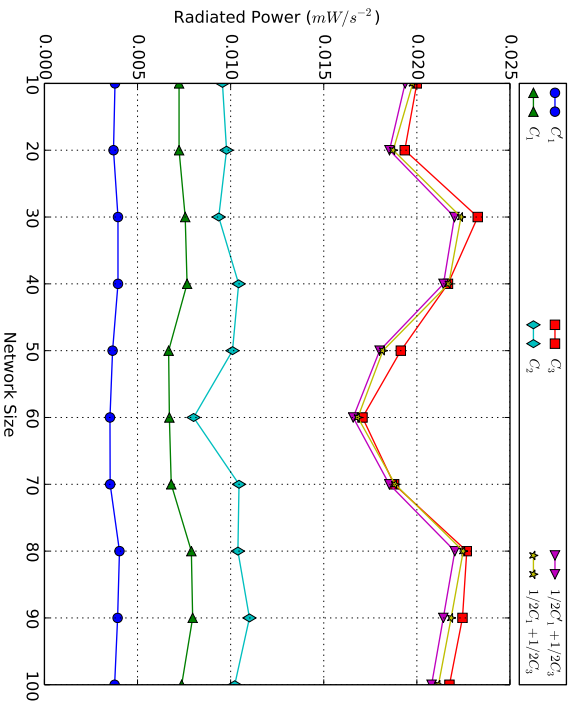
Figure 5.1: Simulation results for the shortest path between the HG and a UE with respect to algorithms of the cluster  $\mathcal{G}_1$ .



(a) Average Radiant Exposure

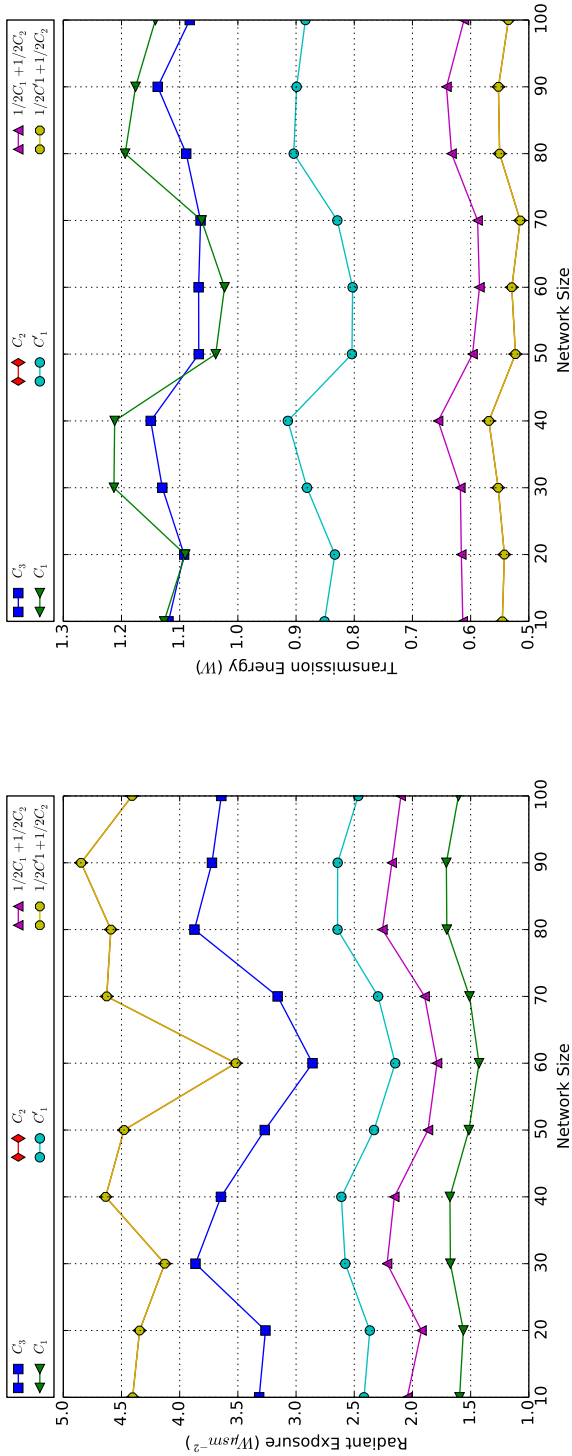


(b) Average Expected energy consumption

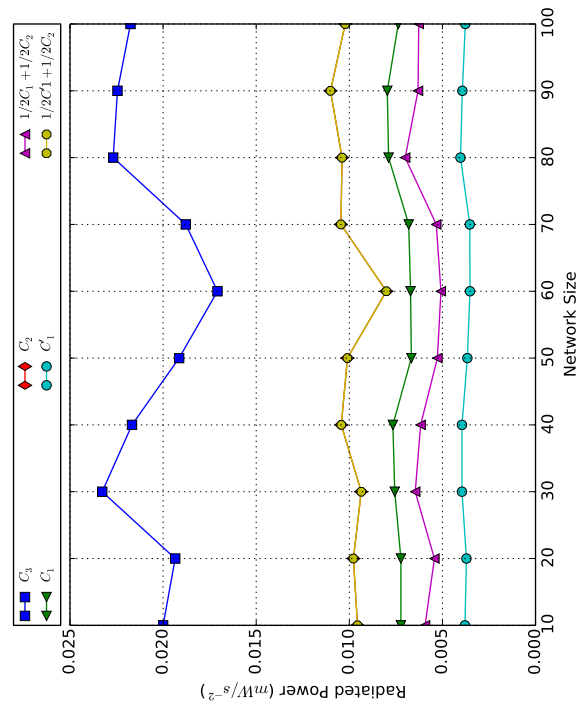


(c) Average Radiated Power

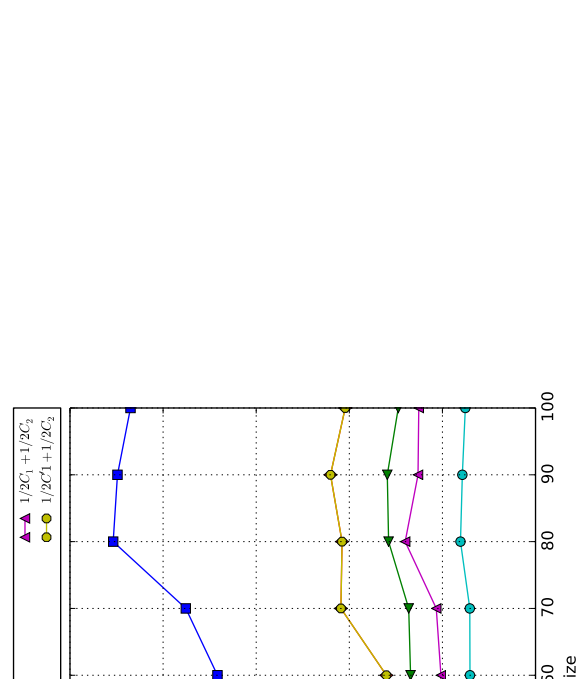
Figure 5.2: Simulation results for the shortest path between the HG and a UE with respect to algorithms of the cluster  $G_2$ .



(a) Average Radiant Exposure



(b) Average Expected energy consumption



(c) Average Radiated Power

Figure 5.3: Simulation results for the shortest path between the HG and a UE with respect to algorithms of the cluster  $\mathcal{G}_3$ .

Finally, the criteria combination  $(\frac{1}{2}\mathcal{C}'_1 + \frac{1}{2}\mathcal{C}_3)$  is not really interesting, since it is worse than  $\mathcal{C}'_1$  and  $\mathcal{C}_3$  optimized individually in terms of radiant exposure (Figure 5.2a) and expected energy consumption (Figure 5.2b). Even though we notice, from Figure 5.2c, a slight decrease in radiated power compared to  $\mathcal{C}_3$ , this is straightforward since the criterion of power density, i.e.  $\mathcal{C}'_1$ , has been taken into consideration in the combination  $(\frac{1}{2}\mathcal{C}'_1 + \frac{1}{2}\mathcal{C}_3)$ .

**Results for  $\mathcal{G}_3$ :** Similarly, regarding this cluster of algorithms, the combination  $(\frac{1}{2}\mathcal{C}_1 + \frac{1}{2}\mathcal{C}_2)$  reduces radiant exposure by almost two compared to  $\mathcal{C}_2$  (Figure 5.3a) while generating 20% more energy consumption (Figure 5.3b). Interestingly, from Figure 5.3a,  $(\frac{1}{2}\mathcal{C}_1 + \frac{1}{2}\mathcal{C}_2)$  generates almost 30% more radiant exposure than  $\mathcal{C}_1$  whereas it reduces by two the energy consumption (Figure 5.3b).

Surprisingly in Figure 5.3, the combination  $(\frac{1}{2}\mathcal{C}_1 + \frac{1}{2}\mathcal{C}_2)$  leads to the exact same simulation results in terms of the three performance metrics than  $\mathcal{C}_2$ . We have interpreted these unexpected outcomes in Section 5.6.

## 5.6 Limitations

The weighting method, although being conceptually straightforward, may not always behave as expected. Weights are often said to reflect the relative importance of the objective functions (i.e., giving the the predominant weight to the most important criterion) but, for example, the combination  $(\frac{1}{3}\mathcal{C}_1 + \frac{1}{3}\mathcal{C}_2 + \frac{1}{3}\mathcal{C}_3)$  leads to almost same radiant exposure and energy consumption results as  $(\mathcal{C}_3)$ . One of the reasons why the weighting method may not lead to satisfactory results is that if some of the objective functions may correlate with each other; in our case, the radiant exposure metric (i.e  $\mathcal{C}_1$ ) is by definition a function of the expected packet time which depends itself on the bandwidth (i.e.  $\mathcal{C}_3$ ). In this case, changing the weights may not produce the expected results. Instead, seemingly bad weights may result in satisfactory solutions and vice versa. This has been shown for more general MCDM problems [114, 115]. Thus, the undesired outcome may be explained by the compensatory character of the weighting method.

## 5.7 Conclusions

In this chapter, we have adapted a primary multi-objective approach for MCR problems which considers factors that can be either predicted or calculated from network information readily available to each node. This is done in order to meet most of the requirements that we have presented in a previous contribution [P3]. In the

same context, we have considered three different *green* analyses in terms of radiated energy, radiated power, and expected energy consumption. Each time, we have investigated the performance metrics for the shortest path between the HG and a given UE with respect to the compared algorithms. To summarize, we list the most relevant contributions of the present chapter:

- We have shown by simulations that in most cases, outcomes of shortest path algorithms having as path-length a composite weighted cost closely follow the user preference weights.
- When combining a radiation-aware criterion (i.e.  $\mathcal{C}_1$  and  $\mathcal{C}_1$ ) with other criteria, algorithms having as path-length functions these combinations might select paths that generate more radiation than the radiation-aware algorithm (e.g.  $\mathcal{C}_1$  and  $\mathcal{C}_1$  optimized individually). In return, they remarkably reduce the energy consumption. Therefore, we can state that these composite costs guarantee a good trade-off between conflicting criteria.
- In some cases, we could have unexpected results, particularly when two or more criteria are correlated (e.g.  $\mathcal{C}_1$  and  $\mathcal{C}_3$ ).

Finally, this study further enhances our understanding of MCR problem challenges when considering *green* criteria (i.e. EM radiation and energy consumption). A future work could extend the presented multi-objective approach in order to tackle the problem of criteria correlation and also to investigate the impact on quality-of-service (e.g. throughput, delay, ...).



# Conclusions & Perspectives

## 6.1 Conclusions

It has been a challenging goal to make path selection based on ecological criteria that are closely linked to the external environment (e.g. EM radiation); instead of the conventional routing metrics inherently dependent on network state (e.g. delay). In this thesis, we have developed a new concept of radiation-aware routing algorithm for heterogeneous home networks in order to reduce radiated emissions level within a given area.

As we aimed to design a new electromagnetic radiation-aware routing metric, it was logical to start by studying EMFs stemming from wireless and wired technologies that a home network might host. First we have thoroughly discussed and analyzed the issues pertaining to modeling such emissions from both Wi-Fi and PLC devices. Then, we have reviewed the most used techniques for this aim and showed why they do not meet our goals. A good understanding of the phenomenon in the context of data routing lead us to define a set of appropriate assumptions and methods. Two theoretical models were developed in order to define a single value for each Wi-Fi and PLC link respectively, that captures its contribution to the cumulative radiation during data transmission.

We have pioneered the Radiant Exposure (RE) quantity, which is a new routing metric for finding minimum radiated emissions paths in multi-hop heterogeneous network. The RE of a path is the expected radiated energy in units of  $\frac{W}{m^2} \cdot s$ , within the radiation-sensitive area, while transmitting a packet along that path. The RE

of a path  $\mathcal{P}$  in a heterogeneous network is link-adaptive and it is calculated as:

$$RE(\mathcal{P}) = \sum_{u \rightarrow v \in \mathcal{P}} \alpha_{u,v} w_{Wi-Fi}(u \rightarrow v) + \beta_{u,v} w_{PLC}(u \rightarrow v) \quad (6.1)$$

Where

$$w_{Wi-Fi}(u \rightarrow v) = \frac{P_{TX}^u}{4\pi r_i^2} * EPT_{uv} \quad (6.2)$$

$$w_{PLC}(u \rightarrow v) = \sum_{B_n \in u \rightarrow v} \frac{30\pi I_{max}^{B_n}{}^2}{4\pi r_{B_n}^2} . EPT_{uv} \left(1 - \cos\left(\pi \frac{B_n}{\lambda}\right)\right)^2 \quad (6.3)$$

$$\alpha_{u,v} = \begin{cases} 1 & \text{if } u \rightarrow v \text{ is a Wi-Fi link} \\ 0 & \text{otherwise} \end{cases} \quad (6.4)$$

$$\beta_{u,v} = \begin{cases} 1 & \text{if } u \rightarrow v \text{ is a PLC link} \\ 0 & \text{otherwise} \end{cases} \quad (6.5)$$

It is worthwhile to mention that the RE metric incorporates the effects of the distance between the radiating sources and the radiation-sensitive area as well as the asymmetry of this radiated energy regarding the two directions of each link. We have studied both effects in the context of this thesis.

Before any implementation, we have investigated the RE metric properties in the light of well-known routing algebra [10, 11]. Moreover, we have discussed both Wi-Fi and PLC EMF models inaccuracies; we have as well shown that such inaccuracies have only a slight effect on the solution performances.

We have proposed and implemented a novel electromagnetic radiation-aware algorithm (EMRARA) for multi-hop wireless networks so that it uses the RE formulation for Wi-Fi links (i.e Equation 6.2), as well as an extension for multi-hop heterogeneous networks (EMRARA-H) which is a modification of Dijkstra's algorithm to support parallel edges in a multi-graph. Specifically, we provided the different implementation steps for both use cases (fully wireless and heterogeneous networks). We have carried out extensive simulations with the aim of emphasizing the effectiveness of

both algorithms to carry data away from a given area in the home environment meaning that they reduce significantly the instantaneous and the time-averaged radio-frequency emissions.

Based on the conclusions of the previous analyses, we have proposed a multi-criteria routing algorithm that combines two green criteria, namely the expected transmission energy and the radiant exposure, with a QoS criterion namely bandwidth. This has been ensured by the adaptation of the weighting function (one of the MCDM methods) for routing purposes. We have then investigated and compared algorithms arising out of different combinations between criteria and preference weights. Extensive simulations lead us to derive the following most relevant conclusions:

- Multi-criteria solution outcomes follow closely the preferences of an end user (expressed as weights).
- Using composite path costs guarantees good trade-off between radiated energy and energy consumption.

Therefore, we are convinced that our contributions represent a first step in the direction of the full understanding of the radiation-aware routing paradigm.

## 6.2 Perspectives & Future Work

Further studies could investigate the following points. Analyzing the impact on the QoS (e.g. the end-to-end delay, throughput,...) of making path decisions based on external environment-dependent metrics. To do so, we have initiated an implementation work with the Quagga [116] software in the simulator NS3 [117]. From a set of well-established routing protocol candidates, for both wired and multi-hop wireless networks, we should choose the most convenient protocol for our network assumptions. An extension of the Open Shortest Path First (OSPF) protocol might guarantee the interpretability between wireless and the wired networks. Furthermore, OSPF appears within the list of candidates advocated by the homenet working group at the IETF. Adopting OSPF for a multi-hop heterogeneous network will not be an easy task. First, RE formulation should be transformed from a link cost to an interface cost. Then, the main difficulty would stem from the asymmetrical nature of the RE metric, so that all OSPF mechanisms based on the bi-directional assumption of the network have to be reconsidered.

Our work could be extended in various research directions. It would be interesting to consider other kind of electromagnetic radiation sources that likely exist in home

---

network, namely 60GHz devices which require suitable EMFs models to formulate and adapt the composite radiation metric. Regarding the MCR problem, it has been shown that, albeit rarely, we get some unexpected results that do not match the preference weights. The reason is twofold: *i)* the eventual correlation between criteria *ii)* the multi-criteria method is used in a priori method, i.e. the user is expected to be able to represent his/her preferences in the form of weights. However, the desired preferences expressed by weights lead sometimes to unsatisfactory results. One solution could be to change the process from a priori to interactive fashion, where a given mechanism (or learning algorithm) tries to guess such weights that would produce a satisfactory trade-offs between different criteria.

# Acronyms

ACK	Acknowledgment.
AODV	Ad hoc On-Demand Distance Vector.
AP	Access Point.
AWGN	Additive White Gaussian Noise.
BAMER	Basic Algorithm for Minimum Energy Routing.
CISPR	International Special Committee on Radio Interference.
CMMBCR	Conditional Max-Min Battery Capacity Routing.
CMRPC	Conditional Maximum Residual Packet Capacity.
CPU	Central Processing Unit.
CST	Computer Simulation Technology.
DSR	Dynamic Source Routing.
EMC	ElectroMagnetic Compatibility.
EMF	ElectroMagnetic Field.
EMI	ElectroMagnetic Interference.
EMRARA	ElectroMagnetic Radiation Aware Routing Algorithm.
EPT	Expected Packet Time.
ETX	Expected Transmission Count.
FDTD	Finite Difference Time Domain.
FEM	Finite Element Method.

---

FS	free space.
H-EMRARA	ElectroMagnetic Radiation Aware Routing Algorithm for Heterogeneous home network.
HD	High Definition.
HF	High Frequency.
HG	Home Gateway.
ICNIRP	International Commission on Non-Ionizing Radiation Protection.
ICT	Information and Communication Technology-enabled.
IEEE	Institute of Electrical and Electronics Engineers.
IETF	Internet Engineering Task Force.
ITE	Information Technology Equipment.
MAC	Medium Access Control.
MANET	Mobile Ad hoc NETwork.
MBCR	Minimal Battery Cost Routing.
MCDM	Multi-Criteria Decision Making.
MCP	Multi-Constrained Path.
MCR	Multi-Criteria Routing.
MCS	Modulation and Coding Scheme.
MMBCR	Min-Max Battery Cost Routing.
MoCA	Multimedia over Coax Alliance.
MoM	Method of Moments.
MR/FDTD	Multiple-Region Finite-Difference Time-Domain.
MTP	Minimal Total Power.
NEC	Numerical Electromagnetics Code.
OSPF	Open Shortest Path First.
PARO	Power-Aware Routing Optimization.
PER	Packet Error Rate.
PLC	Power Line Communication.
QoS	Quality of Service.

RE	Radiant Exposure.
SAR	Specific Absorption Rate.
SD	Standard Definition.
STB	Set Top Box.
TARA	Thermal-Aware Routing Algorithm.
TGn	High Throughput Task Group.
TR	Reversal Technique.
UE	User Equipement.
VoIP	Voice over IP.
WSN	Wireless Sensor Network.



# Appendix A

## Résumé en Français

Les produits et les technologies de communication ont connu durant la dernière décennie des améliorations importantes en termes de diversification de services, ceci a changé la vision des réseaux domestiques.

Les maisons d'aujourd'hui hébergent des équipements de plus en plus sophistiqués offrant une large gamme de services comme HDTV, VoIP, le stockage multimédia, etc. Cette extension technologique n'est pas sans conséquences. En effet, les équipements des Technologies d'Information et de la Communication (TIC) consomment pratiquement un quart de la consommation totale d'électricité dans une maison typique en France, ce qui met en avant la question d'efficacité énergétique dans les réseaux domestiques.

En outre, les émissions électromagnétiques deviennent de plus en plus omniprésentes au sein des maisons, ceci peut inquiéter une tranche importante des utilisateurs, cela peut également ralentir les futures innovations des technologies sans fil. Toutefois, l'augmentation de la connectivité peut aider à résoudre ces problèmes en désactivant les équipements redondants ou en sélectionnant des chemins plus appropriés dans le réseau. Le problème peut être perçu comme un protocole de routage multicritère avec l'introduction de nouvelles métriques vertes. Par conséquent, une solution de routage pour réseau domestique doit supporter des contraintes supplémentaires en parallèle avec celles de QoS.

Nous avons commencé par donner une vue d'ensemble du vaste domaine des maisons intelligentes. Nous avons ainsi présenté quelques solutions dans la littérature visant à optimiser les mécanismes de gestion du réseau dans un environnement domestique. Nous avons par la suite mis l'accent sur les solutions de routage, en

particulier celles qui prennent en considération les exigences vertes de l'utilisateur. Plus précisément, ces exigences concernent l'économie d'énergie et la minimisation des rayonnements électromagnétiques. A travers cet état de l'art, nous avons pu souligner l'absence d'une solution de routage qui répond à ces objectifs écologiques dans un environnement spécifique qui est l'environnement domestique. Cela constitue la principale motivation de ces travaux.

Dans le but de satisfaire les exigences de l'utilisateur préalablement mentionnées, cette thèse contient principalement trois contributions. La première contribution consiste à la proposition d'un nouveau concept de métrique de routage sensible aux rayonnements électromagnétiques, cette métrique peut être utilisée sans modifications avec n'importe quel algorithme de plus court chemin. Elle est désormais nommée Radiant Exposure (RE).

Dans le but d'exprimer RE pour les liens Wi-Fi et CPL (Courant Porteur en Ligne), qui sont les deux technologies les plus présentes dans les foyers d'aujourd'hui, nous avons détaillé notre premier modèle analytique des champs électromagnétiques rayonnés par les équipements Wi-Fi et notre deuxième modèle des champs électromagnétiques provenant des lignes électriques quand celles-ci transportent des données en hautes fréquences. Mais avant tout, nous avons discuté exhaustivement les problèmes liés à la modélisation d'un tel phénomène physique pour des fins de routage. Ce qui nous a amené à considérer un ensemble d'hypothèses simplificatrices ainsi qu'un ensemble de méthodes mathématiques appropriées. Ceci nous a conduit à quantifier les erreurs liés aux approximations du modèle choisi, et montrer par la suite que quoique théoriques ces approximations rejoignent nos exigences.

L'objectif majeur de ces deux modèles est de fournir une valeur unique pour chaque lien qu'il soit Wi-Fi ou CPL permettant de caractériser sa contribution dans l'énergie rayonnée cumulée pendant la transmission des données.

Ainsi la valeur de la métrique RE pour un lien Wi-Fi direct entre un nœud  $u$  ayant une puissance de transmission  $P_{TX}^u$  et un nœud  $v$  est exprimée comme suit :

$$w_{Wi-Fi}(u \rightarrow v) = \frac{P_{TX}^u}{4\pi r_u^2} \cdot \left( \frac{L}{BW_{uv}} + \beta_{uv} \right) \left( \frac{1}{1 - P_{f_{uv}}} \right)$$

Où  $r_u$  est la distance entre le nœud émetteur  $u$  et le point d'investigation,  $L$  est la taille du paquet,  $BW_{uv}$  est la capacité du lien  $u \rightarrow v$ ,  $\beta_{uv}$  est le délai de propagation et  $P_{f_{uv}}$  est la probabilité d'erreur du lien  $u \rightarrow v$ .

Quant à l'expression de la métrique RE pour un lien "logique" CPL entre un nœud  $u$  et un nœud  $v$  qui est généralement composé physiquement de plusieurs branches de lignes électriques linéaires de longueurs  $B_n$ , est donnée comme suit :

$$w_{CPL}(u \rightarrow v) = \sum_{k=1}^N 7.5 \frac{I_{max}^{B_n}{}^2}{r_{B_n}^2} \left(1 - \cos\left(\pi \frac{B_n}{\lambda}\right)\right)^2 \cdot EPT_{uv}$$

Où  $N$  est le nombre de branches linéaires qui composent le lien CPL "logique",  $I_{max}^{B_n}$  est le courant électrique maximal à travers la branche  $B_n$ ,  $r_{B_n}$  est la distance entre le milieu de la branche  $B_n$  et le point d'investigation,  $\lambda$  est la longueur d'onde et finalement  $EPT_{uv}$  est le temps prévu pour délivrer un paquet provenant du nœud  $u$  à destination le nœud  $v$ .

Nous avons ensuite montré analytiquement que cette métrique remplit les conditions suffisantes et nécessaires, notamment l'isotonie et la monotonie, afin de garantir un routage cohérent, optimal et sans boucle. Nous avons également étudié d'autres propriétés de notre métrique RE qui sont l'asymétrie et l'additivité qui sont susceptibles d'influencer les performances du routage.

Par ailleurs, nous avons réalisé des évaluations qualitatives de notre métrique, tout d'abord en analysant les différents compromis que RE peut garantir, ensuite en montrant l'impact de deux paramètres principaux dans l'expression de RE : la distance de la zone sensible aux rayonnements et la capacité du lien.

Dans la deuxième contribution, nous avons présenté les procédures de calcul et d'implémentation de notre métrique pour deux scénarios : un réseau sans fil et un réseau hétérogène. Ceci nous a conduit à étendre la définition initiale de la métrique RE pour couvrir le cas où les liens Wi-Fi et CPL coexistent dans le même réseau. Ainsi le coût d'un chemin  $P_{s,d}$  entre une source  $s$  et une destination  $d$  est exprimé comme suit :

$$\mathcal{C}(P_{s,d}) = \sum_{u \rightarrow v \in P_{s,d}} (\alpha_{u,v} w_{Wi-Fi}(u \rightarrow v) + \beta_{u,v} w_{CPL}(u \rightarrow v))$$

Où

$$\alpha_{u,v} = \begin{cases} 1 & \text{si } u \rightarrow v \text{ est un lien Wi-Fi} \\ 0 & \text{sinon} \end{cases}$$

$$\beta_{u,v} = \begin{cases} 1 & \text{si } u \rightarrow v \text{ est un lien CPL} \\ 0 & \text{sinon} \end{cases}$$

Nous décrivons ensuite nos deux solutions de routage EMRARA et EMRARA-H (extension de EMRARA pour les réseaux hétérogènes) pour trouver les chemins garantissant un niveau minimal d'énergie rayonnée dans les réseaux sans fil et hétérogènes à multi-sauts respectivement. Afin de montrer les performances de nos algorithmes, nous avons développé un simulateur à base de Python, où on a implémenté les modèles proposés, un module de calcul de métrique de routage, et enfin nos algorithmes.

Nous avons également effectué plusieurs évaluations numériques dans la même perspective de mettre en évidence l'efficacité de nos propositions à réduire le niveau des émissions radio-fréquences en comparant avec d'autres solutions de routage bien connues et basées sur des métriques largement utilisées.

Dans certains cas, une optimisation multi-objectifs est nécessaire. Traditionnellement, les algorithmes de routage classiques trouvent les plus courts chemins d'une source vers une destination en considérant un critère unique de QoS. Cependant, pour les réseaux domestiques l'utilisateur pourrait exiger des critères supplémentaires comme indiqué précédemment, à titre d'exemple, l'économie d'énergie ou la minimisation des rayonnements électromagnétique provenant des équipements TIC. Intuitivement, l'amélioration du débit et la minimisation de l'exposition aux rayonnements radiofréquences viennent au détriment de la consommation d'énergie vu l'utilisation d'un plus grand nombre de nœuds en cherchant à s'éloigner le maximum possible de la zone sensible aux rayonnements. C'est dans cette optique où s'inscrit la dernière contribution qui vise à investiguer la possibilité d'atteindre de meilleurs compromis entre les différentes exigences d'utilisateur.

Ainsi, cette contribution consiste à la proposition d'un algorithme de routage multicritère basé sur la méthode à pondération normalisée. Une telle méthode transforme un problème multicritère un problème monocritère en multipliant chaque critère par un poids de pondération, qui exprime entre autre les préférences de l'utilisateur, et ensuite sommer tous les critères pondérés. Les trois critères que nous avons considérés sont RE, la consommation d'énergie et la bande passante.

Nous avons montré par évaluations que, dans la plupart des cas, les résultats des algorithmes de plus court chemin ayant des couts de chemin composés et pondérés

par les préférences utilisateur, suivent exactement ces poids de pondération. Nous avons également conclu que, en utilisant nos algorithmes multi-critères, nous avons pu garantir un meilleur compromis entre deux critères souvent en conflit, notamment l'économie d'énergie et l'exposition aux rayonnements radiofréquences.



# List of Publications

- [P1] H. El Abdellaouy, A. Pelov, L. Toutain, and D. Bernard. Mitigation of Electromagnetic Radiation in Heterogeneous Home Network Using Routing Algorithm. In *Modeling and Optimization in Mobile, Ad Hoc, and Wireless Networks and Workshops (WiOpt). 12th International Symposium on*, pages 326–332, May 2014.
- [P2] H. El Abdellaouy, A. Pelov, L. Toutain, and D. Bernard. Electromagnetic Radiation-Aware Routing Algorithm. In *Consumer Communications & Networking Conference (CCNC) , 2014 IEEE*, pages 119–126, January 2014.
- [P3] H. El Abdellaouy, D. Bernard, A Pelov, and L. Toutain. Green home network requirements. In *Energy Conference and Exhibition (ENERGYCON), 2012 IEEE International*, pages 896–902, Sept 2012.
- [P4] O. Bouchet, J-P. Javaudin, H. El Abdellaouy, A. Kortebi, M. LeBouc, F. Fontaine, F. Coquet, M. Brzozowski, A. Mengi, D. Katsianis, P. Celeda, C. Mayer, H. Guan, B G. Aytekin, and F. Kurt. ACEMIND: The smart integrated home network. ACEMIND: Advanced Convergent and Easily Manageable Innovative Network Design. In *10th IET International Conference on Intelligent Environments (IE 14)*, July 2014.
- [P5] O. Bouchet and H. El Abdellaouy. Deliverable D3.2. HOPE– Home Power Efficiency–Draft Part: General presentation. In *projet ACEMIND*, October 2013.



# Bibliography

- [1] Energie et climat: Chiffres clés. Technical report, ADME (Agence de l'Environnement et de la Maitrise de L'Energie, 2009.
- [2] Special Eurobarometer 73.3. Electromagnetic Fields. Technical report, Directorate General for Health and Consumer Affairs, June 2010.
- [3] ITU-T Recommendation K.61(2003). Guidance to measurement and numerical prediction of electromagnetic fields for compliance with human exposure limits for telecommunication installations. 2003.
- [4] ITU-T Recommendation K.70(2007). Mitigation techniques to limit human exposure to EMFs in the vicinity of radiocommunication stations. 2007.
- [5] Eldad Perahia and Robert Stacey. *Next Generation Wireless LANs: Throughput, Robustness, and Reliability in 802.11n*. Cambridge University Press, 2008.
- [6] Ofcom. The European Broadband Scorecards. March 2014.
- [7] Cisco. Cisco Visual Networking Index (VNI) Services Adoption Forecast, 2013–2018. 2014.
- [8] Ed T. Chown, J. Arkko, A. Brandt, O. Troan, and J. Weil. IPv6 Home Networking Architecture Principles. RFC 7368, 2014.
- [9] T. Norman. Wireless network traffic 2010-2015: forecasts and analysis. Technical report, Analysys Mason, July 2010.
- [10] J.L. Sobrinho. Algebra and algorithms for qos path computation and hop-by-hop routing in the internet. *Networking, IEEE/ACM Transactions on*, 10(4):541–550, Aug 2002.

- 
- [11] Y. Yang and J. Wang. Design Guidelines for Routing Metrics in Multihop Wireless Networks. *INFOCOM 2008. The 27th Conference on Computer Communications. IEEE*, pages 2288–2296, April 2008.
- [12] C. D. Nugent, D. D. Finlay, P. Fiorini, Y. Tsumaki, and E. Prassler. Editorial Home Automation as a Means of Independent Living. *Automation Science and Engineering, IEEE Transactions on*, 5(1):1–9, Jan 2008.
- [13] W.Y. Chen. Emerging home digital networking needs. *Community Networking Proceedings, 1997 Fourth International Workshop on*, pages 7–12, Sep 1997.
- [14] S.S. Intille. Designing a home of the future. *Pervasive Computing, IEEE*, 1(2):76–82, April 2002.
- [15] D.J. Cook, M. Youngblood, III Heierman, E.O., K. Gopalratnam, S. Rao, A. Litvin, and F. Khawaja. Mavhome: an agent-based smart home. *Pervasive Computing and Communications, 2003. (PerCom 2003). Proceedings of the First IEEE International Conference on*, pages 521–524, March 2003.
- [16] M. Chan, D. Estéve, C. Escriba, and E. Campo. A review of smart homes: Present state and future challenges. *Computer Methods and Programs in Biomedicine*, 91(1):55 – 81, 2008.
- [17] R.J. Robles and T. Kim. Review: Context Aware Tools for Smart Home Development. *Int. J. Smart Home*, 4:1–12, Jan 2010.
- [18] M.R. Alam, M.B.I. Reaz, and M.A.M. Ali. A Review of Smart Homes Past, Present, and Future. *Systems, Man, and Cybernetics, Part C: Applications and Reviews, IEEE Transactions on*, 42(6):1190–1203, Nov 2012.
- [19] N. Saito. Ecological Home Network: An Overview. *Proceedings of the IEEE*, 101(11):2428–2435, Nov 2013.
- [20] A. Mihailidis, B. Carmichael, and J. Boger. The use of computer vision in an intelligent environment to support aging-in-place, safety, and independence in the home. *Information Technology in Biomedicine, IEEE Transactions on*, 8(3):238–247, Sept 2004.
- [21] C.L. Wu, C.F. Liao, and LC. Fu. Service-Oriented Smart-Home Architecture Based on OSGi and Mobile-Agent Technology. *Systems, Man, and Cybernetics, Part C: Applications and Reviews, IEEE Transactions on*, 37(2):193–205, March 2007.

- [22] A.E. Nikolaidis, S. Papastefanos, G.A. Doumenis, G.I. Stassinopoulos, and M.P.K. Drakos. Local and remote management integration for flexible service provisioning to the home. *Communications Magazine, IEEE*, 45(10):130–138, October 2007.
- [23] S. Helal, W. Mann, H. El-Zabadani, J. King, Y. Kaddoura, and E. Jansen. The Gator Tech Smart House: a programmable pervasive space. *Computer*, 38(3):50–60, March 2005.
- [24] K. Gill, S.H. Yang, F. Yao, and X. Lu. A zigbee-based home automation system. *Consumer Electronics, IEEE Transactions on*, 55(2):422–430, May 2009.
- [25] A. Brandt, J. Buron, and G. Porcu. Home Automation Routing Requirements in Low-Power and Lossy Networks. RFC 5826, 2010.
- [26] D. Valtchev and I. Frankov. Service gateway architecture for a smart home. *Communications Magazine, IEEE*, 40(4):126–132, Apr 2002.
- [27] M. Starsinic. System architecture challenges in the home M2M network. *Applications and Technology Conference (LISAT), 2010 Long Island Systems*, pages 1–7, May 2010.
- [28] S. Nowak, F.-M. Schaefer, M. Brzozowski, R. Kraemer, and R. Kays. Towards a convergent digital home network infrastructure. *Consumer Electronics, IEEE Transactions on*, 57(4):1695–1703, November 2011.
- [29] J.-P. Javaudin, M. Bellec, P. Jaffre, O. Hoffmann, A. Foglar, and O. Isson. Inter-MAC concept for gigabit home networks. *Personal, Indoor and Mobile Radio Communications, 2009 IEEE 20th International Symposium on*, pages 1–5, Sept 2009.
- [30] ICT OMEGA project. <http://www.ict-omega.eu>.
- [31] IEEE Standard for Broadband over Power Line Networks: Medium Access Control and Physical Layer Specifications. *IEEE Std 1901-2010*, pages 1–1586, Dec 2010.
- [32] Wireless LAN Medium Access Control (MAC) and Physical Layer (PHY) Specifications. *IEEE Std 802.11-2007*, pages 1–1076, June 2007.
- [33] Wireless LAN Medium Access Control (MAC) and Physical Layer (PHY) Specifications Amendment 5: Enhancements for Higher Throughput. *IEEE Std 802.11n-2009*, pages 1–565, Oct 2009.

- [34] Wireless LAN Medium Access Control (MAC) and Physical Layer (PHY) Specifications—Amendment 4: Enhancements for Very High Throughput for Operation in Bands below 6 GHz. *IEEE Std 802.11ac-2013*, pages 1–425, Dec 2013.
- [35] Carrier Sense Multiple Access with Collision Detection (CSMA/CD) Access Method and Physical Layer Specifications. *IEEE Std 802.3-2008*, pages 1–2977, Dec 2008.
- [36] MoCA Standard. <http://www.mocalliance.org/>.
- [37] IEEE Standard for a Convergent Digital Home Network for Heterogeneous Technologies. *IEEE Std 1905.1-2013*, pages 1–93, April 2013.
- [38] T. Meyer, P. Langendorfer, M. Bahr, V. Suraci, S. Nowak, and R. Jennen. An Inter-MAC architecture for heterogeneous gigabit home networks. *Personal, Indoor and Mobile Radio Communications (PIMRC), 2009 IEEE 20th International Symposium on*, pages 1–5, Sept 2009.
- [39] M. Maaser, P. Langendorfer, and S. Nowak. Automated mapping of MAC parameters into generic QoS parameters by Inter-MAC adaptors. *Personal Indoor and Mobile Radio Communications (PIMRC), 2010 IEEE 21st International Symposium on*, pages 2817–2822, Sept 2010.
- [40] S. Sahaly and P. Christin. Inter-MAC forwarding and load balancing per flow. *Personal, Indoor and Mobile Radio Communications, 2009 IEEE 20th International Symposium on*, pages 1–4, Sept 2009.
- [41] M. Brzozowski, S. Nowak, F.-M. Schaefer, R. Jennen, and A. Palo. Inter-MAC – From vision to demonstration: Enabling heterogeneous meshed home area networks. *Electronic Media Technology (CEMT), 2011 14th ITG Conference on*, pages 1–6, March 2011.
- [42] A. Fehske, G. Fettweis, J. Malmodin, and G. Biczok. The global footprint of mobile communications: The ecological and economic perspective. *Communications Magazine, IEEE*, 49(8):55–62, August 2011.
- [43] A.P. Bianzino, C. Chaudet, D. Rossi, and J. Rougier. A Survey of Green Networking Research. *Communications Surveys Tutorials, IEEE*, 14(1):3–20, First 2012.
- [44] EARTH Project. Energy Aware Radio and neTwork tecHnologies. <http://www.ict-earth.eu/>.

- [45] Y.S. Soh, T.Q.S. Quek, M. Kountouris, and H. Shin. Energy Efficient Heterogeneous Cellular Networks. *Selected Areas in Communications, IEEE Journal on*, 31(5):840–850, May 2013.
- [46] S. Nooshabadi. Power-performance versus algorithmic trade-offs in the implementation of wireless multimedia terminals. *Circuits and Systems (MWSCAS), 2010 53rd IEEE International Midwest Symposium on*, pages 700–703, Aug 2010.
- [47] A.P. Chandrakasan, S. Sheng, and R.W. Brodersen. Low-power CMOS digital design. *Solid-State Circuits, IEEE Journal of*, 27(4):473–484, Apr 1992.
- [48] J. Palicot, X. Zhang, P. Leray, and C. Moy. Cognitive Radio and green communications: power consumption consideration. *ISRSSP 2010 – 2nd International Symposium on Radio Systems and Space Plasma*, August 2010.
- [49] L.M. Feeney. *Mobile Ad Hoc Networking*, chapter Energy-Efficient Communication in Ad Hoc Wireless Networks, pages 301–327. IEEE Press, 2004.
- [50] I. Stojmenovic and X. Lin. Power-aware localized routing in wireless networks. *Parallel and Distributed Systems, IEEE Transactions on*, 12(11):1122–1133, Nov 2001.
- [51] J. Li, D. Cordes, and J. Zhang. Power-aware routing protocols in ad hoc wireless networks. *Wireless Communications, IEEE*, 12(6):69–81, Dec 2005.
- [52] S. Singh, M. Woo, and C. S. Raghavendra. Power-aware Routing in Mobile Ad Hoc Networks. *Proceedings of the 4th Annual ACM/IEEE International Conference on Mobile Computing and Networking*, pages 181–190, 1998.
- [53] C-K. Toh. Maximum battery life routing to support ubiquitous mobile computing in wireless ad hoc networks. *Communications Magazine, IEEE*, 39(6):138–147, Jun 2001.
- [54] A. Misra and S. Banerjee. MRPC: maximizing network lifetime for reliable routing in wireless environments. *Wireless Communications and Networking Conference, 2002. WCNC2002. 2002 IEEE*, 2:800–806 vol.2, Mar 2002.
- [55] K. Scott and N. Bambos. Routing and channel assignment for low power transmission in PCS. *Universal Personal Communications, 1996. Record., 1996 5th IEEE International Conference on*, 2:498–502 vol.2, Sep 1996.
- [56] V. Rodoplu and T.H. Meng. Minimum energy mobile wireless networks. *Communications, 1998. ICC 98. Conference Record. 1998 IEEE International Conference on*, 3:1633–1639 vol.3, Jun 1998.

- [57] W.R. Heinzelman, A. Chandrakasan, and H. Balakrishnan. Energy-efficient communication protocol for wireless microsensor networks. *System Sciences, 2000. Proceedings of the 33rd Annual Hawaii International Conference on*, pages 10 pp. vol.2–, Jan 2000.
- [58] S. Doshi, S. Bhandare, and T.X. Brown. An On-demand Minimum Energy Routing Protocol for a Wireless Ad Hoc Network. *SIGMOBILE Mob. Comput. Commun. Rev.*, 6(3):50–66, June 2002.
- [59] J. Gomez, A.T. Campbell, M. Naghshineh, and C. Bisdikian. Conserving transmission power in wireless ad hoc networks. *Network Protocols, 2001. Ninth International Conference on*, pages 24–34, Nov 2001.
- [60] A. Michail and A. Ephremides. Energy efficient routing for connection-oriented traffic in ad-hoc wireless networks. *Personal, Indoor and Mobile Radio Communications. PIMRC 2000. The 11th IEEE International Symposium on*, 2:762–766 vol.2, 2000.
- [61] S. Banerjee and A. Misra. Minimum energy paths for reliable communication in multi-hop wireless networks. *Proceedings of the 3rd ACM international symposium on Mobile ad hoc networking & computing*, pages 146–156, 2002.
- [62] Q. Dong, S. Banerjee, M. Adler, and A. Misra. Minimum Energy Reliable Paths Using Unreliable Wireless Links. *Proceedings of the 6th ACM International Symposium on Mobile Ad Hoc Networking and Computing*, pages 449–459, 2005.
- [63] V. Shrivastava, D. Agrawal, A. Mishra, S. Banerjee, and T. Nadeem. Understanding the Limitations of Transmit Power Control for Indoor Wlans. *Proceedings of the 7th ACM SIGCOMM Conference on Internet Measurement*, pages 351–364, 2007.
- [64] D. Guo. Power amplifier and front end module requirements for IEEE 802.11n applications. *High Frequency Electronics*, 2011.
- [65] ICNIRP guidelines for limiting exposure to time-varying electric, magnetic and electromagnetic fields(up to 300GHz). *Health Physics*, 74, 1998.
- [66] B. Zarikoff and D. Malone. Experiments with radiated interference from in-home power line communication networks. *Communications (ICC), 2012 IEEE International Conference on*, pages 3414–3418, 2012.
- [67] A. Vukicevic. *Electromagnetic Compatibility of Power Line Communication Systems*. PhD thesis, ECOLE POLYTECHNIQUE FEDERALE DE LAUSANNE, 2008.

- [68] A. Mescoco. *Study of Electromagnetic Emissions from Broadband PLC: Characterization, Modeling and Mitigation Methods*. PhD thesis, Télécom Bretagne, Université de Bretagne Occidentale, Dec 2013.
- [69] N. Korovkin, E. Marthe, F. Rachidi, and E. Selina. Mitigation of electromagnetic field radiated by PLC systems in indoor environment. *International Journal of Communication Systems*, 16(5):417–426, 2003.
- [70] P. Favre, C. Candolfi, and P. Krahenbuehl. Radiation and disturbance mitigation in PLC networks. *Electromagnetic Compatibility, 2009 20th International Zurich Symposium on*, pages 5–8, 2009.
- [71] A. Mescoco, P. Pagani, M. Ney, and A Zeddami. Radiation Mitigation for Power Line Communications Using Time Reversal. *Journal of Electrical and Computer Engineering*, 2013.
- [72] IEEE Standard for Safety Levels with Respect to Human Exposure to Radio Frequency Electromagnetic Fields, 3 kHz to 300 GHz. *IEEE Std C95.1-2005*, 2005.
- [73] ITU-T Recommendation K.52 (2004). Guidance on complying with limits for human exposure to electromagnetic fields. 2004.
- [74] ITU-T Recommendation ITU-R BS.1698(2005). Evaluating fields from terrestrial broadcasting transmitting systems operating in any frequency band for assessing exposure to non-ionizing radiation. 2005.
- [75] IEEE P802.11 Wireless LANs. TGn channel models. *IEEE 802.11-03/940r4*, 2004.
- [76] J. McNair, IF. Akyildiz, and M.D. Bender. An inter-system handoff technique for the IMT-2000 system. *INFOCOM 2000. Nineteenth Annual Joint Conference of the IEEE Computer and Communications Societies. Proceedings. IEEE*, 1:208–216 vol.1, 2000.
- [77] Q. Tang, N. Tummala, S.K.S. Gupta, and L. Schwiebert. TARA: Thermal-Aware Routing Algorithm for Implanted Sensor Networks. *DCOSS*, pages 206–217, 2005.
- [78] D. Guezgouz. *Contribution à la modélisation du réseau électrique domestique en vue de la caractérisation du canal de propagation CPL*. PhD thesis, Université François Rabelais Tours, 2010.

- [79] M. Zimmermann and K. Dostert. A Multi-Path Signal Propagation Model for the Power Line Channel in the High Frequency Range. *in Proc. 3rd Int. Symp. Powerline Communications and its Applications, Lancaster, U.K.*, pages 45–51, 1999.
- [80] M. Zimmermann and K. Dostert. A multipath model for the powerline channel. *Communications, IEEE Transactions on*, 50(4):553–559, Apr 2002.
- [81] D. Benyoucef. A New Statistical Model of the Noise Power Density Spectrum for Powerline Communication. *Proceedings of the 7th International symposium on Power-Line Communications and its Applications*, pages 136–141, 2003.
- [82] M. Babic, J. Bausch, T. Kistner, and K. Dostert. Performance Analysis of Coded OFDM Systems at Statistically Representative PLC Channels. *Power Line Communications and Its Applications, 2006 IEEE International Symposium on*, pages 104–109, 2006.
- [83] M. Tlich, A Zeddou, F. Moulin, and F. Gauthier. Indoor Power-Line Communications Channel Characterization Up to 100 MHz—Part I: One-Parameter Deterministic Model. *Power Delivery, IEEE Transactions on*, 23(3):1392–1401, July 2008.
- [84] A.M. Tonello and F. Versolatto. Bottom-Up Statistical PLC Channel Modeling; Part I: Random Topology Model and Efficient Transfer Function Computation. *Power Delivery, IEEE Transactions on*, 26(2):891–898, 2011.
- [85] M. Tlich, A Zeddou, F.P. Gauthier, and P. Pagani. Wideband Indoor Transmission Channel Simulator for Power Line: WITS Software. *Power Delivery, IEEE Transactions on*, 25(2):702–713, April 2010.
- [86] M. Ishihara, D. Umehara, and Y. Morihiro. The Correlation between Radiated Emissions and Power Line Network Components on Indoor Power Line Communications. *Power Line Communications and Its Applications, 2006 IEEE International Symposium on*, pages 314–318, 2006.
- [87] C.R. Paul. A comparison of the contributions of common-mode and differential-mode currents in radiated emissions. *Electromagnetic Compatibility, IEEE Transactions on*, 31(2):189–193, 1989.
- [88] Information Technology Equipment – Radio disturbances characteristics – Limits and methods of measurement. *CISPR 22, Ed. 6.0*, 2008-2009.
- [89] HomePlug AV2 Technology. Raising the Bar for Sustained High-Throughput Performance and Interoperability for Multi-stream Networking Using Existing Powerline Wiring in Home. 2013.

- [90] F. Rachidi and S. Tkachenko. *Electromagnetic Field Interaction with Transmission Lines*. WIT Press, 2008.
- [91] P. Favre, C. Candolfi, M. Schneider, M. Rubinstein, P. Krahenbuehl, and A. Vukicevic. Common mode current and radiations mechanisms in PLC networks. *Power Line Communications and Its Applications, 2007. ISPLC '07. IEEE International Symposium on*, pages 348–354, 2007.
- [92] Numerical Electromagnetics Code (Method of Moments). <http://www.nec2.org/>.
- [93] Computer Simulation Technology. <http://www.cst.com/>.
- [94] A.M. Tonello, F. Versolatto, and S. D'Alessandro. Opportunistic Relaying in In-Home PLC Networks. *Global Telecommunications Conference (GLOBECOM 2010), 2010 IEEE*, pages 1–5, 2010.
- [95] G. Marrocco, D. Statovci, and S. Trautmann. A PLC broadband channel simulator for indoor communications. *Power Line Communications and Its Applications (ISPLC), 2013 17th IEEE International Symposium on*, pages 321–326, March 2013.
- [96] R. Draves, J. Padhye, and B. Zill. Routing in Multi-radio, Multi-hop Wireless Mesh Networks. *Proceedings of the 10th Annual International Conference on Mobile Computing and Networking*, pages 114–128, 2004.
- [97] D.S.J. De Couto. *High-Throughput Routing for Multi-Hop Wireless Networks*. PhD thesis, Massachusetts Institute of Technology, 2004.
- [98] D.S.J. De Couto, D. Aguayo, J. Bicket, and R. Morris. A High-throughput Path Metric for Multi-hop Wireless Routing. *Proceedings of the 9th Annual International Conference on Mobile Computing and Networking*, pages 134–146, 2003.
- [99] A. Hagberg, D. Schult, and P. Swart. *NetworkX Reference, Release 1.7*. 2012.
- [100] C.A.C. Coello, G.B. Lamont, and D.A.V. Veldhuizen. *Evolutionary Algorithms for Solving Multi-Objective Problems (Genetic and Evolutionary Computation)*. Springer-Verlag New York, Inc., Secaucus, NJ, USA, 2006.
- [101] J. Branke, K. Deb, K. Miettinen, and M. Slowinski. *Multiobjective Optimization: Interactive and Evolutionary Approaches, volume 5252 of Lecture Notes in Computer Science*. Springer, Berlin, 2008.

- [102] L.L.H. Andrew and AAN.A. Kusuma. Generalised analysis of a QoS-aware routing algorithm. *Global Telecommunications Conference, 1998. GLOBECOM 1998. The Bridge to Global Integration. IEEE*, 1:1–6 vol.1, 1998.
- [103] S. Chen and K. Nahrstedt. On Finding Multi-constrained Paths. *Communications, 1998. ICC 98. Conference Record. 1998 IEEE International Conference on*, pages 874–879, 1998.
- [104] X. Yuan. Heuristic algorithms for multiconstrained quality-of-service routing. *Networking, IEEE/ACM Transactions on*, 10(2):244–256, Apr 2002.
- [105] P. Van Mieghem and F.A. Kuipers. Concepts of exact QoS routing algorithms. *Networking, IEEE/ACM Transactions on*, 12(5):851–864, Oct 2004.
- [106] T. Korkmaz and M. Krunz. Multi-constrained optimal path selection. *INFOCOM 2001. Twentieth Annual Joint Conference of the IEEE Computer and Communications Societies*, 2:834–843 vol.2, 2001.
- [107] B. Malakooti and I. Thomas. A Distributed Composite Multiple Criteria Routing Using Distance Vector. *Networking, Sensing and Control, 2006. ICNSC '06. Proceedings of the 2006 IEEE International Conference on*, pages 42–47, 2006.
- [108] P. Khadivi, S. Samavi, T.D. Todd, and H. Saidi. Multi-constraint QoS routing using a new single mixed metric. *Communications, 2004 IEEE International Conference on*, 4:2042–2046 Vol.4, June 2004.
- [109] G. Xue and S.K. Makki. Multiconstrained QoS Routing: A Norm Approach. *Computers, IEEE Transactions on*, 56(6):859–863, June 2007.
- [110] D. Yuan. A bicriteria optimization approach for robust OSPF routing. *IP Operations Management, 2003. (IPOM 2003). 3rd IEEE Workshop on*, pages 91–98, Oct 2003.
- [111] Z. Wang and J. Crowcroft. Quality-of-service routing for supporting multimedia applications. *Selected Areas in Communications, IEEE Journal on*, 14(7):1228–1234, 1996.
- [112] S. Gass and T. Saaty. The computational algorithm for the parametric objective function. *Naval Research Logistics Quarterly*, 2(1-2):39–45, 1955.
- [113] L. Zadeh. Optimality and non-scalar-valued performance criteria. *Automatic Control, IEEE Transactions on*, 8(1):59–60, 1963.

- 
- [114] R.E. Steuer. *Multiple Criteria Optimization: Theory, Computation, and Application*. Wiley, New York, 1986.
- [115] L. Tanner. Selecting a text-processing system as a qualitative multiple criteria problem. *European Journal of Operational Research*, 50(2):179 – 187, 1991.
- [116] Quagga Routing Software Suite, GPL licensed. <http://www.nongnu.org/quagga/>.
- [117] NS3 Simulator. <http://www.nsnam.org/>.

Les produits et les technologies de communication ont connu durant la dernière décennie des améliorations importantes en termes de diversification de services, ceci a changé la vision des réseaux domestiques.

Les maisons d'aujourd'hui hébergent des équipements de plus en plus sophistiqués offrant une large gamme de services comme HDTV, VoIP, le stockage multimédia, etc. Cette extension technologique n'est pas sans conséquences. En effet, les équipements des Technologies d'Information et de la Communication (TIC) consomment pratiquement un quart de la consommation totale d'électricité dans une maison typique en France, ce qui met en avant la question d'efficacité énergétique dans les réseaux domestiques. En outre, les émissions électromagnétiques deviennent de plus en plus omniprésentes au sein des maisons, ceci peut inquiéter une tranche importante des utilisateurs, cela peut également ralentir les futures innovations des technologies sans fil. Toutefois, l'augmentation de la connectivité peut aider à résoudre ces problèmes en désactivant les équipements redondants ou en sélectionnant des chemins plus appropriés dans le réseau. Le problème peut être perçu comme un protocole de routage multicritère avec l'introduction de nouvelles métriques vertes. Par conséquent, une solution de routage pour réseau domestique doit supporter des contraintes supplémentaires en parallèle avec celles de QoS.

Nous avons commencé par donner une vue d'ensemble du vaste domaine des maisons intelligentes. Nous avons ainsi présenté quelques solutions dans la littérature visant à optimiser les mécanismes de gestion du réseau dans un environnement domestique. Nous avons par la suite mis l'accent sur les solutions de routage, en particulier celles qui prennent en considération les exigences « vertes » de l'utilisateur. Plus précisément, ces exigences concernent l'économie d'énergie et la minimisation des rayonnements électromagnétiques. A travers cet état de l'art, nous avons pu souligner l'absence d'une solution de routage qui répond à ces objectifs écologiques dans un environnement spécifique qui est l'environnement domestique. Cela constitue la principale motivation de ces travaux.

Dans le but de satisfaire les exigences de l'utilisateur préalablement mentionnés, cette thèse contient principalement trois contributions. La première contribution consiste à la proposition d'un nouveau concept de métrique de routage sensible aux rayonnements électromagnétiques qui peut être utilisée sans modifications avec n'importe quel algorithme de plus court chemin. Nous avons ensuite montré analytiquement que cette métrique remplit les conditions suffisantes et nécessaires afin de garantir un routage cohérent, optimal et sans boucle. Cette métrique est désormais nommée Radiant Exposure (RE). Dans le but d'exprimer RE pour les liens Wi-Fi et CPL (Courant Porteur en Ligne), qui sont les deux technologies les plus présentes dans les foyers d'aujourd'hui, nous avons détaillé notre premier modèle analytique des champs électromagnétiques rayonnés par les équipements Wi-Fi et notre deuxième modèle des champs électromagnétiques provenant des lignes électriques quand celles-ci transportent des données en hautes fréquences. Mais avant tout, nous avons discuté exhaustivement les problèmes liés à la modélisation d'un tel phénomène physique pour des fins de routage. Ce qui nous a amené à considérer un ensemble d'hypothèses simplificatrices ainsi qu'un ensemble de méthodes mathématiques appropriées. L'objectif majeur de ces deux modèles est de fournir une valeur unique pour chaque lien qu'il soit Wi-Fi ou CPL permettant de caractériser sa contribution dans l'énergie rayonnée cumulée pendant la transmission des données.

Dans la deuxième contribution, nous avons présenté les procédures de calcul et d'implémentation de notre métrique pour deux scénarios : un réseau sans fil et un réseau hétérogène. Ceci nous a conduit à étendre la définition initiale de la métrique RE pour couvrir le cas où les liens Wi-Fi et CPL coexistent dans le même réseau.

Nous décrivons ensuite nos deux solutions de routage EMRARA et EMRARA-H pour trouver les chemins garantissant un niveau minimal d'énergie rayonnée dans les réseaux sans et hétérogènes à multi-sauts respectivement. Afin de montrer les performances de nos algorithmes, nous avons développé un simulateur à base de Python, où on a implémenté les modèles proposés, un module de calcul de métrique de routage, et enfin nos algorithmes.

La dernière contribution consiste à la proposition d'un algorithme de routage multicritère basé sur la méthode à pondération normalisée. Une telle méthode transforme un problème multicritère à un problème monocritère en multipliant chaque critère par un poids de pondération, qui exprime entre autre les préférences de l'utilisateur, et ensuite sommer tous les critères pondérés. Les trois critères que nous avons considérés sont RE, la consommation d'énergie et la bande passante.

**Mots-clés :** Routage, Réseaux, Gestion de l'énergie, Rayonnement électromagnétique, Wi-Fi, CPL

The recent improvements in communication technologies and products in terms of services' diversification have a direct effect on home environment. Nowadays, homes host increasingly sophisticated devices providing a wide range of services such as HDTV, VoIP, multimedia storage, gaming, music and so on. This extension does not come for free. Indeed, Information and Communication Technology-enabled (ICT) devices consume about the quarter of the total power consumption within a typical home network, which puts forward the issue of energy efficiency in the home network. In addition, electromagnetic radiation emissions are increasing within homes and may create fear likely to slow down future innovations for certain community of people. Nevertheless the increasing connectivity may help to solve these problems by disabling redundant devices or select more appropriate paths in the network. The problem can be viewed as a multi-criteria routing protocol generalization with the introduction of new metrics. A home network routing solution has therefore to support additional constraints in conjunction with QoS criteria.

It has been a challenging goal to make path selection based on ecological criteria that are closely linked to the external environment (e.g. EM radiation); instead of the conventional routing metrics inherently dependent on network state (e.g. delay). In this thesis, we develop a new concept of radiation-aware routing algorithm for heterogeneous home networks in order to reduce radiated emissions level within a given area. The first contribution is the proposal of two models of electromagnetic radiated emissions stemming from Wi-Fi and PLC links based on a set of assumptions and mathematical approximation methods. We have then formulated a link-adaptive radiation-aware routing metric.

The second contribution is the proposal of the Radiant Exposure (RE), which is a new routing metric for finding minimum radiated emissions paths in multi-hop heterogeneous network. The RE of a path is the expected radiated energy in units of  $W.s/m^2$ , within the radiation-sensitive area, while transmitting a packet along that path.

The RE metric incorporates the effects of the distance between the radiating sources and the radiation-sensitive area as well as the asymmetry of this radiated energy regarding the two directions of each link. We describe the design and implementation of RE as routing metric that can  $\_t$  any shortest path algorithm. For practical networks, using RE metric also maximizes the network throughput. We show by simulations that using RE metric reduces significantly radiated energy compared to the widely used minimum-hop count metric.

The third contribution consists of proposing a multi-criteria routing algorithm built upon the well-known normalized weighting function. Such method transforms a multi-objective problem into a mono-objective problem by multiplying each objective function by a weighting factor and summing up all the weighted criteria. We involve the user in the process of selecting weights in line with their preferences. The three criteria considered here are radiant exposure (RE), expected energy consumption and bandwidth.

**Keywords :** Routing, Networks, Energy Efficiency, Electromagnetic Fields, Wi-Fi, PLC



n° d'ordre : 2015telb0342

Télécom Bretagne

Technopôle Brest-Iroise - CS 83818 - 29238 Brest Cedex 3

Tél : + 33(0) 29 00 11 11 - Fax : + 33(0) 29 00 10 00